Electronic Supplementary Material (ESI) for Organic & Biomolecular Chemistry.

Electronic Supplementary Information

A Supramolecular Host for Phosphatidylglycerol (PG) Lipids with Antibacterial Activity

Elliot S. Williams, Hassan Gneid, Sarah R. Marshall, Mario J. González, Jorgi A. Mandelbaum, and Nathalie Busschaert

Department of Chemistry, Tulane University, New Orleans, Louisiana 70118, United States. Email: nbusschaert@tulane.edu

Table of Contents

S1. General

Compound names were generated from ChemDraw 16.0.1.4 following IUPAC nomenclature. Solvents, reagents, and inorganic salt were purchased by Sigma Aldrich, TCI, or Combi Blocks and used without further purification. Reactions were performed under a nitrogen atmosphere in oven-dried glassware. HPLC traces were collected on a Thermo Fisher Scientific Vanquish Flex UHPLC with variable wavelength detector, using a Hypersil GOLD C18 column (150 mm length, 3.0 mm diameter, 3 µm particle size). 'Solvent A' was 0.1% (v/v) HCOOH in water and 'solvent B' was 0.1% (v/v) HCOOH in acetonitrile. Gradient was from 10% B to 90% B in 15 min, followed by 4 minutes at 90% B. The detection wavelength was set at 254 nm or 280 nm. ^{1}H NMR and ^{13}C NMR spectra were collected on a Bruker 500 MHz NMR, Varian 400 MHz, or a Bruker Avance 300 MHz spectrometer. ^{13}C NMR spectra were proton decoupled. MestreNova was used for NMR visualization. Chemical shifts (δ) are reported in parts per million (ppm), calibrated to the residual solvent peak in DMSO-d_6 δ = 2.50 (^{1}H) and δ = 39.5 (^{13}C), and coupling constants (*J*) are given in Hertz (Hz). The following abbreviations are used for spin multiplicity: s = singlet, d = doublet, t = triplet, q = quartet, dd = doublet of doublets, td = triplet of doublet, m = multiplet. ^{13}C signals arising from the quaternary carbon bearing the boronic acid group were not always observed and therefore not always listed. NMR signals arising from the boroxine form of boronic acid and the self-cyclized forms of **1**, **5**, and **6** were sometimes observed, however not reported.[1] Infrared (IR) spectra were recorded on a Nexus 670 Avatar FTIR spectrometer; only selected maximum absorbances (ν_{max}) of the most intense peaks are reported (cm^{-1}). High resolution electron spray ionization (ESI) mass spectra were recorded on a Bruker micrOTOF. The lipids POPG (1-palmitoyl-2-oleoyl-sn-glycero-3-phospho-(1'-rac-glycerol) (sodium salt)), POPC (1-palmitoyl-2-oleoyl-glycero-3-phosphocholine), DDPG (1,2-didecanoyl-sn-glycero-3-phospho-(1'-rac-glycerol) (sodium salt)), and DHPC (1,2-dihexanoyl-sn-glycero-3-phosphocholine) were purchased from Avanti Polar Lipids, Inc. UV-Vis titrations were performed on an Agilent Cary 100 UV-Vis spectrophotometer equipped with stirring function and Peltier temperature controller. Fluorescence spectra were recorded on an Agilent Cary Eclipse fluorescence spectrophotometer equipped with stirring function and Peltier temperature controller. For the fluorescence experiments, 3 mL macrocuvettes with 10 mm pathlength were used and all solutions were stirred using a cuvette stir bar (Sigma-Aldrich #Z363545). The pK_a experiments used a microcuvette with 2 mm pathlength. For the Alizarin Red S (ARS) K_a approximation assay, 65 mm tall cuvettes with 10 mm pathlength were purchased from Firefly Sci. (Type 508). Bacterial strains were purchased from the American Type Culture Collection (ATCC). Bacterial growth curves, mechanistic studies, imaging and hemolysis assays were performed using a BioTek Cytation 5 Cell Imaging Multi-Mode Reader. Control antibiotics were used as provided by the suppliers: clindamycin hydrochloride (Sigma-Aldrich #PHR1159), indolicidin (GenScript #RP11242), gramicidin (BioVision #B1624), and nisin (Sigma-Aldrich #N5764). Fluorophores for the antibacterial mode of action studies were used as provided by the supplier and stored at -20 °C in the dark (stock solutions were always prepared fresh on the day of use): $DiSC_3(5)$ (3,3'-dipropylthiadicarbocyanine iodide, AnaSpec #AS-84923), Sytox Green (Invitrogen #S7020), Laurdan (6-dodecanoyl-2-dimethylaminonaphthalene, Invitrogen #D250) and DPH (1,6-diphenyl-1,3,5-hexatriene**,** Sigma-Aldrich #D208000). Phosphate buffered saline (PBS) was purchased from Gibco (#10-010-031) and washed single donor human red blood cells were purchased from Innovative Research, Inc. (IWB3ALS)

S2. Synthesis and characterization

General procedure. The library of boronic acid containing ureas was synthesized from the reaction of the appropriate amine (containing the boronic acid) with excess isocyanate in anhydrous pyridine. After the reaction was complete, the round-bottom flask was attached to a rotary evaporator and the pyridine was removed by reduced pressure (using an azeotropic mixture with toluene). The ureas were subsequently purified using an extraction-based method adapted from Dennis Hall.[1] The method takes advantage of the ability of boronic acids to bind sugars. By adding the polyol sorbitol, and either acid or base, the polarity of each boronic acid compound can be tuned and thus separated from starting material and side products. For this method, the dry crude mixture was dissolved in 15 mL of a 5% w/w NaOH solution and transferred to a separatory funnel. After the crude basic solution had been transferred, 15 mL of diethyl ether was used to transfer the remaining crude material from the round-bottom flask to the separatory funnel, and an additional 75 mL of diethyl ether, 2 mL of 5% v/v HCl solution, and 75 mL deionized H_2O were added to the extraction funnel to ensure that the aqueous solution became acidic. The flask was shaken, allowed to settle for five minutes, and the acidic layer was removed while retaining the organic layer. This step should remove the staring amine from the crude mixture. Next, 1.2 equivalents of sorbitol (based on the starting amount of boronic acid) were added to the extraction funnel, as well as a 1 mL of a 5% w/w NaOH solution and 75 mL deionized H_2O. The flask was shaken, allowed five minutes to settle, and the basic layer was collected in a beaker and chilled in an ice bath. The organic layer (which contains the isocyanate and other organic side products) was discarded. To the aqueous layer (which contains the product complexed to sorbitol) was slowly added 5% v/v HCl to release the product from the sorbitol, which leads to precipitation of the final product. The final product was filtered off by vacuum filtration and dried in a vacuum desiccator overnight. To collect the product from the filter paper, the filter paper was washed with acetone, and the solvent transferred to a scintillation vial. The acetone was removed using a rotary evaporator, leaving a sticky viscous product. A small addition (< 5 mL) of dichloromethane (DCM) to the viscous product converted the product to a powder, due to its insolubility in DCM. The DCM was removed using a rotary evaporator and the product was dried on high vacuum overnight.

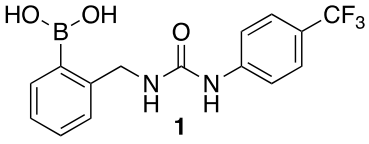

1

(2-((3-(4-(trifluoromethyl)phenyl)ureido)methyl)phenyl)boronic acid, (1). In an oven-dried 25 mL round bottom flask equipped with stir bar, (2-(aminomethyl)phenyl)boronic acid (126 mg, 0.83 mmol, 1 eq) and 4-(trifluoromethyl)phenyl isocyanate (300 µL, 2.10 mmol, 2.5 eq) were stirred in 6 mL anhydrous pyridine at 50˚C for 18 hours under a N_2 atmosphere. Compound **1** was purified using the sorbitol extraction method described in the 'general procedure', yielding a white solid (86 mg, 0.25 mmol, 30% yield). Purity (HPLC): 98.5%. ^{1}H NMR (500 MHz, DMSO-d_6, ppm) δ 9.08 (s, 1 H), 8.21 (s, 2 H), 7.61 – 7.50 (m, 5 H), 7.40 – 7.29 (m, 2 H), 7.29 – 7.15 (m, 1 H), 6.70 (t, ^3J = 6.0 Hz, 1 H), 4.43 (d, ^3J = 6.0 Hz, 2 H); ^{13}C NMR (126 MHz, DMSO-d_6, ppm) δ 155.0, 144.1 (q, $^4J_{C\text{-}F}$ = 1.5 Hz), 143.8, 133.9, 129.2, 127.9, 126.0 – 125.9 (m), 125.9 (shown in insert), 124.5 (q, $^1J_{C\text{-}F}$ = 271.0 Hz), 121.0 (q, $^2J_{C\text{-}F}$ = 32.0 Hz), 117.3, 43.2. HRMS (ESI+) for $C_{15}H_{15}BF_3N_2O_3$ $[M+H]^+$: *m/z* = 339.1189 (found), 339.1131 (calculated); IR (neat): *v* (cm^{-1}) = 2969, 1737, 1321, 1112, 1068.

(3-(3-(4-(trifluoromethyl)phenyl)ureido)phenyl)boronic acid, (2). 3-Aminophenylboronic acid (219 mg, 1.60 mmol, 1 eq) and 4-(trifluoromethyl)phenyl isocyanate (260 µL, 1.82 mmol, 1.1 eq) were stirred in 6 mL anhydrous pyridine at room temperature for 20 hours under a N_2 atmosphere. Compound **2** was purified using the sorbitol extraction method

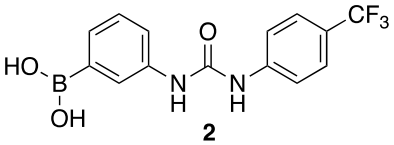

2

described in the 'general procedure', yielding a beige solid (391 mg, 1.21 mmol, 76% yield). Purity (HPLC): 98.3%. ^{1}H NMR (500 MHz, DMSO-d_6, ppm) δ 9.06 (s, 1 H), 8.69 (s, 1 H), 7.95 (s, 2 H), 7.70 (s, 1 H), 7.68 – 7.57 (m, 5 H), 7.43 (d, ^{3}J = 7.5 Hz, 1 H), 7.26 (t, ^{3}J = 7.5 Hz, 1 H); ^{13}C NMR (75 MHz, DMSO-d_6, ppm) δ 152.4, 143.6 (q, $^{4}J_{C\text{-}F}$ = 1.5 Hz), 138.4, 128.2, 127.8, 126.1 (q, $^{3}J_{C\text{-}F}$ = 3.5 Hz), 124.6 (q, $^{1}J_{C\text{-}F}$ = 271.0 Hz), 124.5, 121.6 (q, $^{2}J_{C\text{-}F}$ = 32.0 Hz), 120.5, 117.8; HRMS (ESI+) for $C_{14}H_{13}BF_3N_2O_3$ $[M+H]^+$: *m/z* = 325.0967 (found), 325.0974 (calculated); IR (neat): *v* (cm^{-1}) = 3267, 1735, 1643, 1324, 1070.

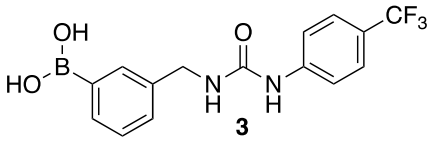

3

(**3-((3-(4-(trifluoromethyl)phenyl)ureido)methyl)phenyl) boronic acid, (3).** In a 25 mL round bottom flask, (3-(aminomethyl)phenyl)boronic acid, hydrochloric acid (293 mg, 1.56 mmol, 1 eq) and 4-(trifluoromethyl)phenyl isocyanate (600 µL, 4.20 mmol, 2.7 eq) were dissolved in 20 mL anhydrous pyridine and the resulting mixture was stirred at room temperature for 18 hours under a N_2 atmosphere. Compound **3** was purified using the sorbitol extraction method described in the 'general procedure', yielding a white solid (230 mg, 0.68 mmol, 44% yield). Purity (HPLC): 95.1%. ^{1}H NMR (500 MHz, DMSO-d_6, ppm) δ 8.94 (s, 1 H), 7.98 (s, 2 H), 7.73 (s, 1 H), 7.71 – 7.64 (m, 1 H), 7.64 – 7.53 (m, 4 H), 7.38 – 7.24 (m, 2 H), 6.73 (t, ^{3}J = 6.0 Hz, 1 H), 4.31 (d, ^{3}J = 6.0 Hz, 2 H);^{13}C NMR (75 MHz, DMSO-d_6, ppm) δ 154.8, 144.2 (q, $^{4}J_{C\text{-}F}$ = 1.5 Hz), 138.7, 133.0, 132.6, 129.0, 127.3, 125.9 (q, $^{3}J_{C\text{-}F}$ = 4.0 Hz), 124.6 (q, $^{1}J_{C\text{-}F}$ = 271.0 Hz), 120.9 (q, $^{2}J_{C\text{-}F}$ = 32.0 Hz), 117.2, 42.9; HRMS (ESI+) for $C_{15}H_{15}BF_3N_2O_3$ $[M+H]^+$: *m/z* = 339.1120 (found), 339.1131 (calculated). IR (neat): *v* (cm^{-1}) = 3342, 2998, 1739, 1641, 1552, 1324.

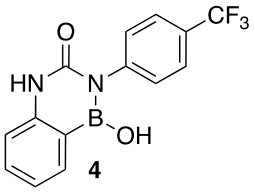

4

1-hydroxy-2-(4-(trifluoromethyl)phenyl)-1,4-dihydrobenzo[*c*][1,5,2]diaza-borinin-3(2*H*)-one, (4). In a 25 mL round bottom flask, (2-aminophenyl) boronic acid (256 mg, 1.87 mmol, 1 eq) and 4-(trifluoromethyl)phenyl isocyanate (500 µL, 3.5 mmol, 1.9 eq) were dissolved in 6 mL anhydrous pyridine and stirred at 25˚C for 18 hours under a N_2 atmosphere. Compound **4** was purified using the sorbitol extraction method described in the 'general procedure', yielding a white solid (526 mg, 1.72 mmol, 92% yield). Purity (HPLC): 96.4%. ^{1}H NMR (500 MHz, DMSO-d_6, ppm) δ 10.44 (s, 1 H), 9.19 (s, 1 H), 8.01 (dd, *J* = 8.0, 1.5 Hz, 1 H), 7.77 (m, 2 H), 7.50 (td, *J* = 8.0, 1.5 Hz, 1 H), 7.43 (m, 2 H), 7.11 (d, *J* = 8.0 Hz, 1 H), 7.07 (t, *J* = 8.0 Hz, 1 H); ^{13}C NMR (75 MHz, DMSO-d_6, ppm) δ 153.8, 145.5, 143.2 (q, $^{3}J_{C\text{-}F}$ = 1.5 Hz), 132.8, 132.7, 129.9, 126.9 (q, $^{2}J_{C\text{-}F}$ = 32.0 Hz), 125.5 (q, $^{1}J_{C\text{-}F}$ = 270.0 Hz), 125.4 (q, $^{3}J_{C\text{-}F}$ = 4.0 Hz), 120.9, 114.4; HRMS (ESI+) for $C_{14}H_{11}BF_3N_2O_2$ $[M+H]^+$: *m/z* = 307.0853 (found), 307.0869 (calculated). IR (neat): *v* (cm^{-1}) = 3372, 3004, 2696, 1737, 1388, 1324.

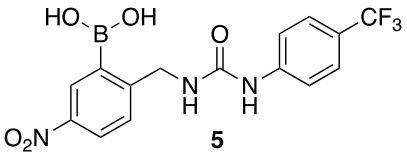

5

(5-nitro-2-((3-(4-(trifluoromethyl)phenyl)ureido)methyl) phenyl)boronic acid, (5). In a 25 mL round bottom flask equipped with a magnetic stir bar, (2-(aminomethyl)-4-nitrophenyl)boronic acid (74 mg, 0.38 mmol, 1.0 eq) and 4-(trifluoromethyl)phenyl isocyanate (160 µL, 1.12 mmol, 3.0 eq) were dissolved in 6 mL anhydrous pyridine and stirred at 60˚C for 18 hours under a N_2 atmosphere. Compound **5** was purified using the sorbitol extraction method described in the 'general procedure', yielding a pale-yellow solid (36 mg, 0.094 mmol, 25% yield). Purity (HPLC): 97.3%. ^{1}H NMR (500 MHz, DMSO-d_6, ppm) δ 9.25 (s, 1 H), 8.66 (s, 2 H), 8.37 (d, *J* = 2.5 Hz, 1 H), 8.21 (dd, *J* = 8.5, 2.5 Hz, 1 H), 7.61 – 7.55 (m, 5 H), 6.89 (t, *J* = 6.0 Hz, 1 H), 4.55 (d, *J* = 6.0 Hz, 2 H); ^{13}C NMR (101 MHz, DMSO-d_6, ppm) δ 156.0, 153.1, 146.6, 144.9, 129.4, 129.2, 126.8 (q, $^{3}J_{C\text{-}F}$ = 4.0 Hz), 125.0, 122.0 (q, $^{2}J_{C\text{-}F}$ = 32.0 Hz), 122.6 (q, $^{1}J_{C\text{-}F}$ = 271.0 Hz), 118.1, 43.8; HRMS (ESI+) for $C_{15}H_{14}BF_3N_3O_5$ $[M+H]^+$: *m/z* = 384.0971 (found), 384.0982 (calculated); IR (neat): *v* (cm^{-1}) = 3353, 1741, 1542, 1519, 1324, 1114, 1068.

(2-((3-(2-ethylhexyl)ureido)methyl)-5-nitrophenyl)boro-nic acid, (6). In a 25 mL round bottom flask equipped with a magnetic stir bar, (2-(aminomethyl)-4-nitrophenyl) boronic acid (83 mg, 0.42 mmol, 1 eq) and 2-ethylhexyl isocyanate (165 mg, 1.06 mmol, 2.52 eq) were dissolved in 6 mL anhydrous pyridine and stirred at 60˚C for 18 hours under a N_2 atmosphere. Compound **6** was purified using the sorbitol extraction method described in the 'general procedure', yielding a pale-yellow solid (45 mg, 0.13 mmol, 31% yield). Purity (HPLC): 98.2%. ^{1}H NMR (500 MHz, DMSO-d_6, ppm) δ 8.80 (s, 2 H), 8.29 (d, J = 2.5 Hz, 1 H), 8.17 (dd, J = 8.5, 2.5 Hz, 1 H), 7.53 (d, J = 8.5 Hz, 1 H), 6.56 (t, J = 6.0 Hz, 1 H), 6.11 (t, J = 6.0 Hz, 1 H), 4.37 (d, J = 6.0 Hz, 2 H), 2.94 – 2.89 (m, 2 H), 1.33 – 1.10 (m, 9 H), 0.87 – 0.76 (m, 6 H); ^{13}C NMR (75 MHz, DMSO-d_6, ppm) δ 158.7, 152.8, 145.6, 128.9, 128.0, 123.8, 42.8, 42.1, 39.3 (behind DMSO peak), 30.3, 28.3, 23.6, 22.5, 13.9, 10.8; HRMS (ESI+) for $C_{16}H_{27}BN_3O_5$ $[M+H]^+$: m/z = 352.2037 (found), 352.2047 (calculated); IR (neat): v (cm^{-1}) = 3397, 2925, 1741, 1517, 1344.

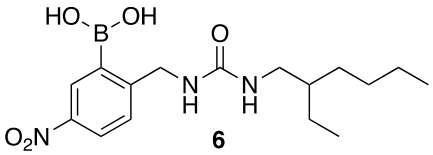

6

(3-nitro-5-(3-(4-(trifluoromethyl)phenyl)ureido)phenyl)boron-ic acid, (7). In a 25 mL round bottom flask equipped with a magnetic stir bar, (3-amino-5-nitrophenyl)boronic acid, hydrochloric acid (98 mg, 0.45 mmol, 1 eq) and 4-(trifluoro-methyl)phenyl isocyanate (200 µL, 1.40 mmol, 3.1 eq) were dissolved in 6 mL anhydrous pyridine and stirred at 60˚C for 18 hours under a N_2 atmosphere. Compound **7** was purified using the sorbitol extraction method described in the 'general procedure', yielding a pale-yellow solid (120 mg, 0.325 mmol, 72% yield). Purity (HPLC): 97.4%. ^{1}H NMR (500 MHz, DMSO-d_6, ppm) δ 9.31 (s, 1 H), 9.26 (s, 1 H), 8.65 (t, J = 2.0 Hz, 1 H), 8.51 (s, 2 H), 8.28 (d, J = 2.0, 1 H), 8.00 (d, J = 2.0 Hz, 1 H), 7.75 – 7.61 (m, 4 H); ^{13}C NMR (75 MHz, DMSO-d_6, ppm) δ 152.3, 147.8, 143.1, 140.0, 130.2, 124.5 (q, $^1J_{C\text{-}F}$ = 272.0 Hz), 126.1 (q, $^3J_{C\text{-}F}$ = 4.0 Hz), 122.5 (q, $^2J_{C\text{-}F}$ = 32.0 Hz), 121.8, 118.2, 113.9; HRMS (ESI+) for $C_{14}H_{12}BF_3N_3O_5$ $[M+H]^+$: m/z = 370.0835 (found), 370.0825 (calculated); IR (neat): v (cm^{-1}) = 3322, 2969, 1739, 1369, 1328, 1216.

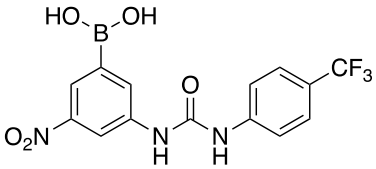

7

(3-(3-(2-ethylhexyl)ureido)-5-nitrophenyl)boronic acid, (8). In a 25 mL round bottom flask equipped with a magnetic stir bar, 3-amino-5-nitrophenyl)boronic acid, hydrochloric acid (98 mg, 0.45 mmol, 1 eq) and 2-ethylhexyl isocyanate (186 µL, 1.06 mmol, 2.36 eq) were dissolved in 6 mL anhydrous pyridine and stirred at 60˚C for 18 hours under a N_2 atmosphere. Compound **8** was purified using the sorbitol extraction method described in the 'general procedure', yielding a pale-yellow solid (75 mg, 0.22 mmol, 49% yield). Purity (HPLC): 97.5%. ^{1}H NMR (500 MHz, DMSO-d_6, ppm) δ 8.84 (s, 1 H), 8.63 (t, J = 2.5 Hz, 1 H), 8.37 (s, 2 H), 8.17 (d, J = 2.5 Hz, 1 H), 7.86 (d, J = 2.5 Hz, 1 H), 6.21 (t, J = 6.0 Hz, 1 H), 3.16 – 2.99 (m, 2 H), 1.49 – 1.35 (m, 1 H), 1.36 – 1.20 (m, 8 H), 0.94 – 0.82 (m, 6 H); ^{13}C NMR (75 MHz, DMSO-d_6, ppm) δ 155.1, 147.8, 141.2, 129.2, 120.6, 112.8, 41.7, 39.3 (behind DMSO peak), 30.4, 28.4, 23.7, 22.5, 14.0, 10.8; HRMS (ESI+) for $C_{15}H_{25}BN_3O_5$ $[M+H]^+$: m/z = 338.1881 (found), 338.1890 (calculated); IR (neat): v (cm^{-1}) = 3299, 2929, 2857, 1737, 1556, 1521, 1336.

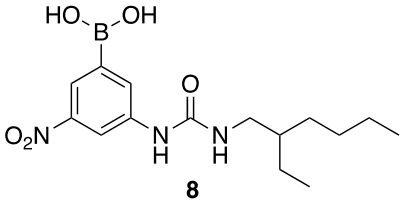

8

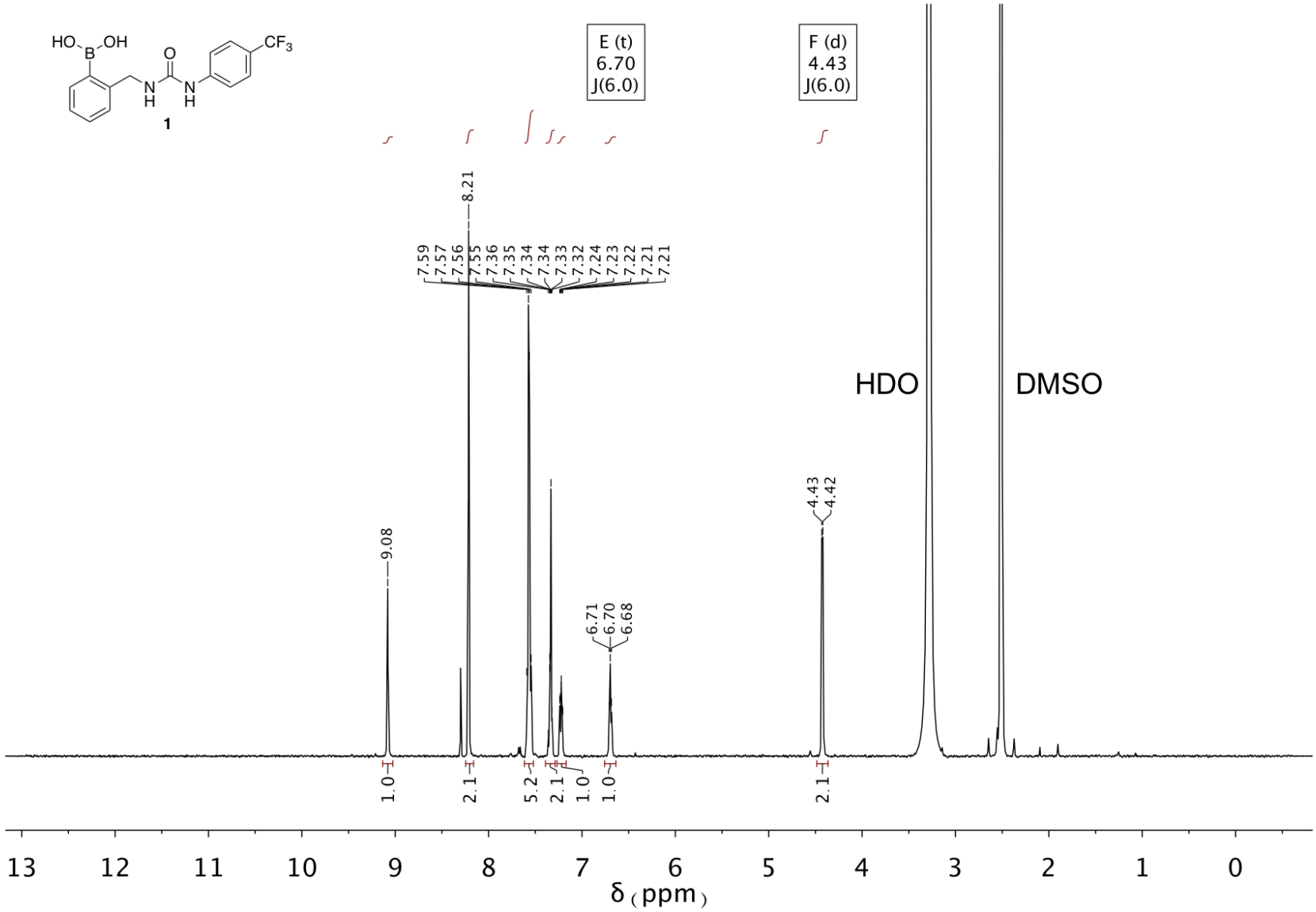

Figure S1. ^{1}H NMR (500 MHz) spectrum of compound **1** in 99.5% DMSO-d_6 : 0.5% H_2O at 310 K.

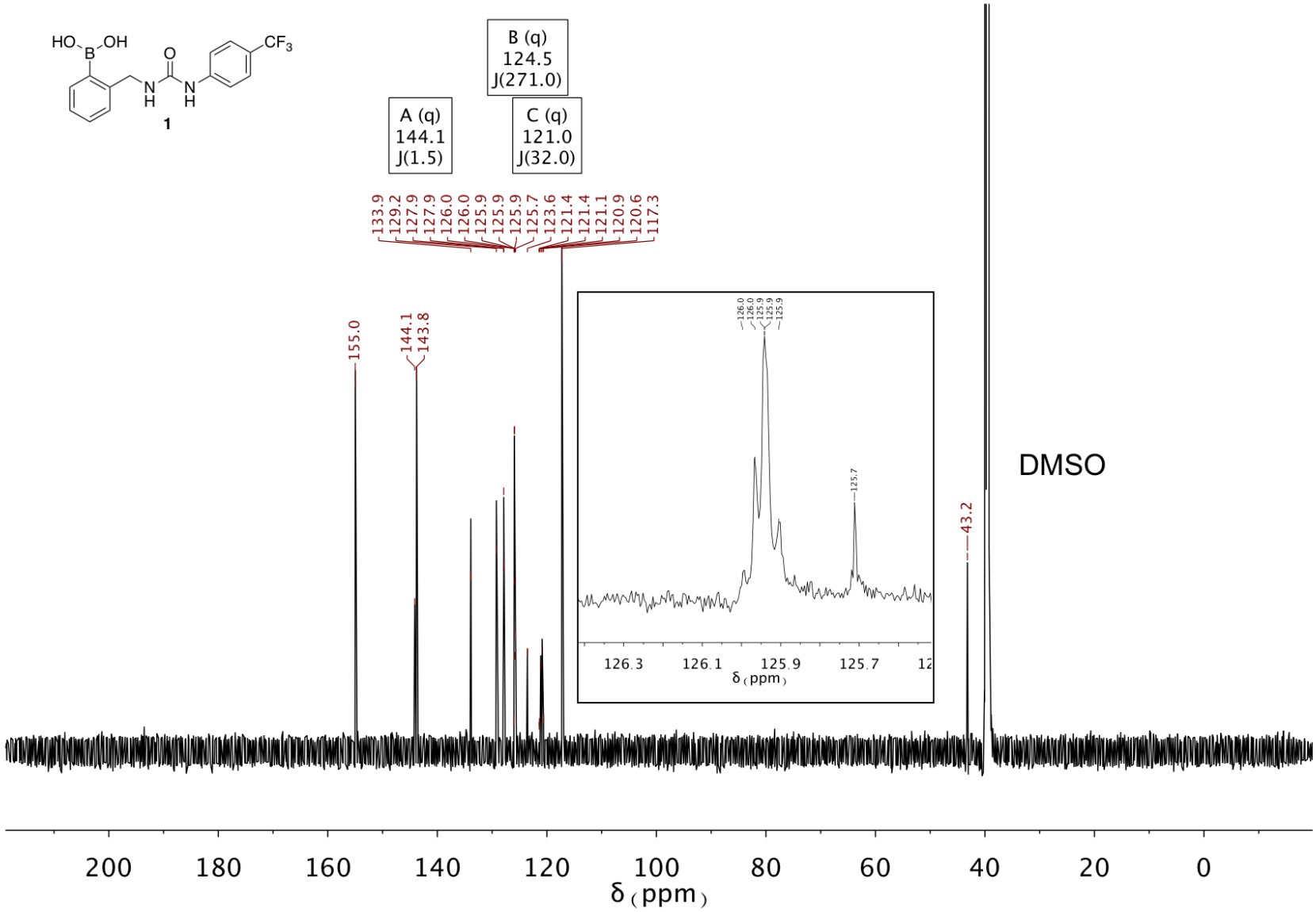

Figure S2. ^{13}C NMR (126 MHz) spectrum of compound **1** in 99.5% DMSO-d_6 : 0.5% H_2O at 298 K.

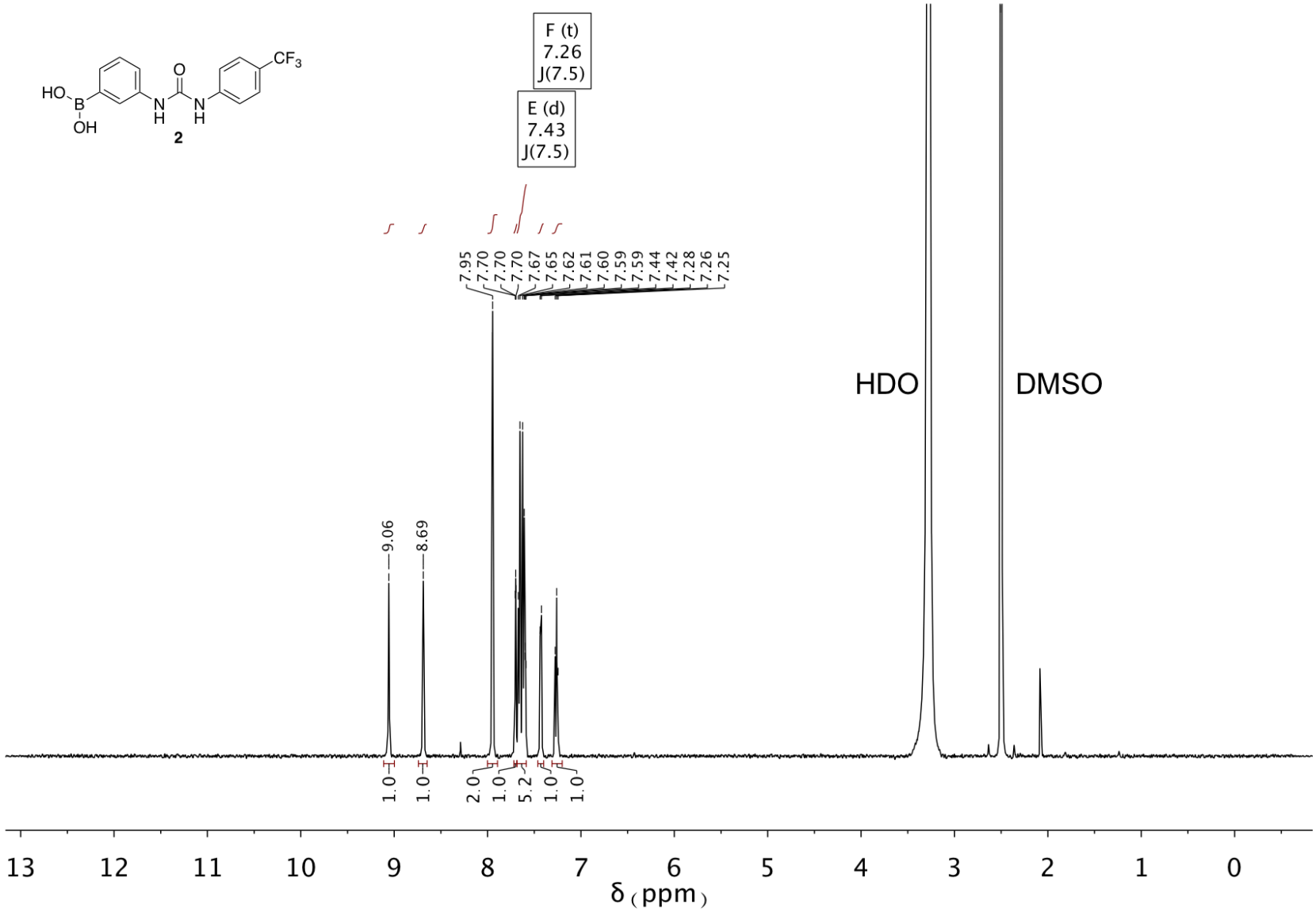

Figure S3. ^{1}H NMR (500 MHz) spectrum of compound **2** in 99.5% DMSO-d_6 : 0.5% H_2O at 310 K.

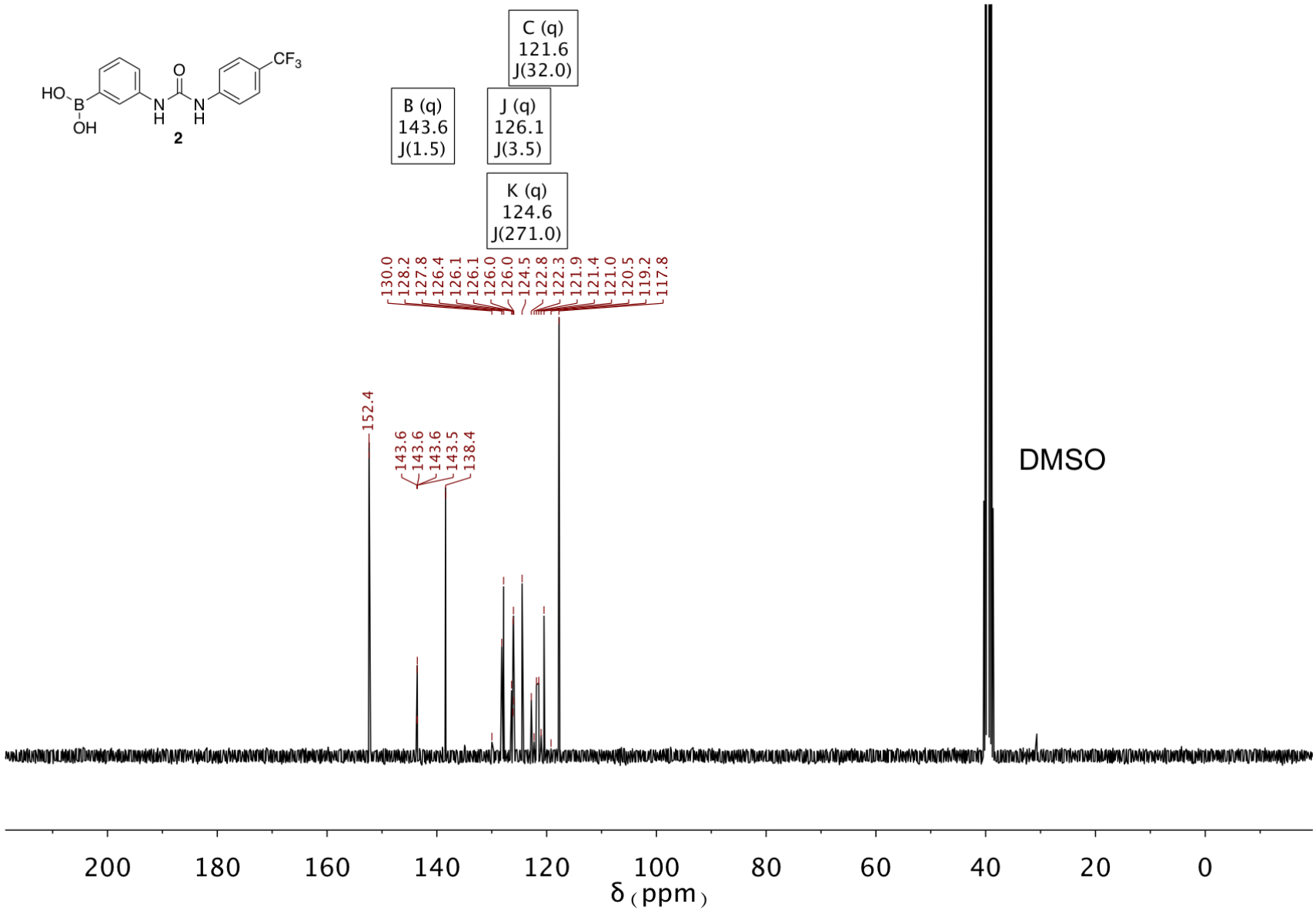

Figure S4. ^{13}C NMR (75 MHz) spectrum of compound **2** in 99.5% DMSO-d_6 : 0.5% H_2O at 298 K.

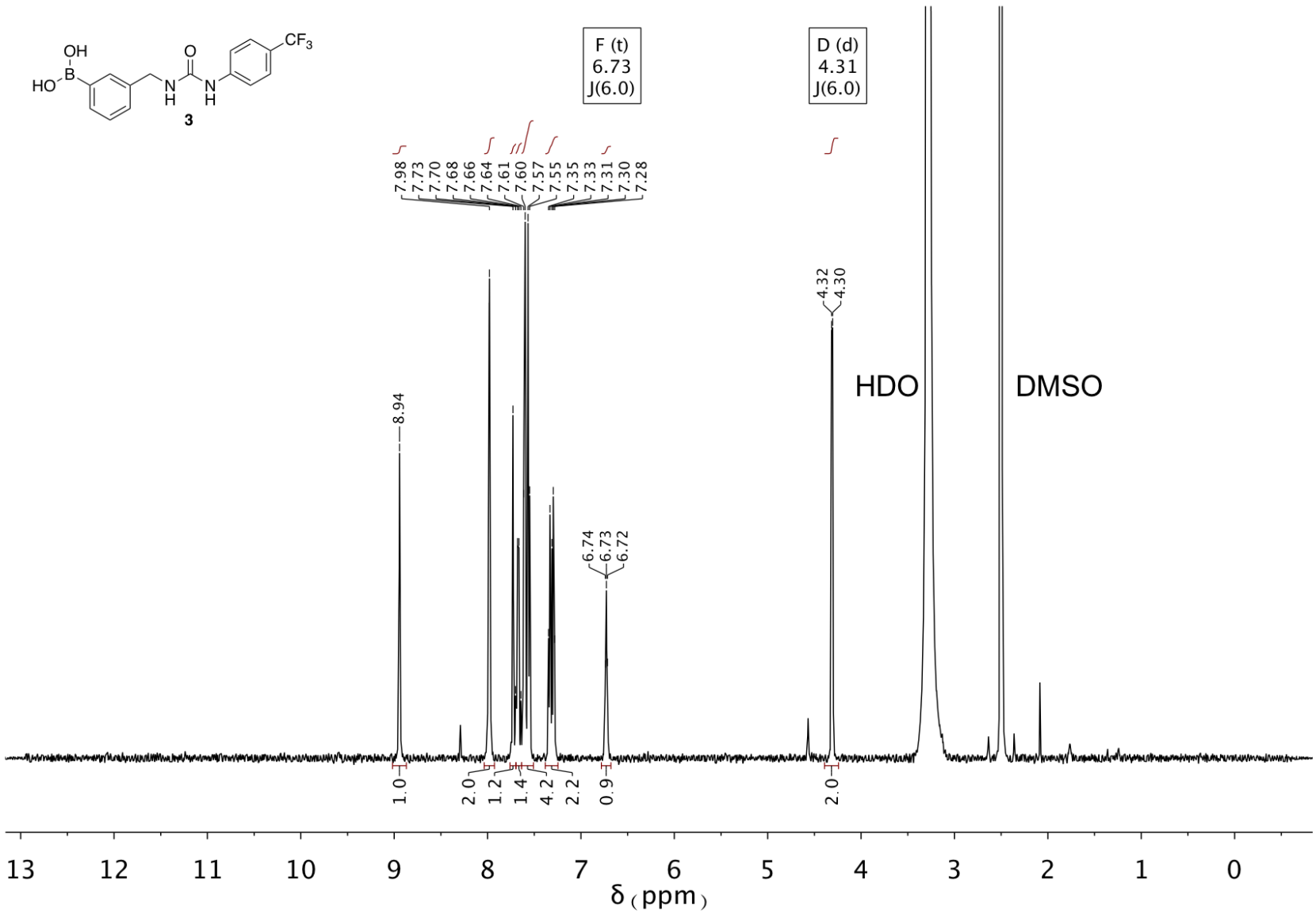

Figure S5. ^{1}H NMR (500 MHz) spectrum of compound **3** in 99.5% DMSO-d_6 : 0.5% H_2O at 310 K.

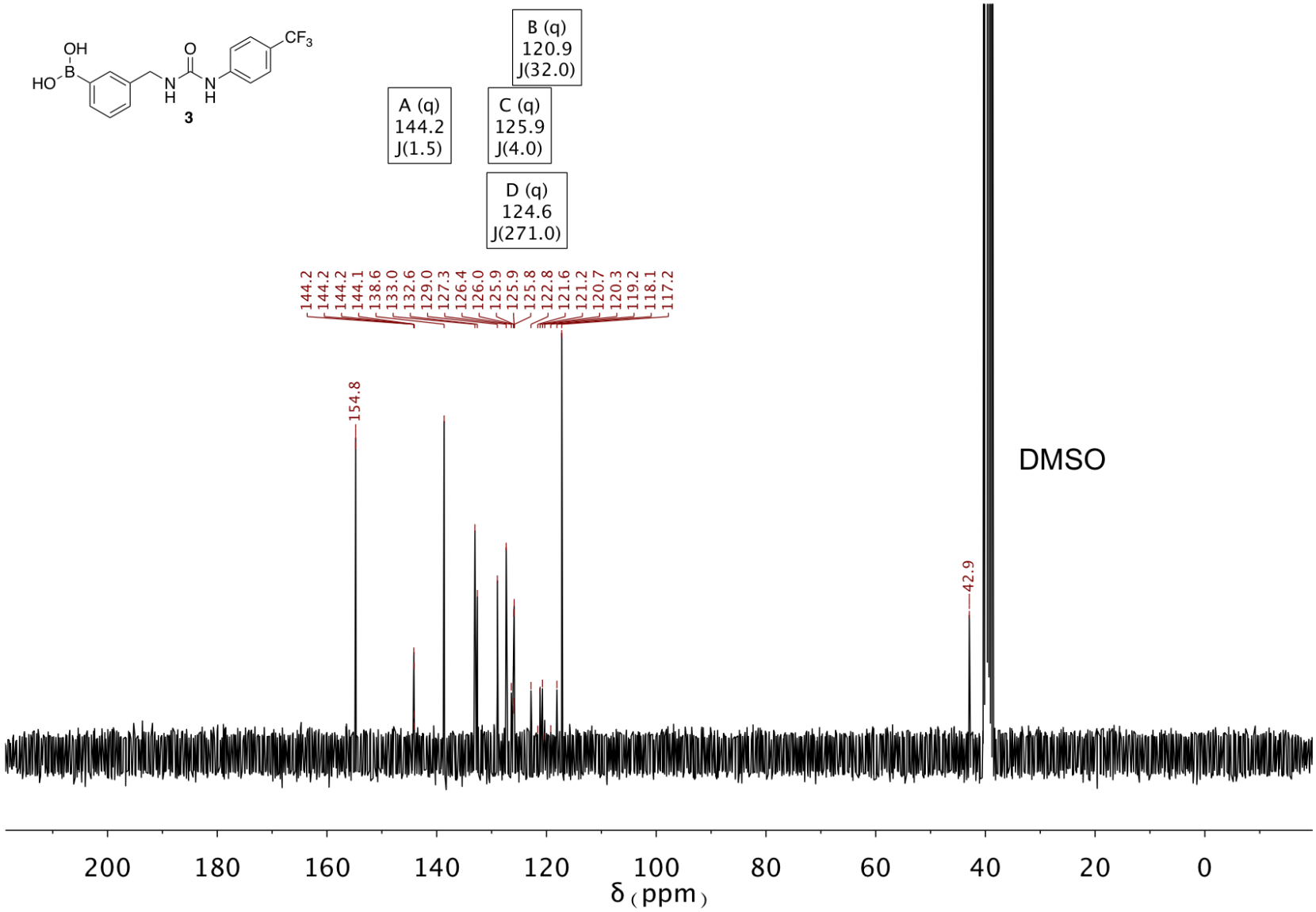

Figure S6. ^{13}C NMR (75 MHz) spectrum of compound **3** in 99.5% DMSO-d_6 : 0.5% H_2O at 298 K.

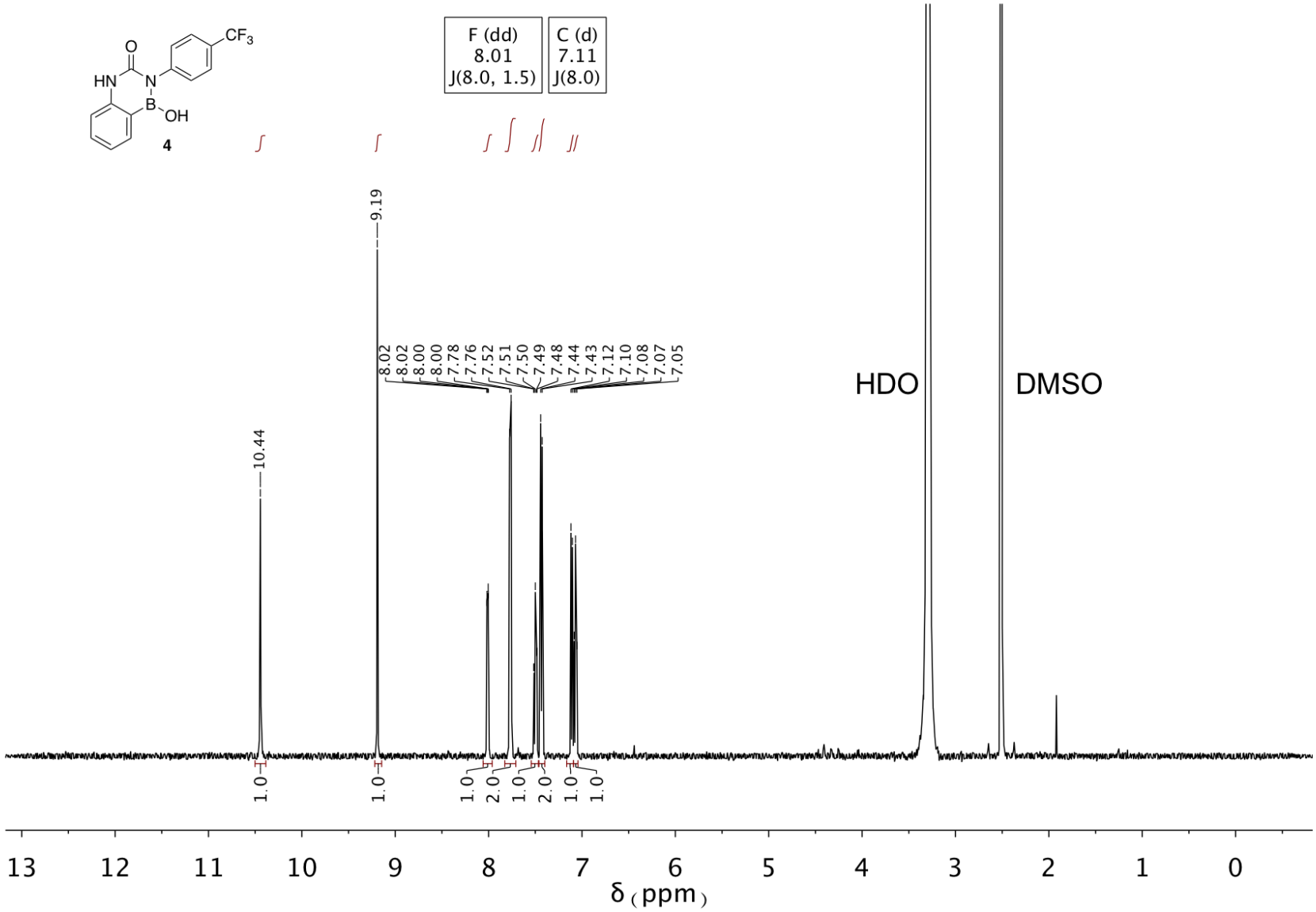

Figure S7. ^{1}H NMR (500 MHz) spectrum of compound **4** in 99.5% DMSO-d_6 : 0.5% H_2O at 310 K.

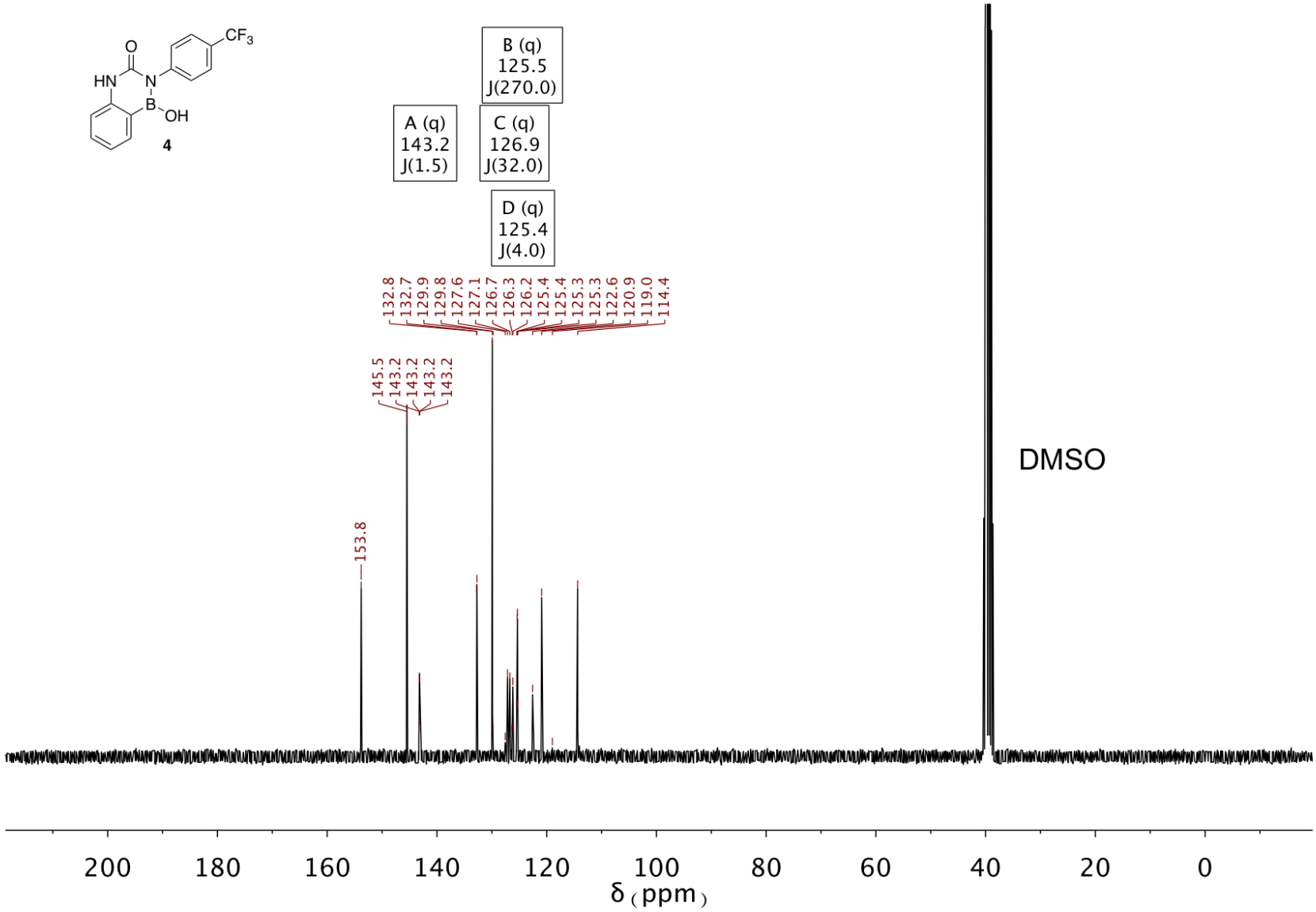

Figure S8. ^{13}C NMR (75 MHz) spectrum of compound **4** in 99.5% DMSO-d_6 : 0.5% H_2O at 298 K.

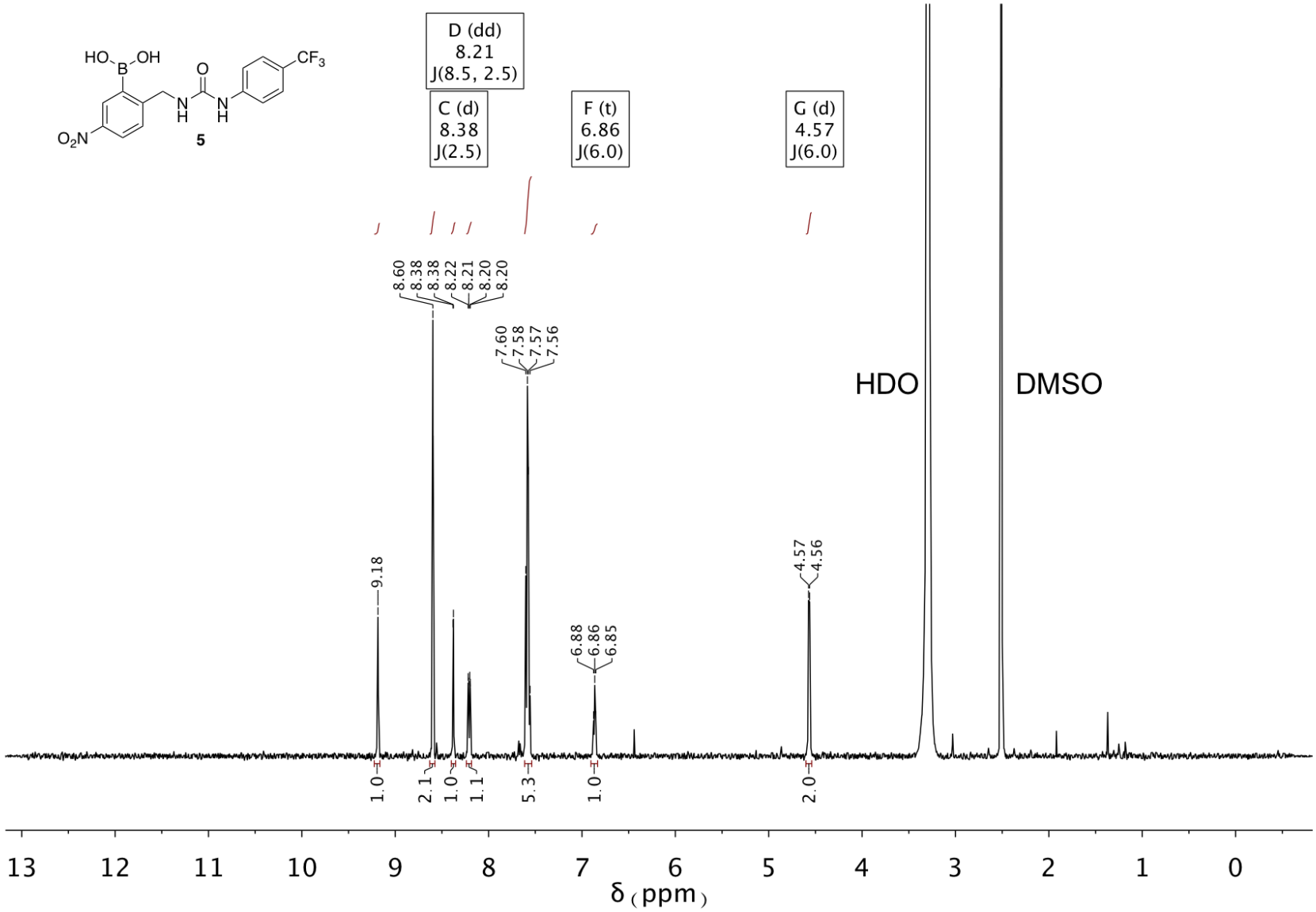

Figure S9. ^{1}H NMR (500 MHz) spectrum of compound **5** in 99.5% DMSO-d_6 : 0.5% H_2O at 310 K.

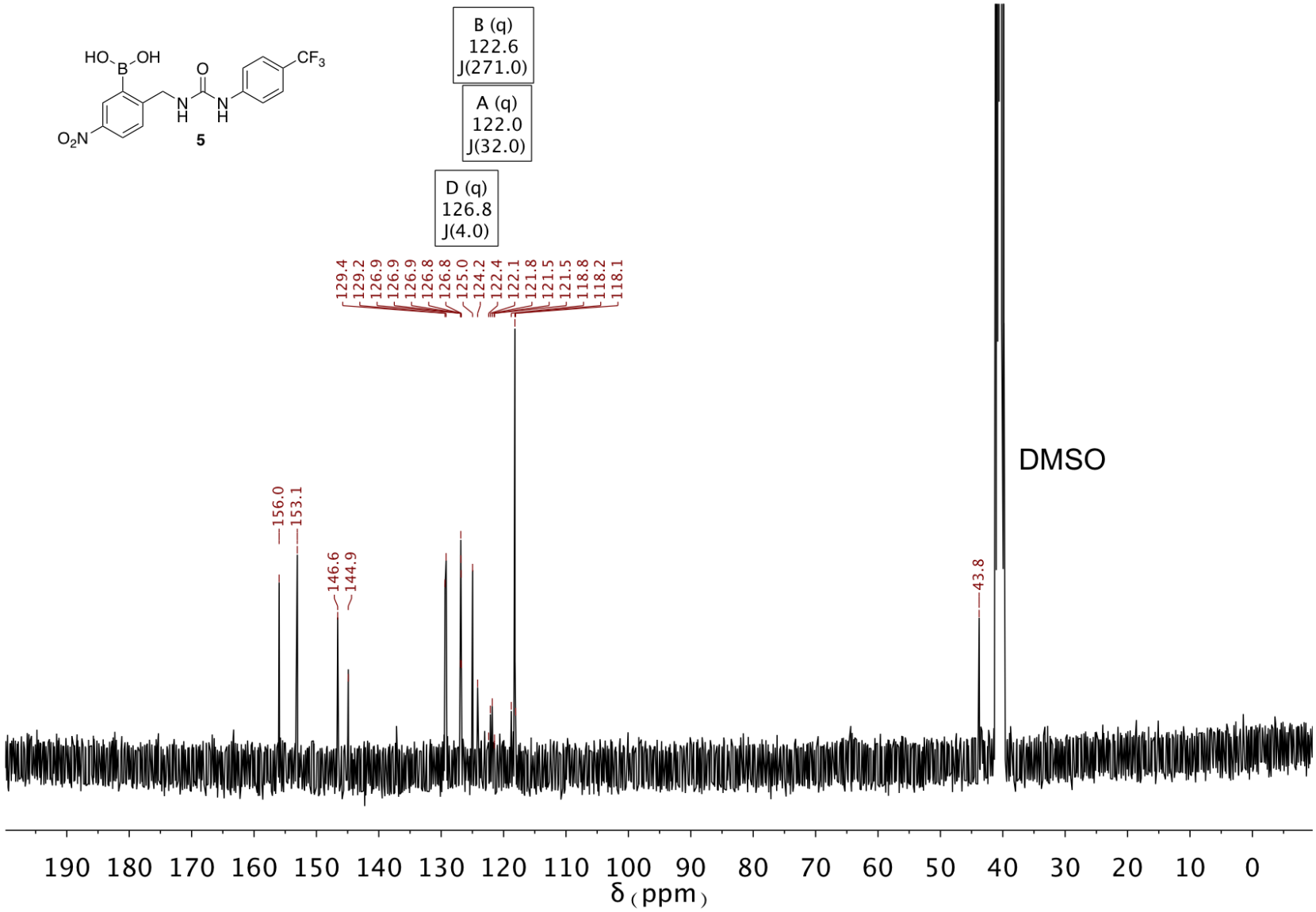

Figure S10. ^{13}C NMR (100 MHz) spectrum of compound **5** in 99.5% DMSO-d_6 : 0.5% H_2O at 298 K.

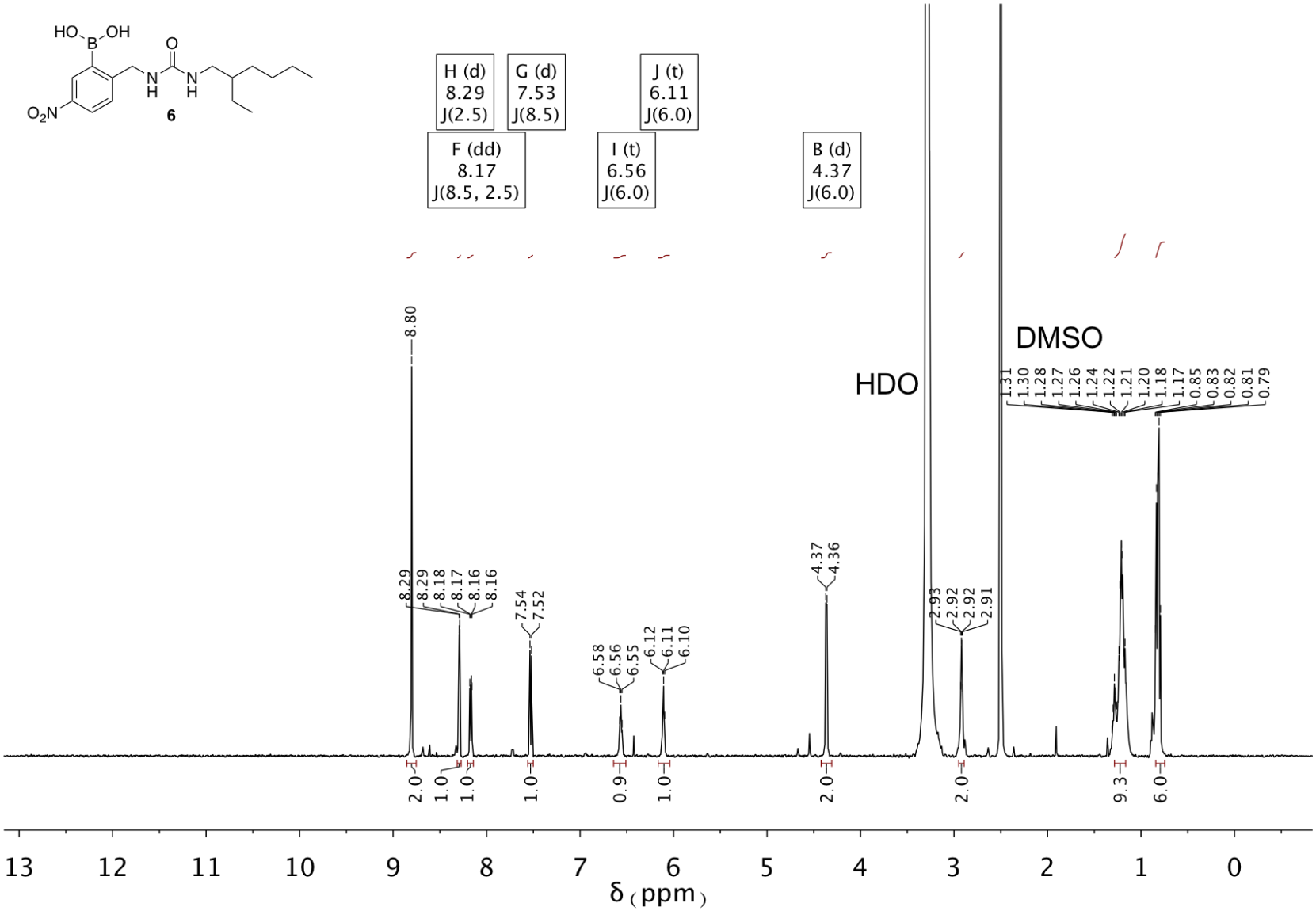

Figure S11. ^{1}H NMR (500 MHz) spectrum of compound **6** in 99.5% DMSO-d_6 : 0.5% H_2O at 310 K.

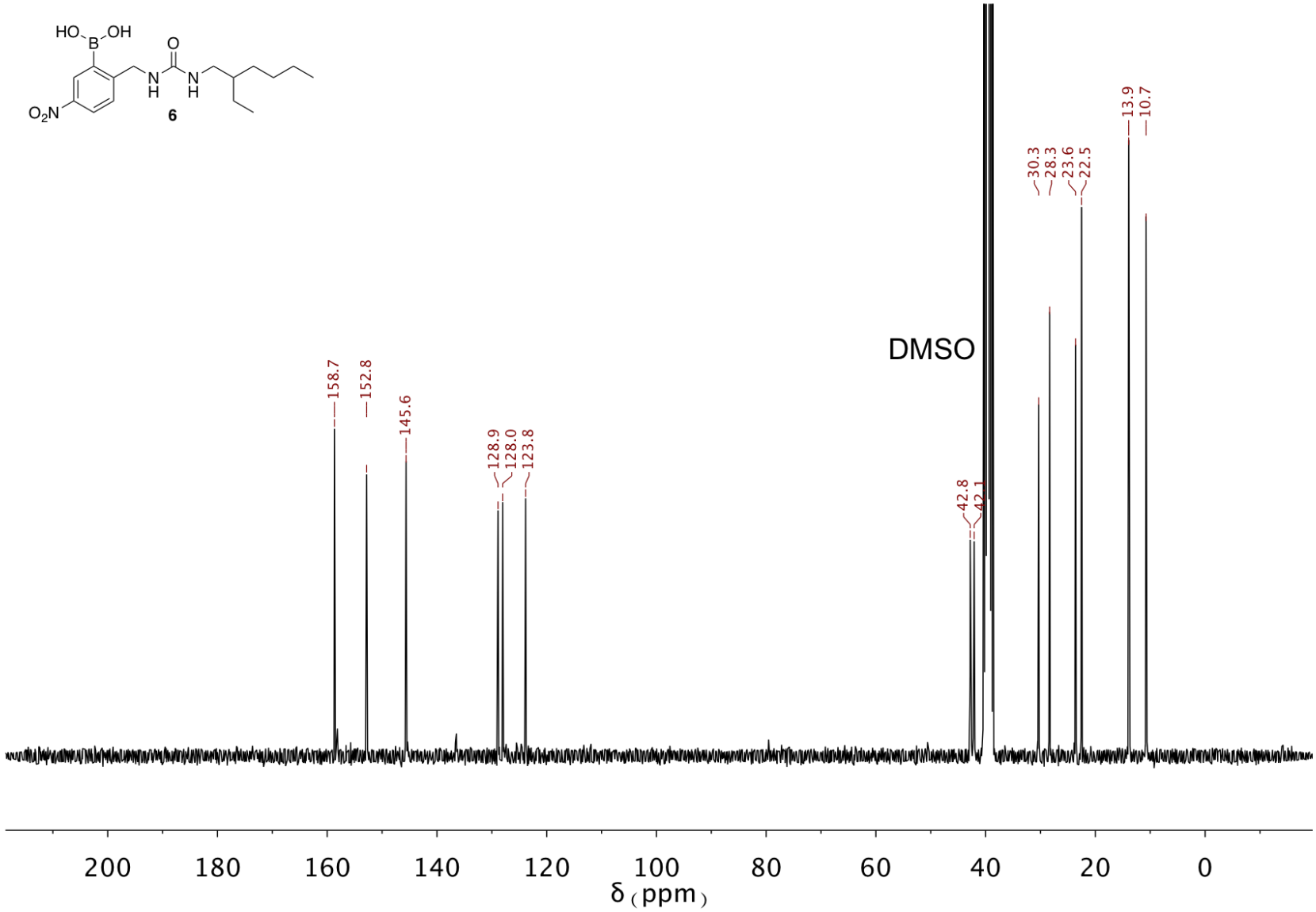

Figure S12. ^{13}C NMR (75 MHz) spectrum of compound **6** in 99.5% DMSO-d_6 : 0.5% H_2O at 298 K.

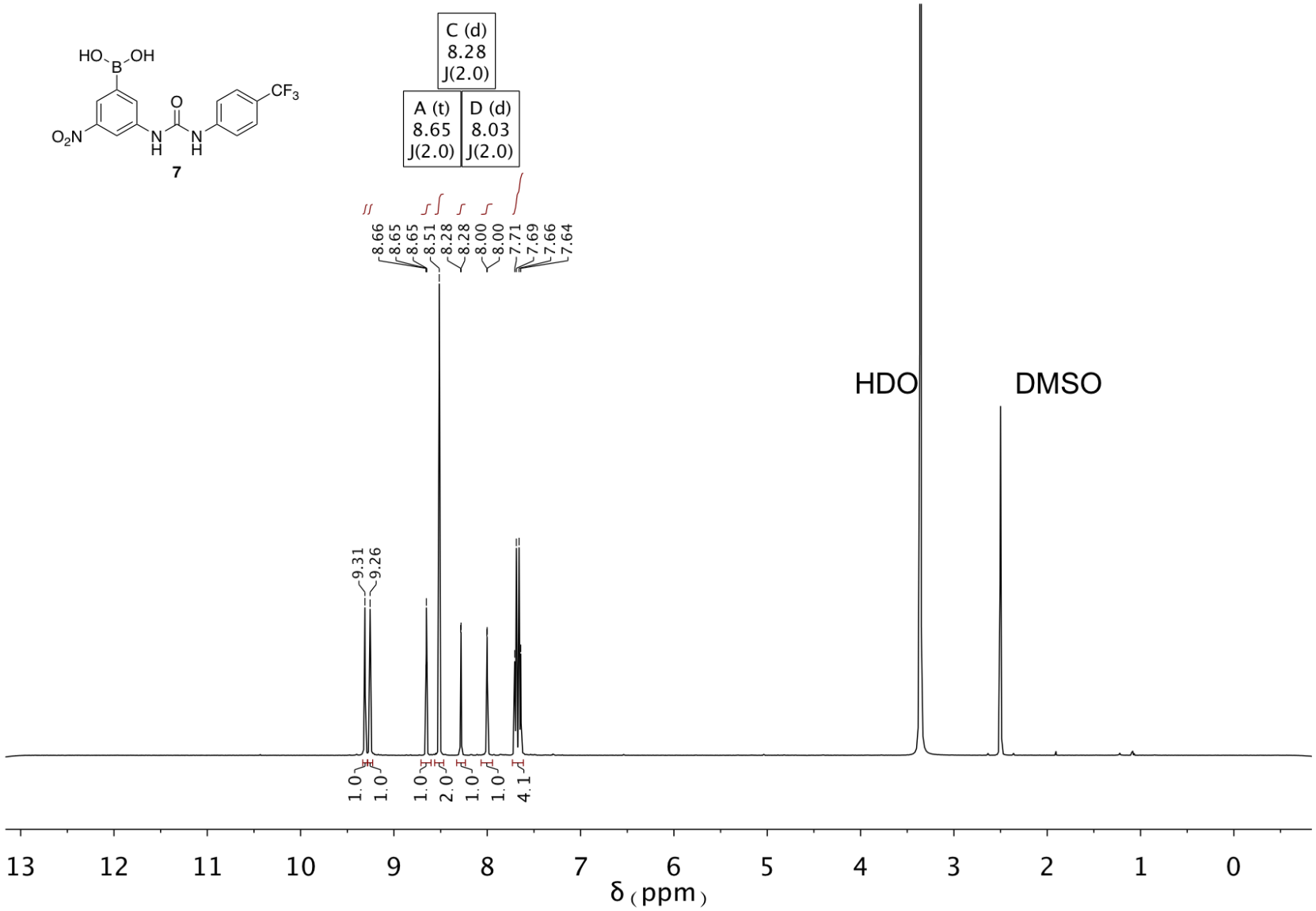

Figure S13. ^{1}H NMR (500 MHz) spectrum of compound **7** in 99.5% DMSO-d_6 : 0.5% H_2O at 310 K.

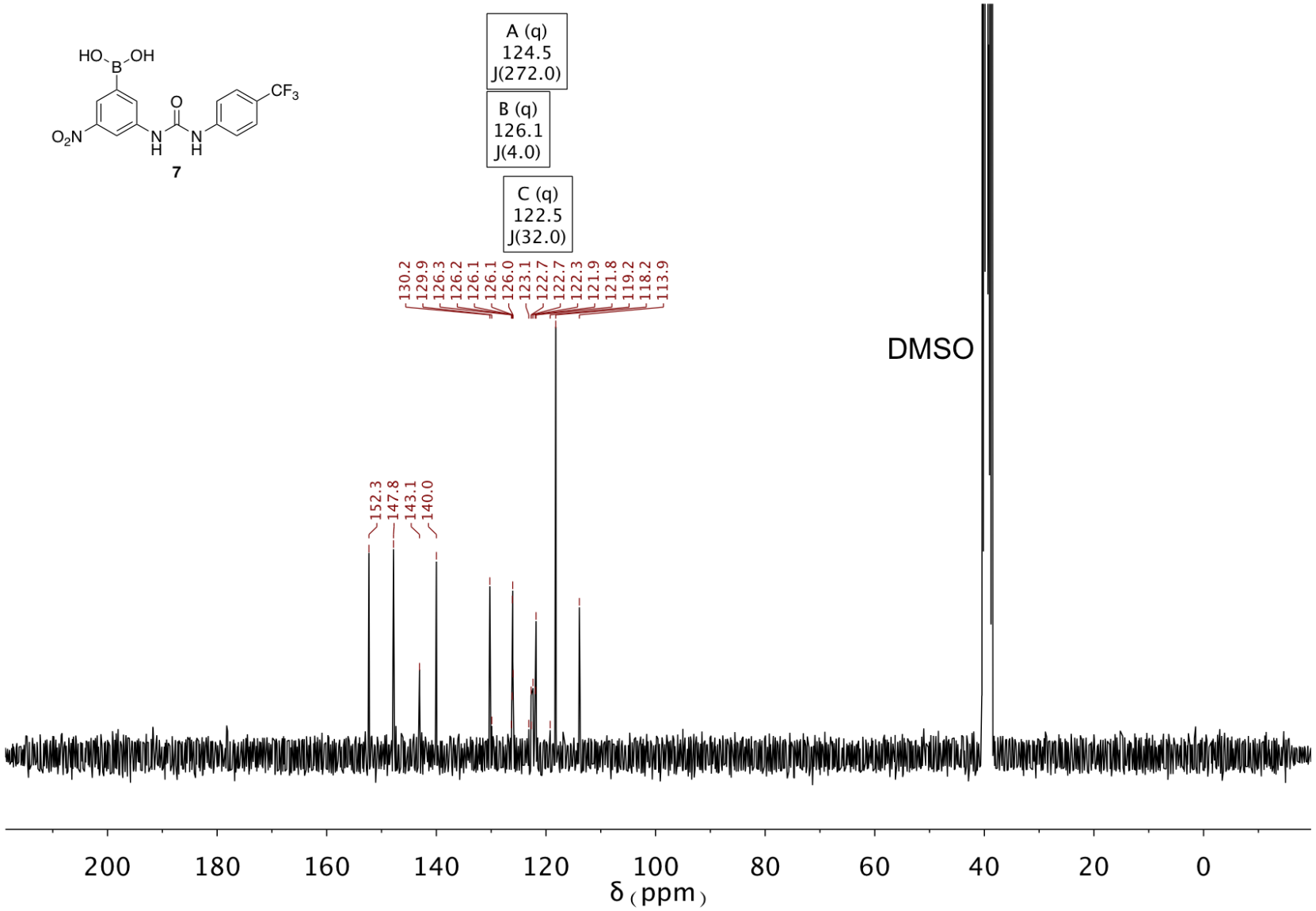

Figure S14. ^{13}C NMR (75 MHz) spectrum of compound **7** in 99.5% DMSO-d_6 : 0.5% H_2O at 298 K

.

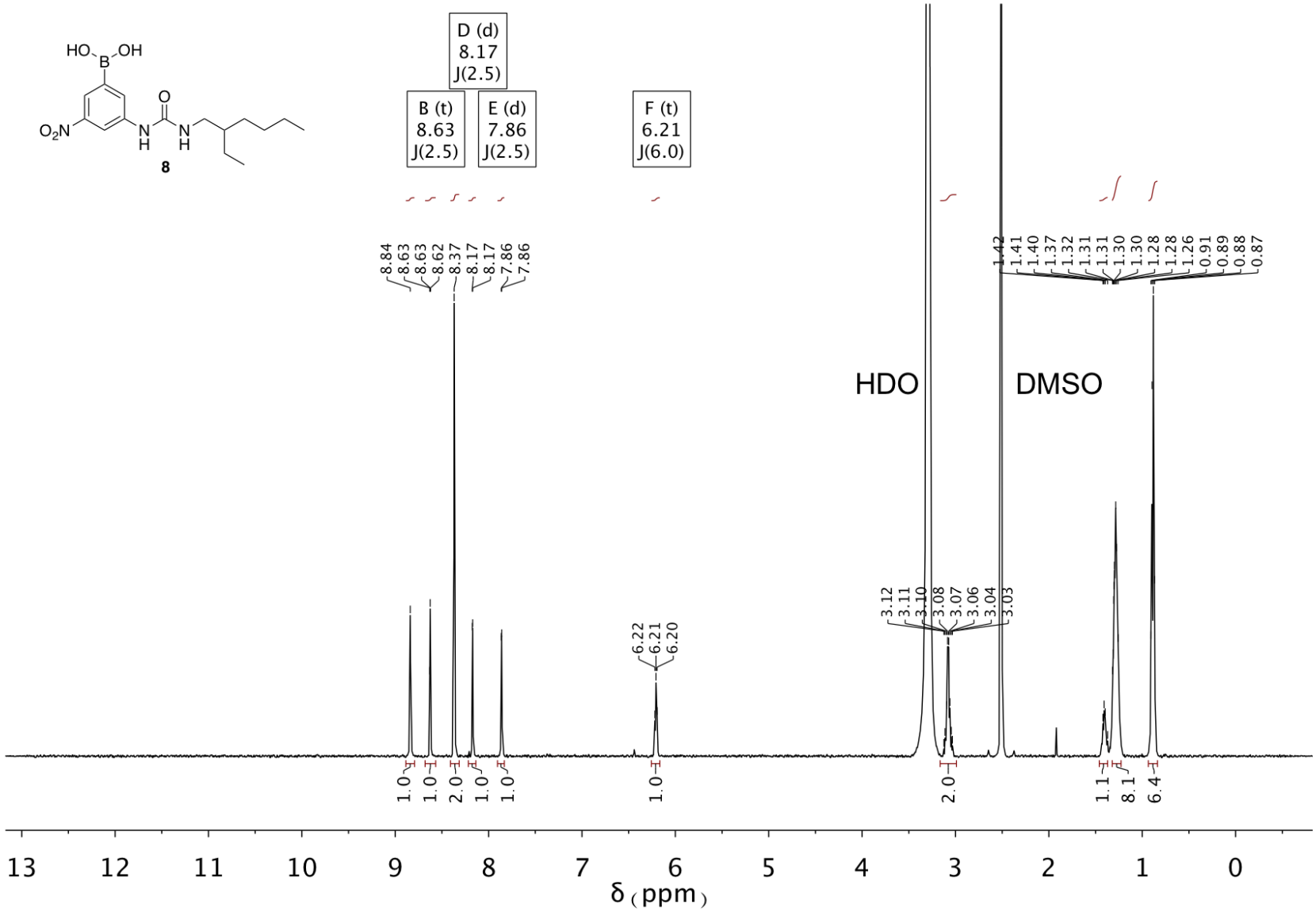

Figure S15. ^{1}H NMR (500 MHz) spectrum of compound **8** in 99.5% DMSO-d_6 : 0.5% H_2O at 310 K.

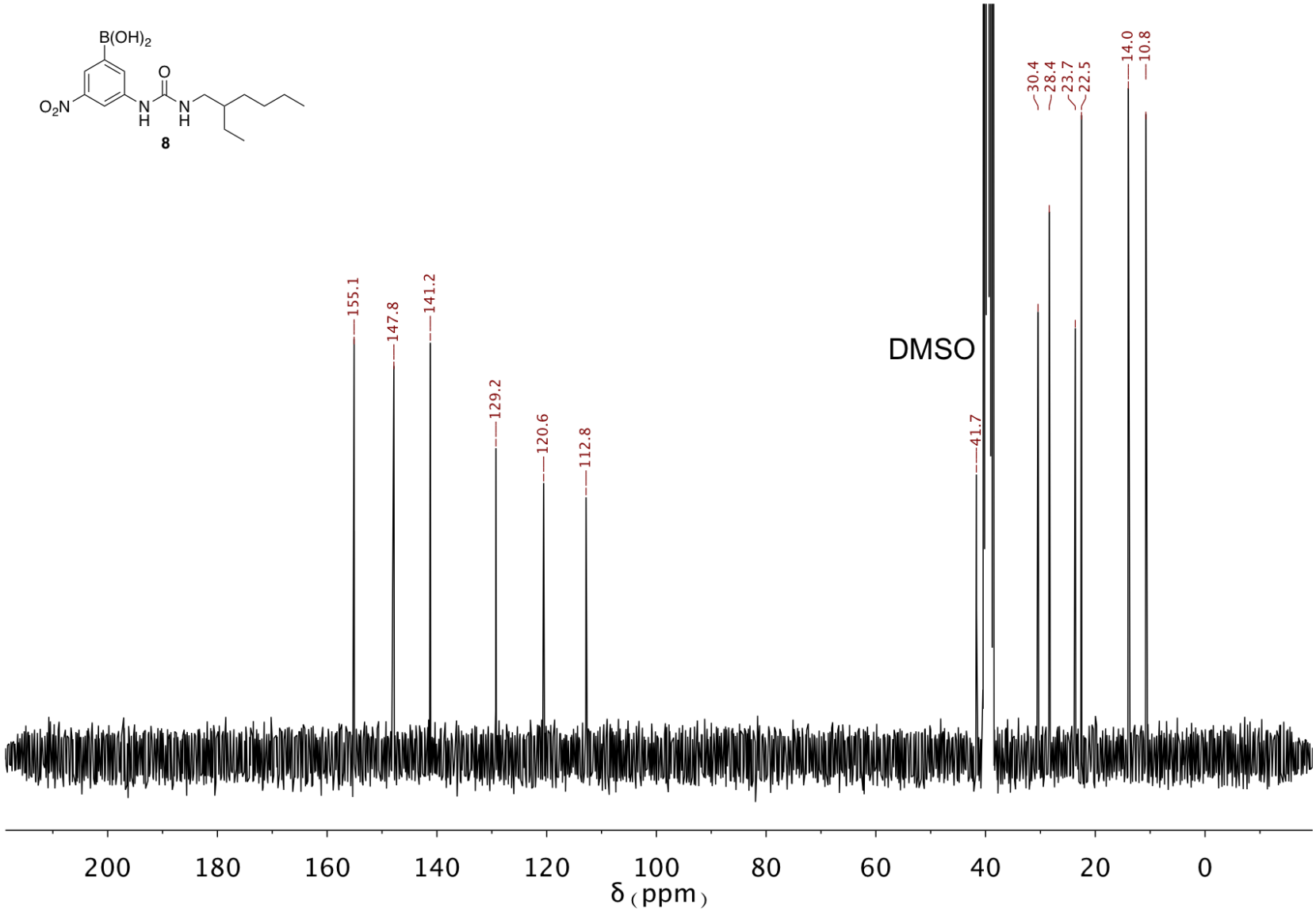

Figure S16. ^{13}C NMR (75 MHz) spectrum of compound **8** in 99.5% DMSO-d_6 : 0.5% H_2O at 298

S3. Determination of pK_a

We determined the pK_a of each boronic acid to quantify the Lewis acidity and thus the amount of activation for exchange with *cis*-1,2 diols. A 100 µM solution of each boronic acid (BA) was dissolved in a solution of 25% acetonitrile and 75% buffer (75 mM phosphate buffer). The pH of the solution was recorded and 500 µL was transferred to a microcuvette with 2 mm pathlength and the absorbance spectrum was measured using an Agilent Cary 100 UV-Vis spectrophotometer. Next, aliquots of a NaOH solution were added to increase the pH by approximately 0.1 units per addition. The resultant change in pH was recorded and the new absorbance spectrum was measured. This was repeated until pH ≈ 11. Next, an absorbance ratio of two independent wavelength vs pH was plotted in OriginPro 2018b (b9.5.5.409 (Academic)) and fitted with a sigmoidal curve.[2] The inflection point of the sigmoidal curve (LOGx0) was taken as the pK_a value. The experiment was performed in triplicate to estimate experimental error. For control compound phenylboronic acid (**PBA**), a trial with 75 mM phosphate buffer was used to adjust the obtained pK_a's to a system without acetonitrile. The pK_a of unsubstituted phenylboronic acid (**PBA**) was found to be 8.87 in 100% aqueous phosphate buffer (in agreement with previous literature reports),[3, 4] and 9.64 in 25% acetonitrile, 75% phosphate buffer. The difference between these two pK_a values of **PBA** (ΔpK_a = 0.77) was subtracted from the experimental pK_a values of **1-8** to find the adjusted values estimated as the pK_a in 100% aqueous solutions. A table with the obtained pK_a values is given in the main manuscript. The obtained graphs are shown in **Figure S17** - **Figure S26**.

(a)

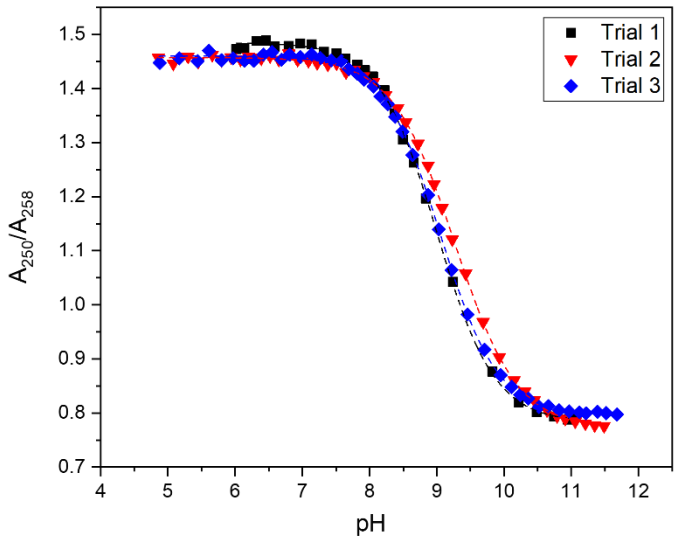

(b)

Model	DoseResp		
Equation	y = A1 + (A2-A1)/(1 + 10^((LOGx0-x)*p))		
Trial	1	2	3
A1	0.78 ± 0.00	0.77 ± 0.00	0.80 ± 0.00
A2	1.48 ± 0.00	1.46 ± 9.11E-04	1.46 ± 0.00
LOGx0	9.00 ± 0.01	9.27 ± 0.01	9.06 ± 0.01
Adj. R-Square	0.99955	0.9998	0.99966

(c)

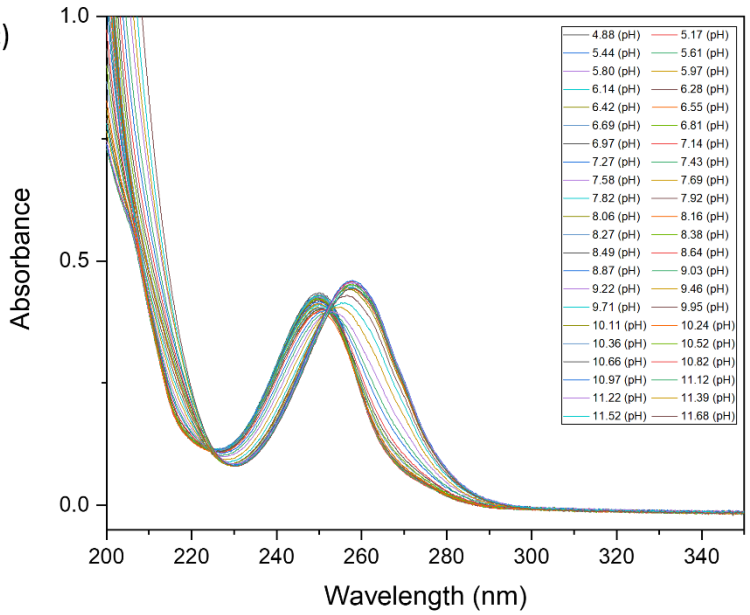

Figure S17. pK_a determination of **1** in 25% acetonitrile : 75% buffer (75 mM phosphate buffer). The pH was adjusted with dilute NaOH. (a) Graph of pH vs A_{250}/A_{258} for **1**. Dashed lines represent the fit of each graph using the DoseResp model in OriginPro 2018b. Three independent repeats were conducted. (b) Chart of the fitted curve include information on the calculated parameters, quality of the fit, and pK_a (LOGx0) for each trial. (c) Absorbance spectra of 100 µM **1** in 25% acetonitrile and 75% buffer (75 mM phosphate buffer) at various pH (representative repeat).

(a)

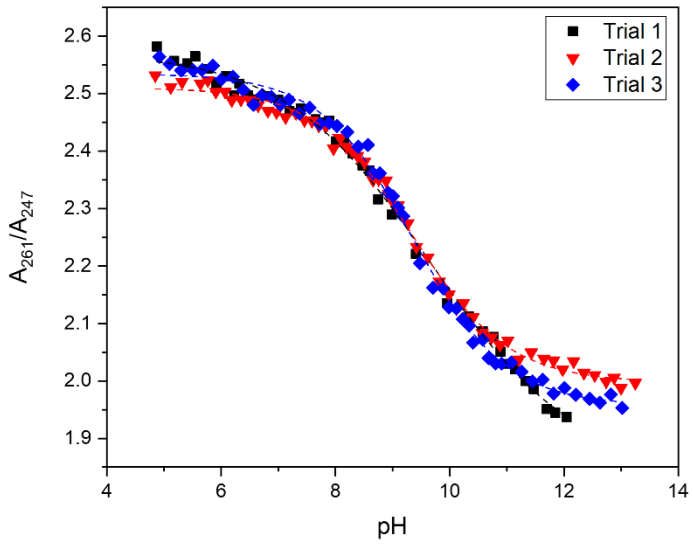

(b)

Model	DoseResp		
Equation	y = A1 + (A2-A1)/(1 + 10^((LOGx0-x)*p))		
Trial	1	2	3
A1	1.84 ± 0.03	2.00 ± 0.00	1.96 ± 0.01
A2	2.57 ± 0.01	2.51 ± 0.00	2.53 ± 0.01
LOGx0	9.67 ± 0.12	9.35 ± 0.03	9.37 ± 0.04
Adj. R-Square	0.99534	0.99658	0.99548

(c)

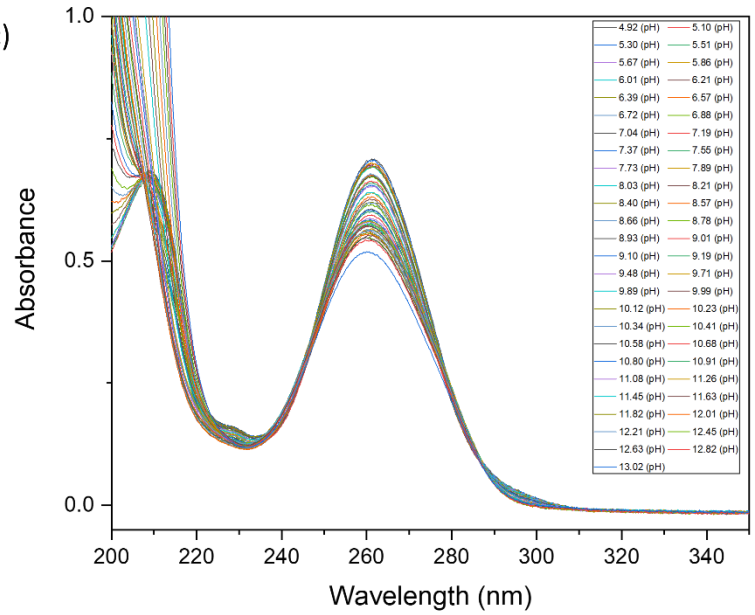

Figure S18. pK_a determination of **2** in 25% acetonitrile : 75% buffer (75 mM phosphate buffer). The pH was adjusted with dilute NaOH. (a) Graph of pH vs A_{261}/A_{247} for **2**. Dashed lines represent the fit of each graph using the DoseResp model in OriginPro 2018b. Three independent repeats were conducted. (b) Chart of the fitted curve include information on the calculated parameters, quality of the fit, and pK_a (LOGx0) for each trial. (c) Absorbance spectra of 100 µM **2** in 25% acetonitrile and 75% buffer (75 mM phosphate buffer) at various pH (representative repeat).

(a)

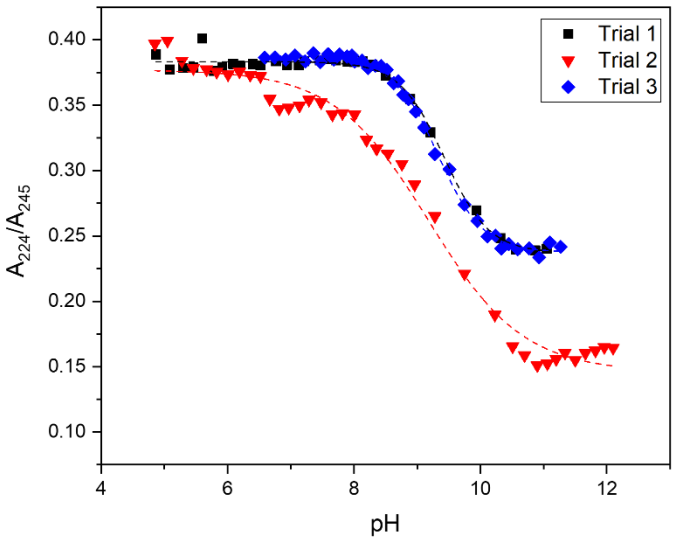

(b)

Model	DoseResp		
Equation	y = A1 + (A2-A1)/(1 + 10^((LOGx0-x)*p))		
Trial	1	2	3
A1	0.24 ± 0.00	0.15 ± 0.01	0.24 ± 0.00
A2	0.38 ± 0.00	0.38 ± 0.00	0.39 ± 9.82E-04
LOGx0	9.43 ± 0.05	9.18 ± 0.08	9.32 ± 0.02
Adj. R-Square	0.99076	0.98622	0.9971

(c)

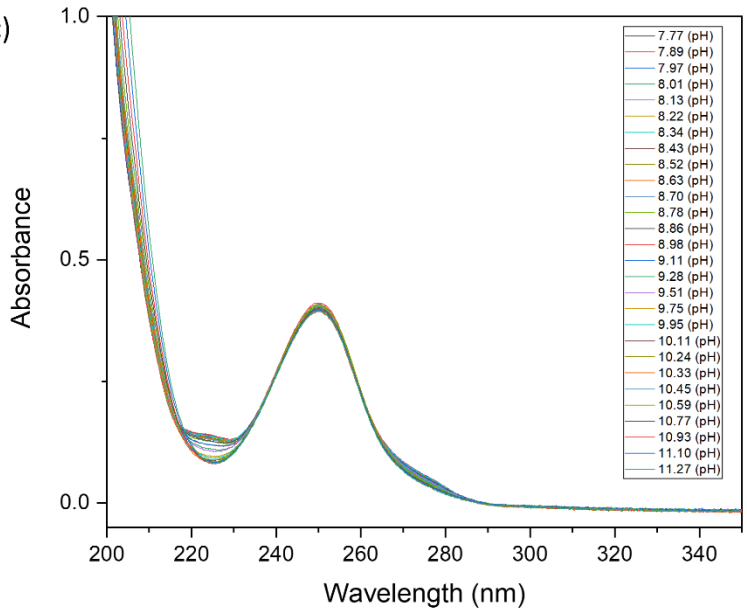

Figure S19. pK_a determination of **3** in 25% acetonitrile : 75% buffer (75 mM phosphate buffer). The pH was adjusted with dilute NaOH. (a) Graph of pH vs A_{224}/A_{245} for **3**. Dashed lines represent the fit of each graph using the DoseResp model in OriginPro 2018b. Three independent repeats were conducted. (b) Chart of the fitted curve include information on the calculated parameters, quality of the fit, and pK_a (LOGx0) for each trial. (c) Absorbance spectra of 100 µM **3** in 25% acetonitrile and 75% buffer (75 mM phosphate buffer) at various pH (representative repeat).

(a)

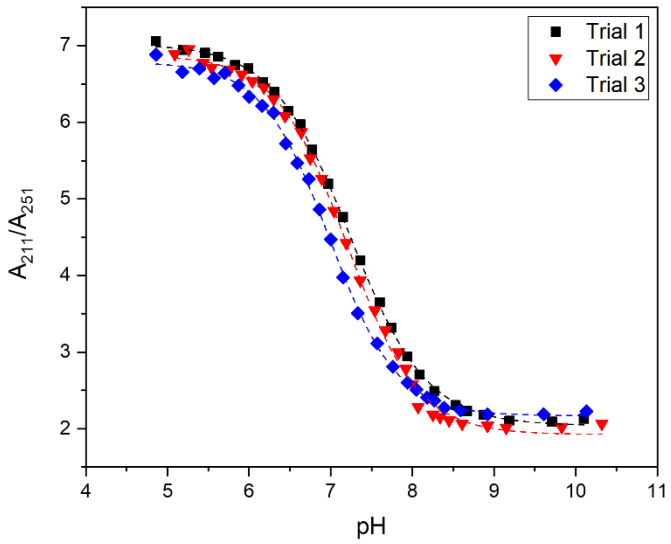

(b)

Model	DoseResp		
Equation	y = A1 + (A2-A1)/(1 + 10^((LOGx0-x)*p))		
Trial	1	2	3
A1	2.04 ± 0.02	1.93 ± 0.04	2.17 ± 0.03
A2	7.02 ± 0.02	6.88 ± 0.04	6.79 ± 0.03
LOGx0	7.23 ± 0.01	7.20 ± 0.02	6.99 ± 0.01
Adj. R-Square	0.99969	0.99807	0.99909

(c)

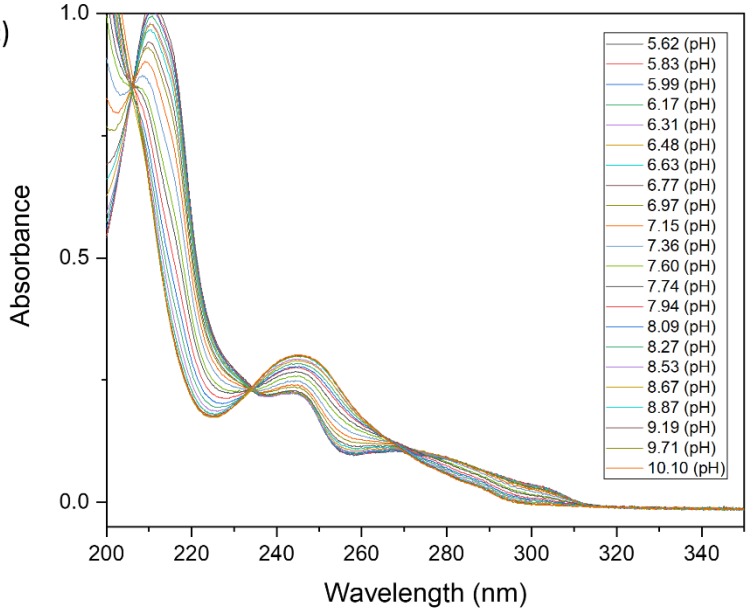

Figure S20. pK_a determination of **4** in 25% acetonitrile : 75% buffer (75 mM phosphate buffer). The pH was adjusted with dilute NaOH. (a) Graph of pH vs A_{211}/A_{251} for **4**. Dashed lines represent the fit of each graph using the DoseResp model in OriginPro 2018b. Three independent repeats were conducted. (b) Chart of the fitted curve include information on the calculated parameters, quality of the fit, and pK_a (LOGx0) for each trial. (c) Absorbance spectra of 100 µM **4** in 25% acetonitrile and 75% buffer (75 mM phosphate buffer) at various pH (representative repeat).

(a)

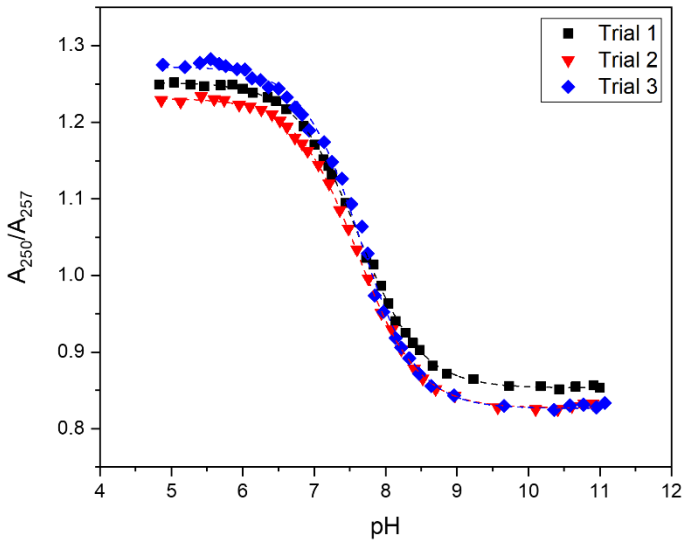

(b)

Model	DoseResp		
Equation	y = A1 + (A2-A1)/(1 + 10^((LOGx0-x)*p))		
Trial	1	2	3
A1	0.85 ± 0.00	0.83 ± 0.00	0.83 ± 0.00
A2	1.25 ± 0.00	1.23 ± 0.00	1.27 ± 0.00
LOGx0	7.62 ± 0.01	7.61 ± 0.01	7.64 ± 0.02
Adj. R-Square	0.99967	0.99962	0.99758

(c)

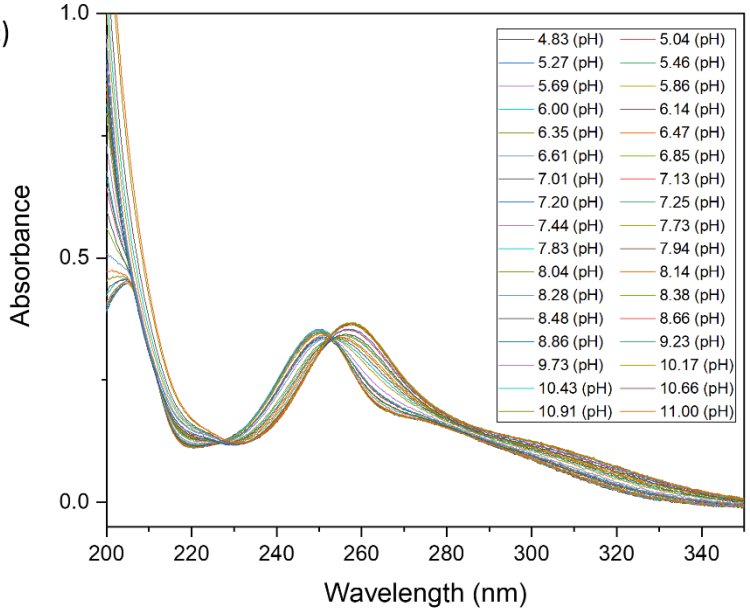

Figure S21. pK_a determination of **5** in 25% acetonitrile : 75% buffer (75 mM phosphate buffer). The pH was adjusted with dilute NaOH. (a) Graph of pH vs A_{250}/A_{257} for **5**. Dashed lines represent the fit of each graph using the DoseResp model in OriginPro 2018b. Three independent repeats were conducted. (b) Chart of the fitted curve include information on the calculated parameters, quality of the fit, and pK_a (LOGx0) for each trial. (c) Absorbance spectra of 100 µM **5** in 25% acetonitrile and 75% buffer (75 mM phosphate buffer) at various pH (representative repeat).

(a)

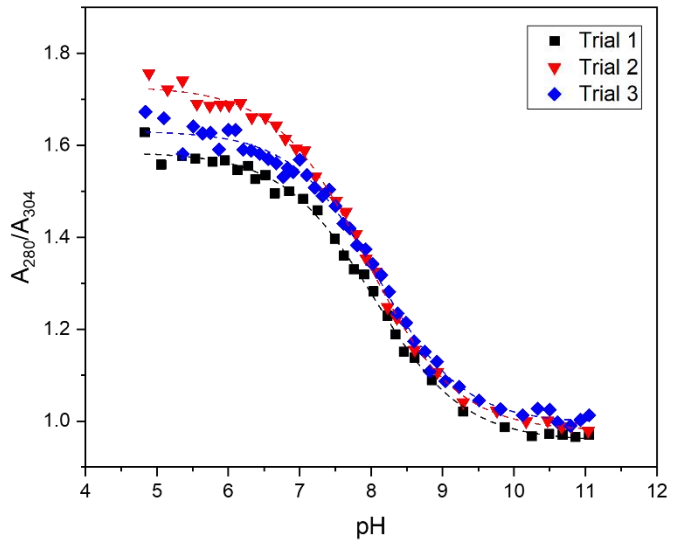

(b)

Model	DoseResp		
Equation	y = A1 + (A2-A1)/(1 + 10^((LOGx0-x)*p))		
Trial	1	2	3
A1	0.96 ± 0.01	0.98 ± 0.01	1.00 ± 0.01
A2	1.58 ± 0.01	1.73 ± 0.01	1.63 ± 0.01
LOGx0	8.03 ± 0.03	7.93 ± 0.02	8.09 ± 0.03
Adj. R-Square	0.99646	0.99752	0.99407

(c)

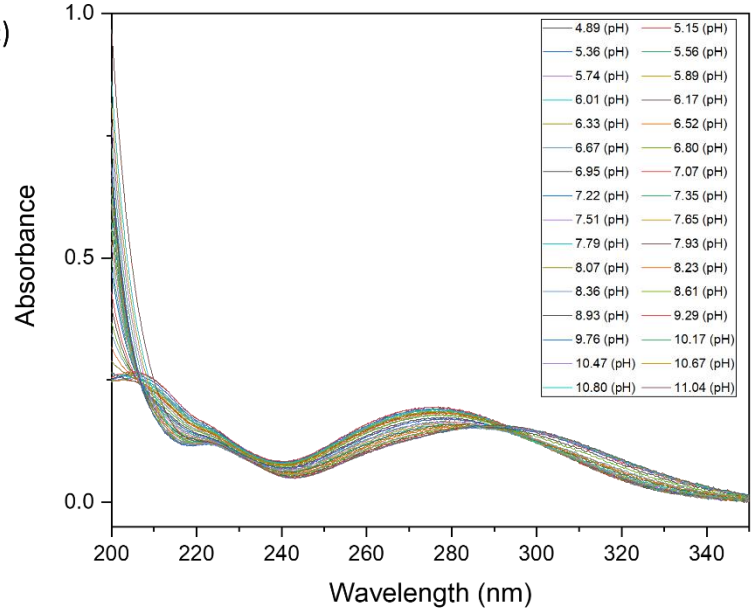

Figure S22. pK_a determination of **6** in 25% acetonitrile : 75% buffer (75 mM phosphate buffer). The pH was adjusted with dilute NaOH. (a) Graph of pH vs A_{280}/A_{304} for **6**. Dashed lines represent the fit of each graph using the DoseResp model in OriginPro 2018b. Three independent repeats were conducted. (b) Chart of the fitted curve include information on the calculated parameters, quality of the fit, and pK_a (LOGx0) for each trial. (c) Absorbance spectra of 100 µM **6** in 25% acetonitrile and 75% buffer (75 mM phosphate buffer) at various pH (representative repeat).

(a)

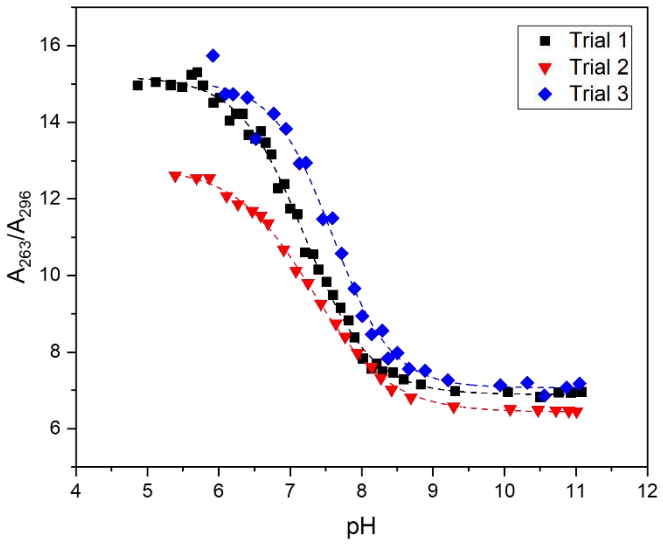

(b)

Model	DoseResp		
Equation	y = A1 + (A2-A1)/(1 + 10^((LOGx0-x)*p))		
Trial	1	2	3
A1	6.90 ± 0.07	6.44 ± 0.04	7.07 ± 0.13
A2	15.19 ± 0.09	12.83 ± 0.07	15.08 ± 0.21
LOGx0	7.20 ± 0.02	7.30 ± 0.02	7.59 ± 0.04
Adj. R-Square	0.99621	0.99871	0.98902

(c)

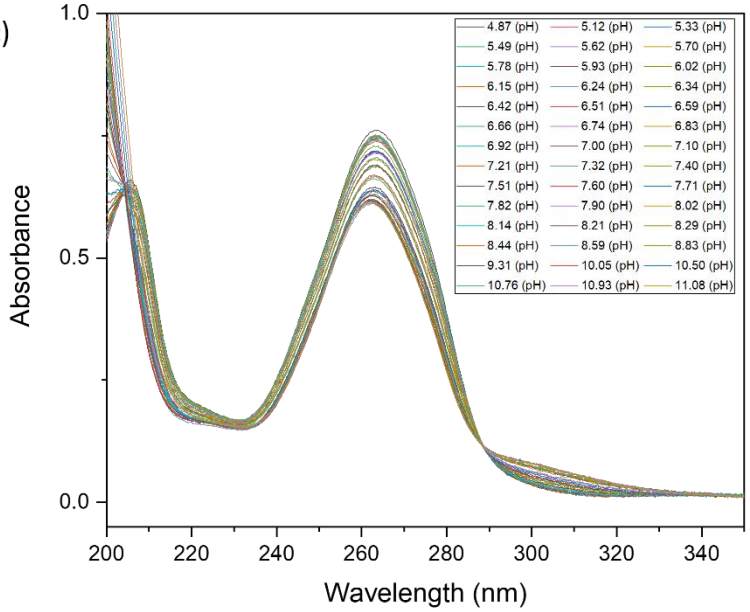

Figure S23. pK_a determination of **7** in 25% acetonitrile : 75% buffer (75 mM phosphate buffer). The pH was adjusted with dilute NaOH. (a) Graph of pH vs A_{263}/A_{296} for **7**. Dashed lines represent the fit of each graph using the DoseResp model in OriginPro 2018b. Three independent repeats were conducted. (b) Chart of the fitted curve include information on the calculated parameters, quality of the fit, and pK_a (LOGx0) for each trial. (c) Absorbance spectra of 100 µM **7** in 25% acetonitrile and 75% buffer (75 mM phosphate buffer) at various pH (representative repeat).

(a)

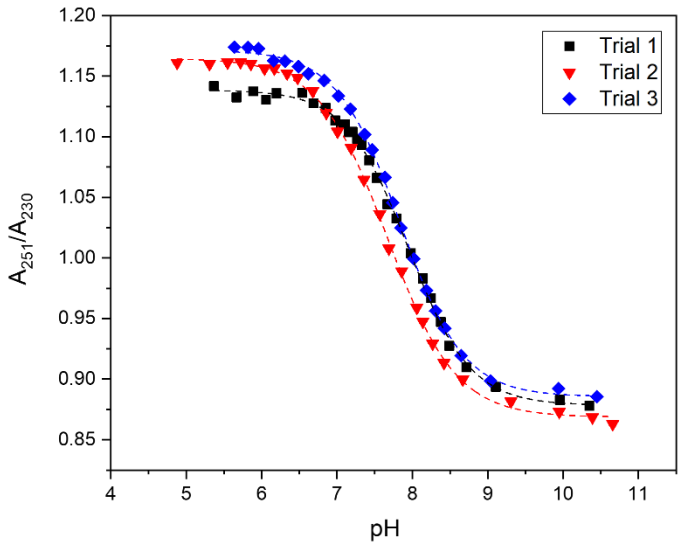

(b)

Model	DoseResp		
Equation	y = A1 + (A2-A1)/(1 + 10^((LOGx0-x)*p))		
Trial	1	2	3
A1	0.88 ± 0.00	0.87 ± 0.00	0.89 ± 0.00
A2	1.14 ± 0.00	1.16 ± 0.00	1.17 ± 0.00
LOGx0	7.95 ± 0.01	7.67 ± 0.01	7.84 ± 0.01
Adj. R-Square	0.99853	0.9992	0.99915

(c)

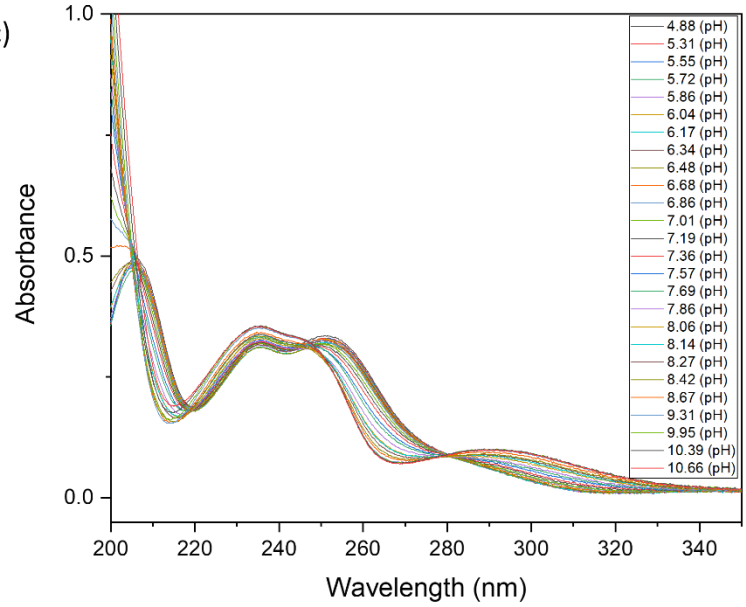

Figure S24. pK_a determination of **8** in 25% acetonitrile : 75% buffer (75 mM phosphate buffer). The pH was adjusted with dilute NaOH. (a) Graph of pH vs A_{251}/A_{230} for **8**. Dashed lines represent the fit of each graph using the DoseResp model in OriginPro 2018b. Three independent repeats were conducted. (b) Chart of the fitted curve include information on the calculated parameters, quality of the fit, and pK_a (LOGx0) for each trial. (c) Absorbance spectra of 100 µM **8** in 25% acetonitrile and 75% buffer (75 mM phosphate buffer) at various pH (representative repeat).

(a)

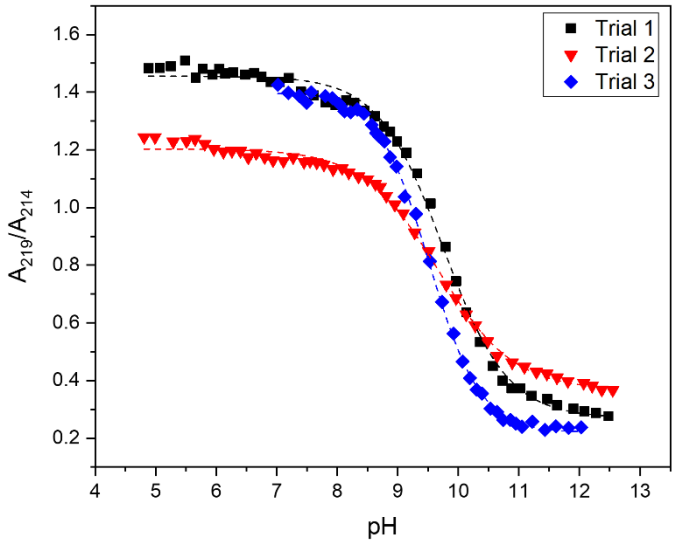

(b)

Model	DoseResp		
Equation	y = A1 + (A2-A1)/(1 + 10^((LOGx0-x)*p))		
Trial	1	2	3
A1	0.27 ± 0.01	0.37 ± 0.01	0.22 ± 0.01
A2	1.46 ± 0.01	1.20 ± 0.00	1.40 ± 0.01
LOGx0	9.74 ± 0.02	9.66 ± 0.03	9.52 ± 0.01
Adj. R-Square	0.99689	0.99713	0.99912

(c)

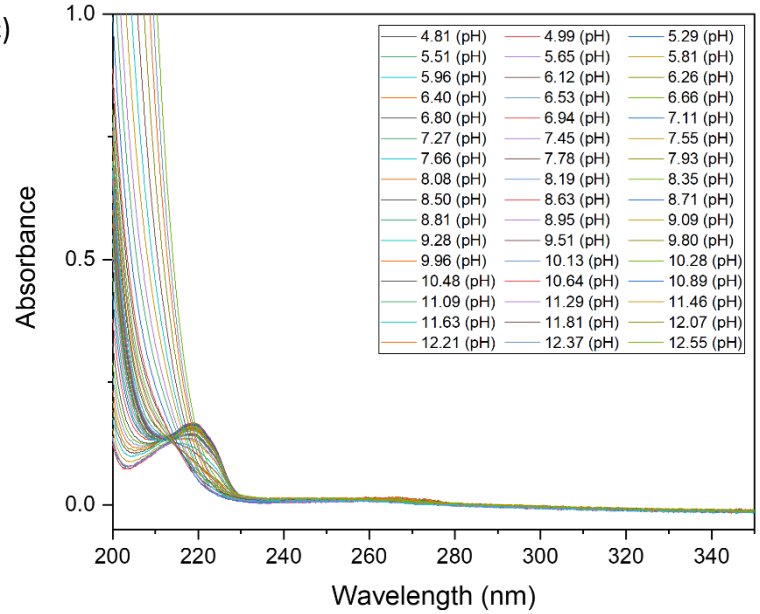

Figure S25. pK_a determination of **PBA** in 25% acetonitrile : 75% buffer (75 mM phosphate buffer). The pH was adjusted with dilute NaOH. (a) Graph of pH vs A_{219}/A_{214} for **PBA**. Dashed lines represent the fit of each graph using the DoseResp model in OriginPro 2018b. Three independent repeats were conducted. (b) Chart of the fitted curve include information on the calculated parameters, quality of the fit, and pK_a (LOGx0) for each trial. (c) Absorbance spectra of 100 µM **PBA** in 25% acetonitrile and 75% buffer (75 mM phosphate buffer) at various pH (representative repeat).

(a)

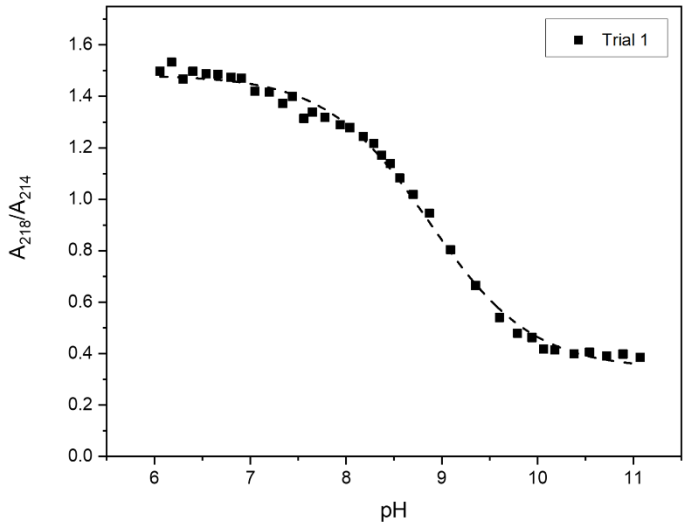

(b)

Model	DoseResp
Equation	y = A1 + (A2-A1)/(1 + 10^((LOGx0-x)*p))
A1	0.34 ± 0.02
A2	1.48 ± 0.01
LOGx0	8.87 ± 0.03
Adj. R-Square	0.99549

(c)

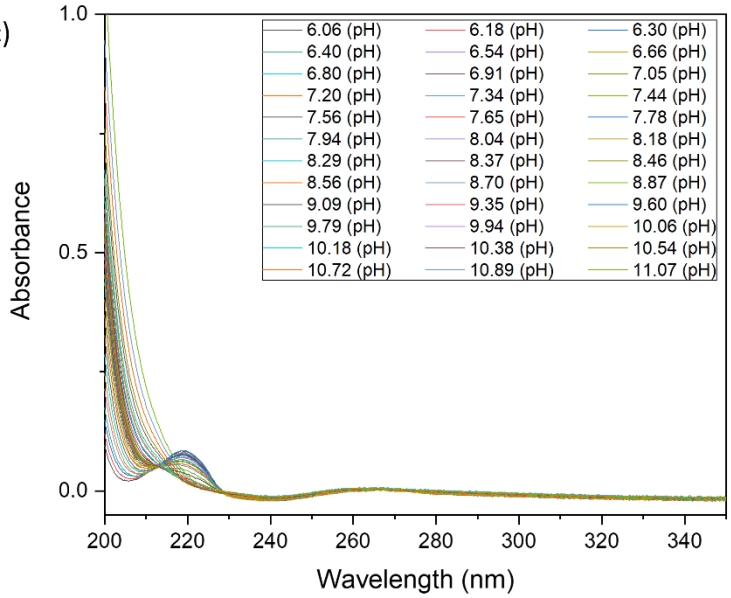

Figure S26. pK_a determination of **PBA** in 75 mM phosphate buffer. The pH was adjusted with dilute NaOH. (a) Graph of pH vs A_{218}/A_{214} for **PBA**. Dashed lines represent the fit of each graph using the DoseResp model in OriginPro 2018b. (b) Chart of the fitted curve include information on the calculated parameters, quality of the fit, and pK_a (LOGx0). (c) Absorbance spectra of 100 µM **1** in 75 mM phosphate buffer at various pH.

S4. ^{1}H NMR Titrations

^{1}H NMR titrations of compounds **1-8** with DDPG-TMA and DHPC were performed on a Bruker 500 MHz instrument in a solvent system of 99.5% DMSO-d_6:0.5% Milli-Q H_2O at 37˚C. The instrument was locked to DMSO-d_6. Both lipids were purchased from *Avanti Polar Lipids, Inc*: DHPC (catalog# 850305) and DDPG (catalog# 840434). DDPG contains the target lipid headgroup prevalent in bacteria and DHPC represents the most common mammalian membrane lipid headgroup. Prior to the experiment, the sodium counterion of DDPG was exchanged for the sterically hindered counterion tetramethylammonium (TMA). The ion exchange procedure is listed in section S4.1. The length of the hydrophobic tail varied between (10:0) PG and (6:0) PC to ensure proper solubility of both lipids in DMSO. In our analysis, compounds **1-8** were viewed as the host and lipids were views as the guest. The titrations were performed using a 3 mM host solution starting point, to which aliquots of a solution containing 45 mM guest and 3 mM host were added using a Hamilton gas-tight syringe. The ^{1}H NMR spectrum was obtained upon each addition. Before measuring the NMR spectra, an incubation period of at least 3 minutes was used to improve peak resolution. All titrations were repeated a minimum of 3 times, and association constants are reported as the average of these 3 repeats with errors representing standard deviations. A repeat with 1 mM host and 15 mM guest was also done to ensure the observed binding constants were not influenced by potential aggregation. The titration results are shown in sections S4.2. and S4.3. A table with the obtained association constants is given in the main manuscript.

For fast exchange binding constant determination, the downfield shift in the urea N-H peaks were measured in MestreNova, and these values were used to calculate association constants (K_a) using the online tool BindFit[5] assuming a 1:1 stoichiometry for binding. Compounds **1** and **5-8** exhibited slow exchange when titrated with DDPG-TMA. In this case, an integration ratio of the peaks belonging to the host and the host-guest complex were applied to a mass-balance equation shown in the formulas below:

$$1{:}\,1 \text{ Mass Balance Equation: } [\mathrm{H}] + [\mathrm{G}] \rightleftharpoons [\mathrm{HG}] \qquad (1)$$

$$1{:}\,1 \text{ Association Constant: } \mathrm{K_a} = \frac{[\mathrm{HG}]}{[\mathrm{H}][\mathrm{G}]} \qquad (2)$$

To solve for formula (2) we need to know the concentrations of [HG], [H], [G]. The unbound Host concentration [H] can be determined by multiplying the integration of a Host proton peak (i_H) by the initial host concentration $[H]_0$ and divided by the sum of the host proton integration (i_H) and the integration of the same proton of the host guest complex (i_{HG}) as shown in formula (3). This same approach can be applied to determine the Host guest complex concentration [HG] according to formula (4):

$$\text{Unbound Host Concentration: } [\mathrm{HG}] = \frac{i_H[H]_o}{i_{HG} + i_H} \qquad (3)$$

$$\text{Host Guest Complex: } [\mathrm{HG}] = \frac{i_{HG}[H]_o}{i_{HG} + i_H} \qquad (4)$$

With [HG] determined we can then use formula (5) to determine the unbound guest concentration [G] from the mass balance equation:

$$\text{Unbound Guest Concentration: } [G] = [G]_o - [HG] \qquad (5)$$

With the concentrations of [H], [G], and [HG] determined, we can add the values to formula (2) and determine the association constant K_a of a 1:1 binding event.

S4.1. DDPG-TMA ion exchange procedure

0.35 mmol of DDPG (Na^+) was dissolved in 1:1 isopropanol:chloroform. The solution was passed through a BioTage Isolute® SCX ion exchange column (6 mL) and collected in a pre-weighed 50 mL round bottom flask. The solvent system was removed under reduced pressure using a rotary evaprator and the flask was dried overnight under high vacuum. The next day, the flask was weighed and the amount of neutral phospholipid was calculated assuming 100% protonation. This value was used to determine how much tetramethylammonium hydroxide (TMA-OH) was required to generate the TMA^+ salt of the lipid. A small sample of DDPG (H^+) was collected and processed on ^1H and ^{31}P NMR (Bruker 300 MHz) to ensure the lipid was completely protonated. The ^{31}P NMR displayed a single peak, indicating complete conversion. The dried neutral lipid was dissolved in 25 mL H_2O and the lipid solution was stirred. Initially, neutral DDPG (H^+) is insoluble in water but as the pH increases towards 7, the ionized lipid becomes soluble. The pH meter was calibrated with pH standards prior to the titration. A 1:10 and 1:100 dilution of TMA-OH was created in fresh UltraPure water. TMA-OH was purchased from Sigma Aldrich (331635-250ML). Dropwise additions of 1:10 TMA-OH were slowly added until the pH registered ~5.50. Then, the 1:100 TMA-OH was carefully added dropwise until the pH registered 7.00. Care was taken to ensure the final pH was exact. The lipid solution was transferred by glass pipette into two 50 mL Falcon® tubes, sealed, and emersed in liquid N_2 until thoroughly frozen. The frozen Falcon® tubes were unsealed and lyophilized using a Labconco Free Zone Bench Top Freeze Dryer until completely dry. The final product was confirmed by ^1H and ^{31}P NMR. The proton peak belonging to TMA, δ 3.09 (s, 12H), properly integrated and the ^{31}P NMR displayed a single peak at 0.93 ppm.

DDPG-TMA: (94% yield, 0.33 mmol) ^1H NMR (300 MHz, DMSO-d_6, ppm) δ 5.71 (s, 1 H), 5.11 – 5.00 (m, 1 H), 4.95 (s, 1 H), 4.27 (dd, *J* = 12.0, 3.1 Hz, 1 H), 4.08 (dd, *J* = 12.0, 6.9 Hz, 1 H), 3.78 – 3.54 (m, 4 H), 3.09 (s, 12 H), 2.31 – 2.22 (m, 4 H), 1.50 (s, 4 H), 1.23 (s, 24 H), 0.93 – 0.77 (m, 6 H). ^{31}P NMR (121 MHz, DMSO-d_6, ppm) δ 0.93 (br.).

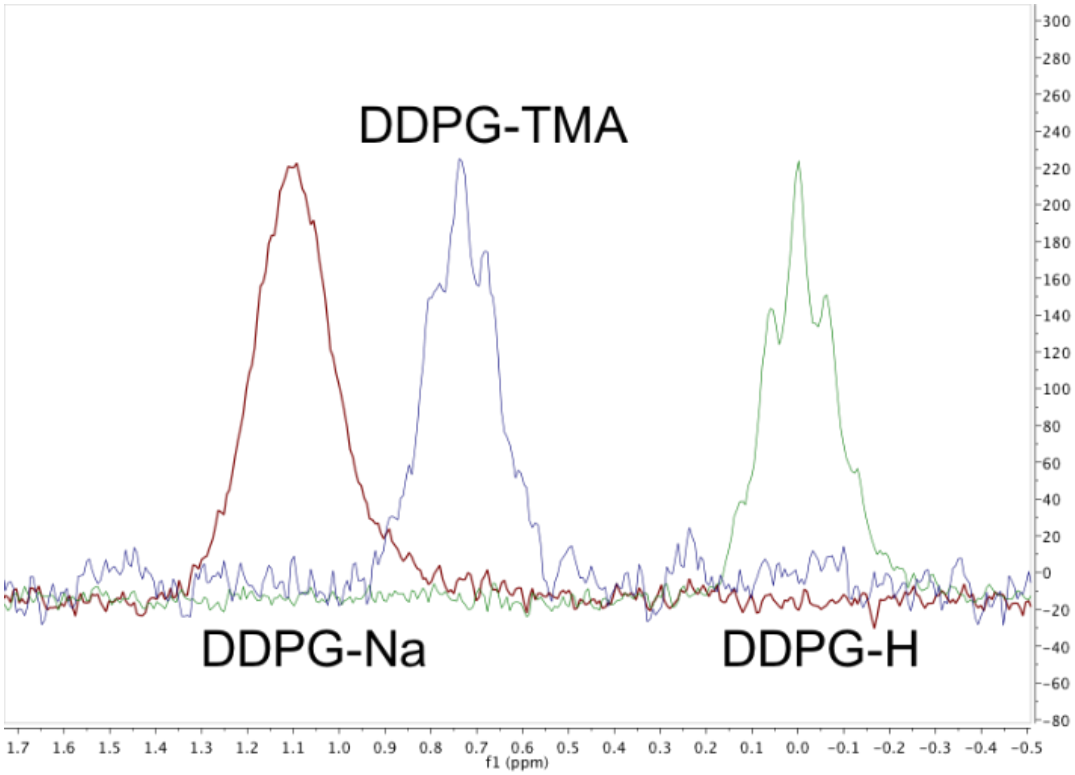

Figure S27. Superimposed ^{31}P NMR (121 MHz) spectra of DDPG-Na^+, DDPG-H^+, and DDPG-TMA^+ in $CDCl_3$ at 298 K, demonstrating the complete conversion for each step.

S4.2. DHPC ^{1}H NMR titration results

Below are the results of the ^{1}H NMR titrations of boronic acids **1-8** with the phosphatidylcholine lipid DHPC. When the change in chemical shift was < 0.1 ppm, the data was not fitted, and very weak binding was assumed.

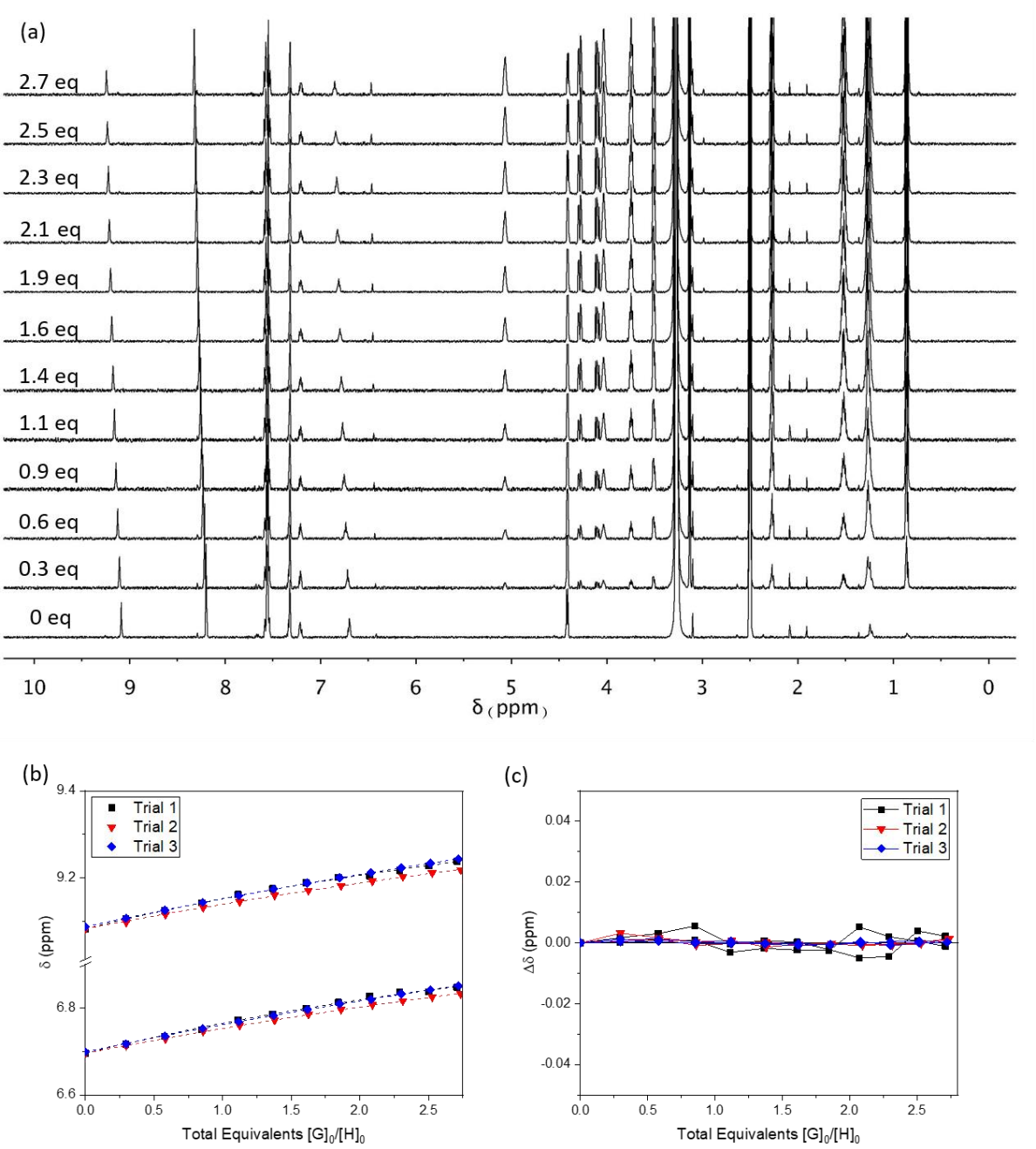

Figure S28. ^{1}H NMR titration of **1** with DHPC in 99.5% DMSO-d_6:0.5% Milli-Q H_2O at 310 K. (a) Stacked spectra plot of a representative titration. (b) Fitplot for the urea NHs at δ_A = 9.09 ppm and δ_B= 6.71 ppm using global analysis and 1:1 binding stoichiometry. The symbols of each trial report the chemical shift in ppm and the dashed lines represent the calculated fit of each curve. Data from 3 independent repeats are overlaid. (c) Plot of the residuals for urea NHs at δ_A = 9.09 ppm and δ_B= 6.71 ppm using global analysis and 1:1 binding stoichiometry. Data from 3 independent repeats are overlaid.

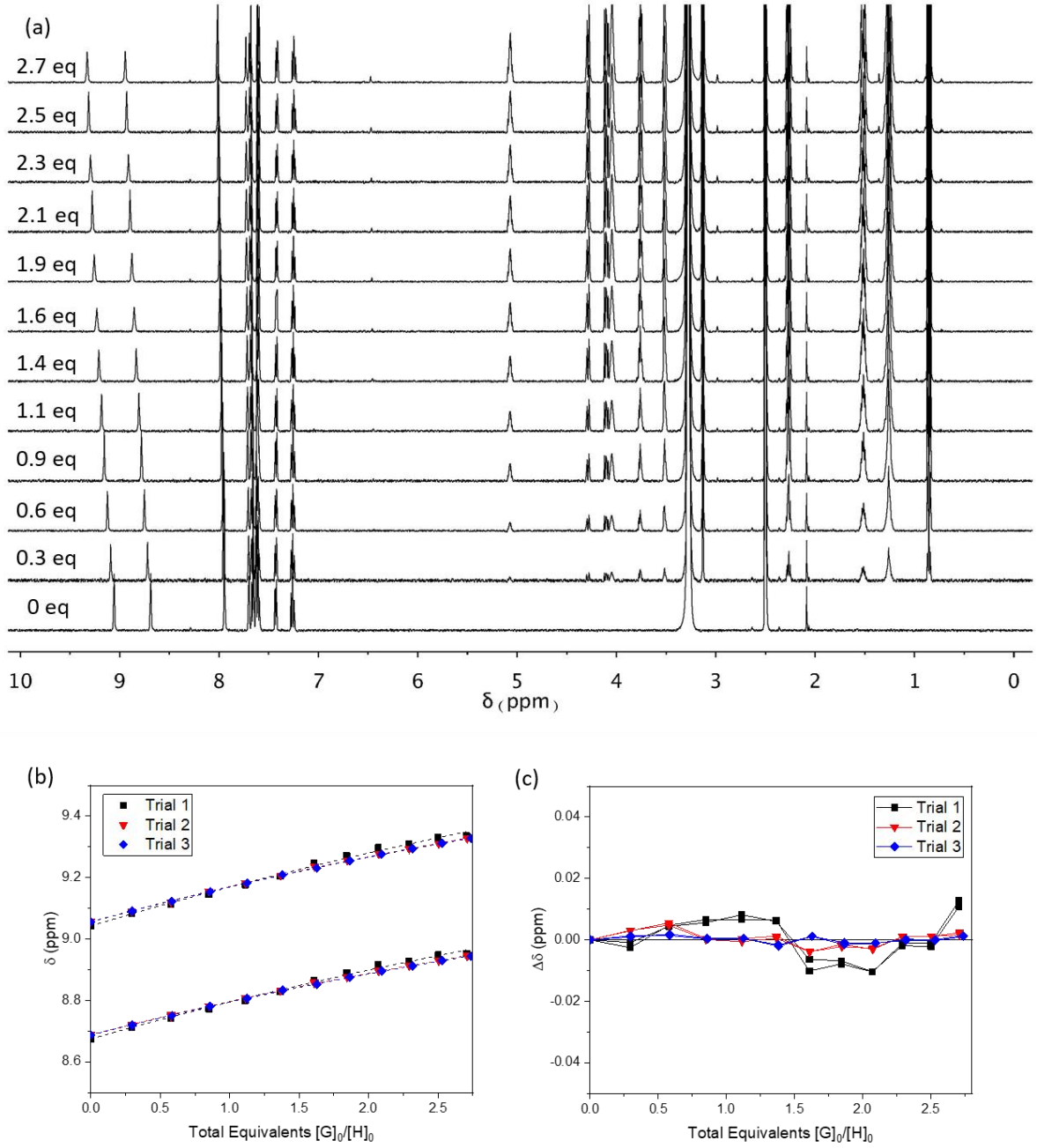

Figure S29. ^{1}H NMR titration of **2** with DHPC in 99.5% DMSO-d_6:0.5% Milli-Q H_2O at 310 K. (a) Stacked spectra plot of a representative titration. (b) Fitplot for the urea NHs at δ_A = 9.06 ppm and δ_B= 8.69 ppm using global analysis and 1:1 binding stoichiometry. The symbols of each trial report the chemical shift in ppm and the dashed lines represent the calculated fit of each curve. Data from 3 independent repeats are overlaid. (c) Plot of the residuals for urea NHs at δ_A = 9.06 ppm and δ_B= 8.69 ppm using global analysis and 1:1 binding stoichiometry. Data from 3 independent repeats are overlaid.

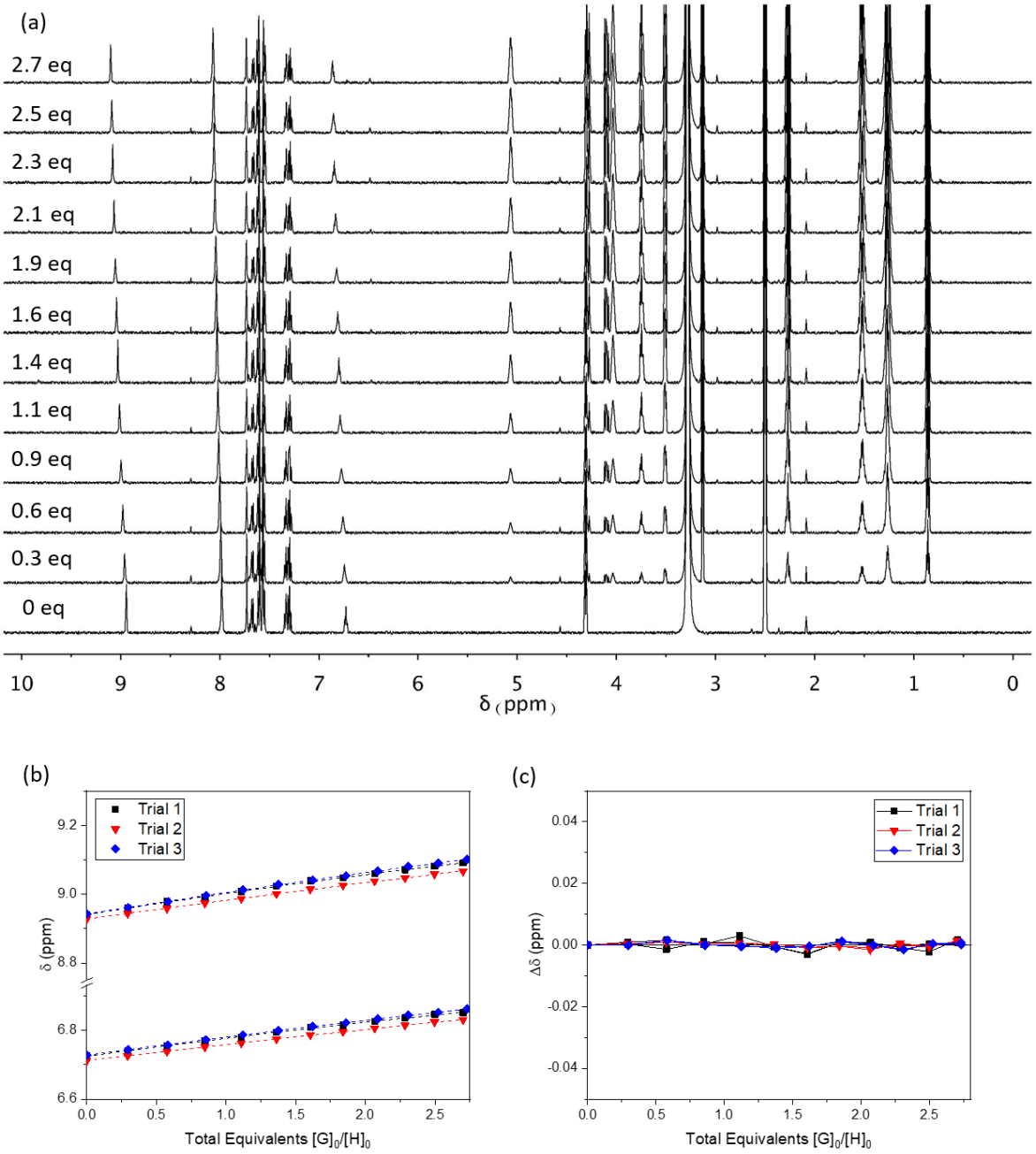

Figure S30. ^{1}H NMR titration of **3** with DHPC in 99.5% DMSO-d_6:0.5% Milli-Q H_2O at 310 K. (a) Stacked spectra plot of a representative titration. (b) Fitplot for the urea NHs at δ_A = 8.94 ppm and δ_B= 6.73 ppm using global analysis and 1:1 binding stoichiometry. The symbols of each trial report the chemical shift in ppm and the dashed lines represent the calculated fit of each curve. Data from 3 independent repeats are overlaid. (c) Plot of the residuals for urea NHs at δ_A = 8.94 ppm and δ_B= 6.73 ppm using global analysis and 1:1 binding stoichiometry. Data from 3 independent repeats are overlaid.

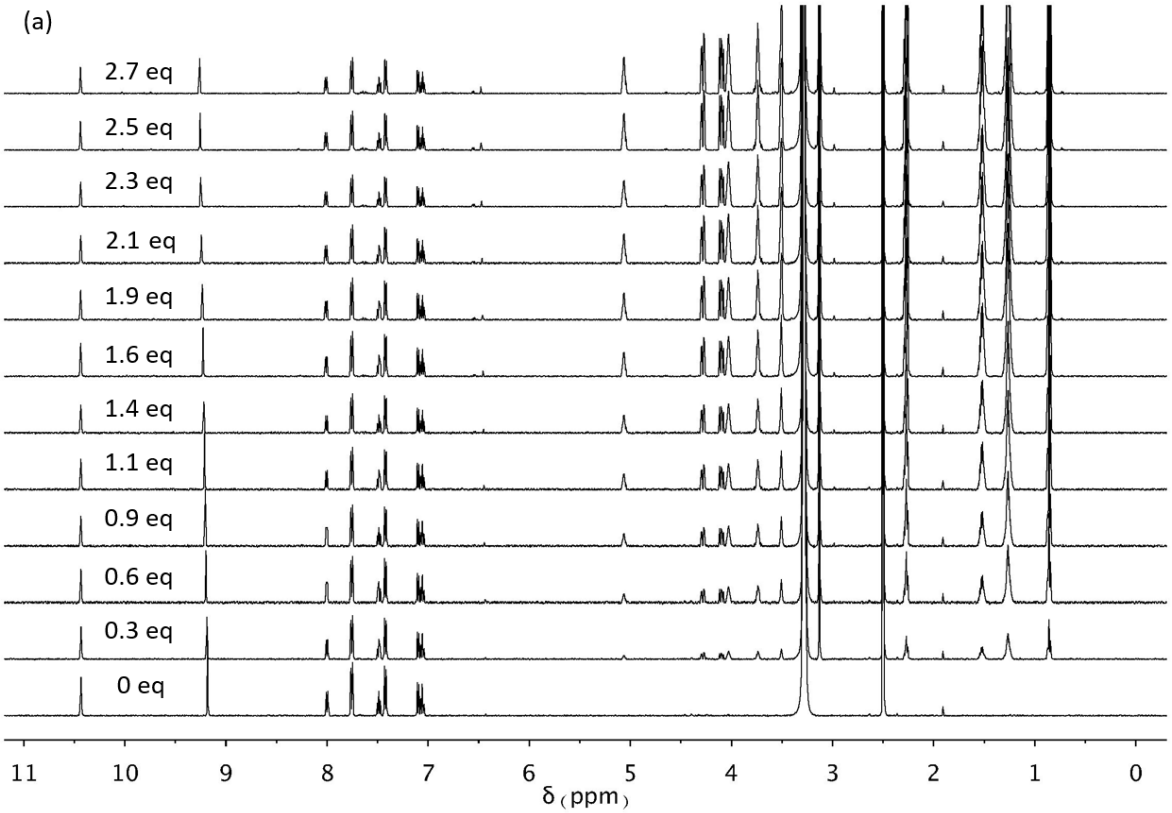

Figure S31. ^{1}H NMR titration of **4** with DHPC in 99.5% DMSO-d_6:0.5% Milli-Q H_2O at 310 K. (a) Stacked spectra plot of a representative titration. The resultant chemical shift due to the host and guest interaction was too small to quantify (<0.03 ppm).

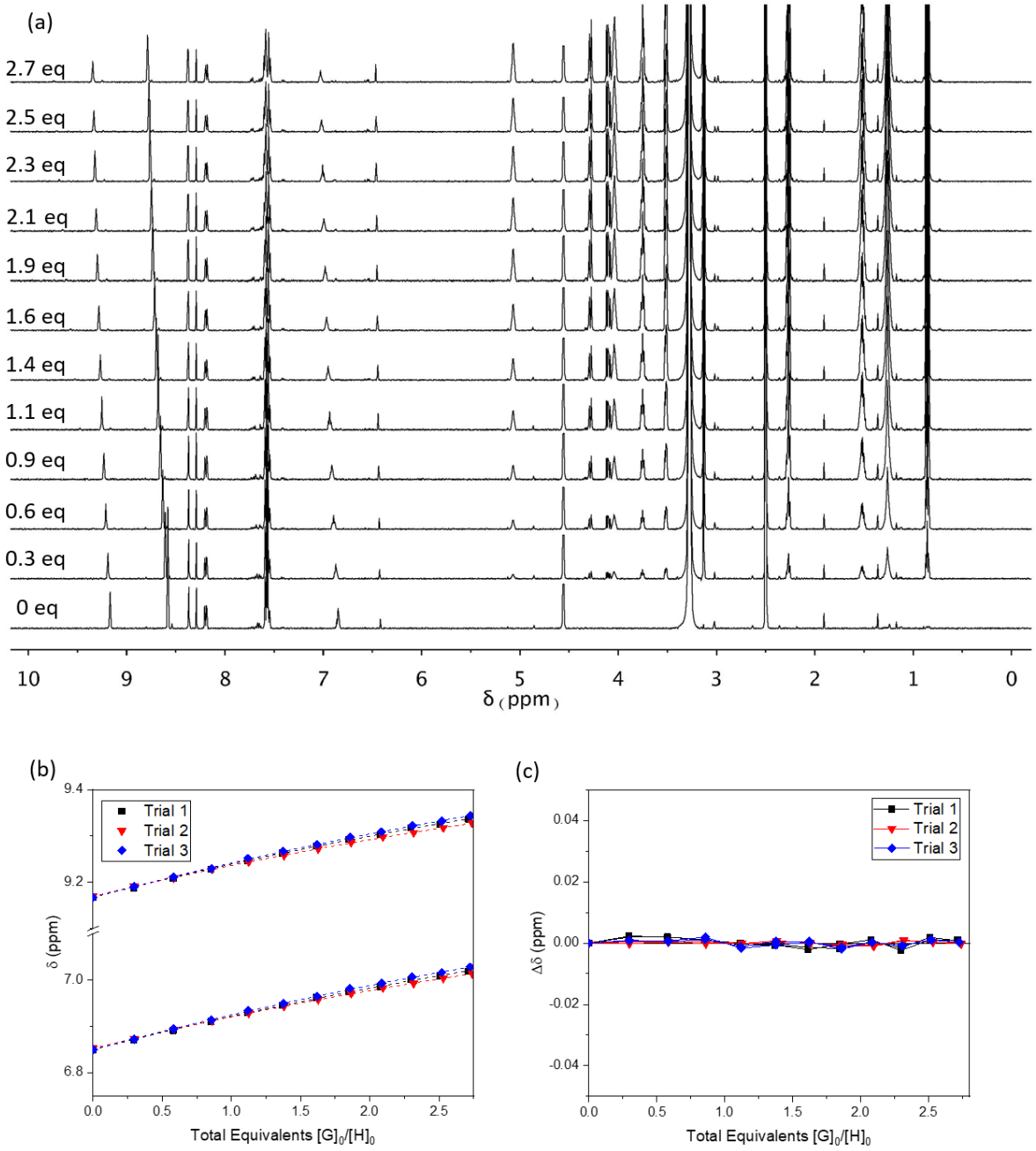

Figure S32. ^{1}H NMR titration of **5** with DHPC in 99.5% DMSO-d_6:0.5% Milli-Q H_2O at 310 K. (a) Stacked spectra plot of a representative titration. (b) Fitplot for the urea NHs at δ_A = 9.18 ppm and δ_B= 6.86 ppm using global analysis and 1:1 binding stoichiometry. The symbols of each trial report the chemical shift in ppm and the dashed lines represent the calculated fit of each curve. Data from 3 independent repeats are overlaid. (c) Plot of the residuals for urea NHs at δ_A = 9.18 ppm and δ_B= 6.86 ppm using global analysis and 1:1 binding stoichiometry. Data from 3 independent repeats are overlaid.

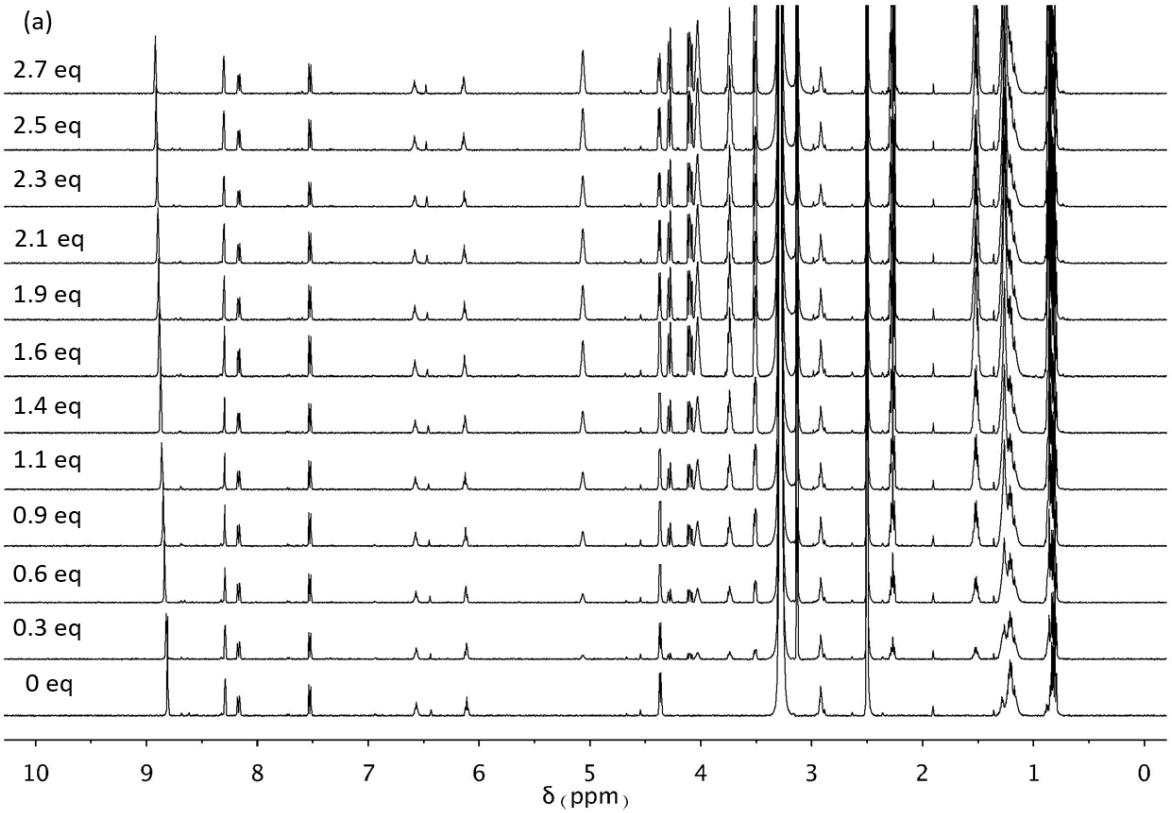

Figure S33. ^{1}H NMR titration of **6** with DHPC in 99.5% DMSO-d_6:0.5% Milli-Q H_2O at 310 K. (a) Stacked spectra plot of a representative titration. The resultant chemical shift due to the host and guest interaction was too small to quantify (<0.03 ppm).

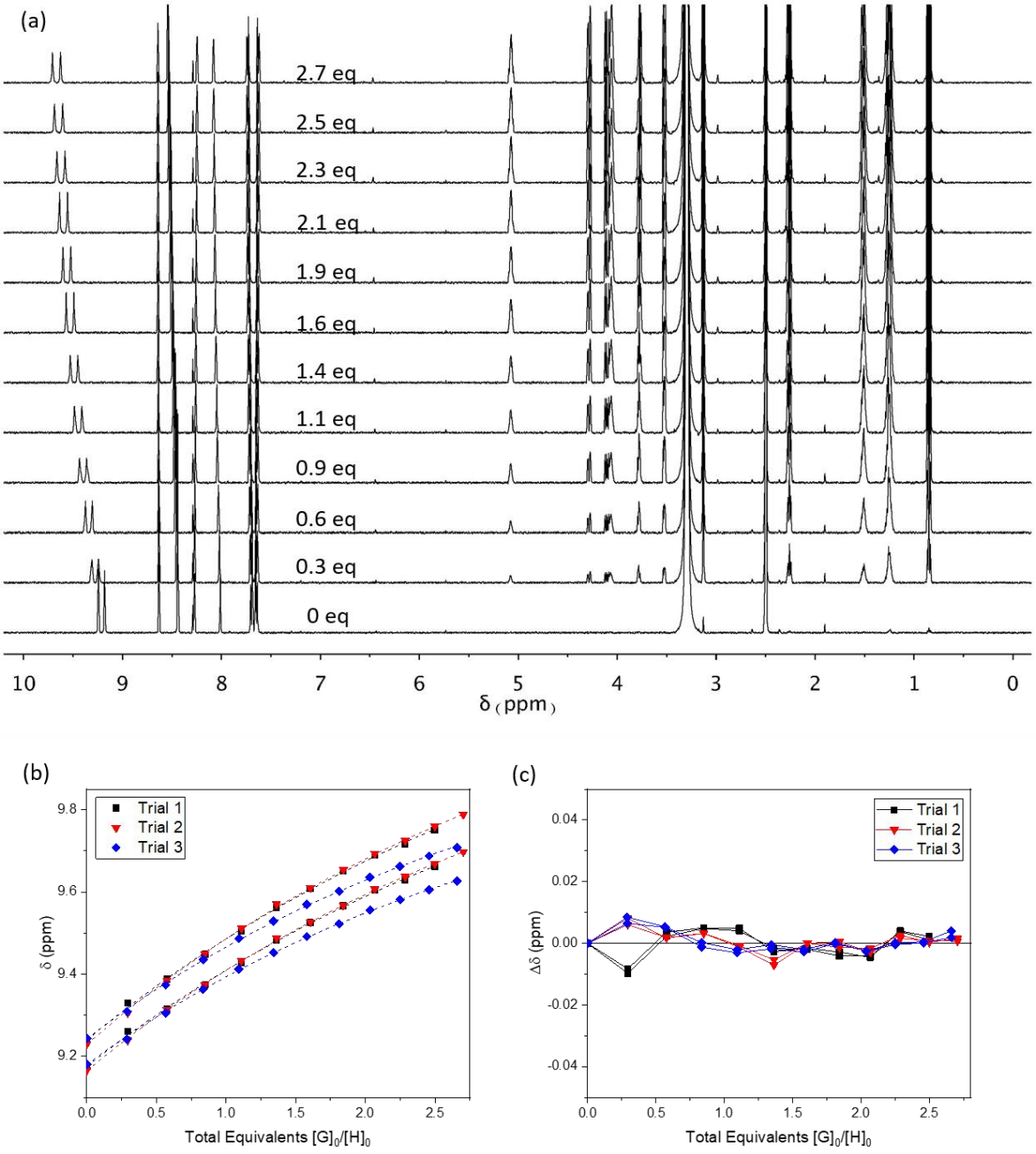

Figure S34. ^{1}H NMR titration of **7** with DHPC in 99.5% DMSO-d_6:0.5% Milli-Q H_2O at 310 K. (a) Stacked spectra plot of a representative titration. (b) Fitplot for the urea NHs at δ_A = 9.25 ppm and δ_B= 9.18 ppm using global analysis and 1:1 binding stoichiometry. The symbols of each trial report the chemical shift in ppm and the dashed lines represent the calculated fit of each curve. Data from 3 independent repeats are overlaid. (c) Plot of the residuals for urea NHs at δ_A = 9.25 ppm and δ_B= 9.18 ppm using global analysis and 1:1 binding stoichiometry. Data from 3 independent repeats are overlaid.

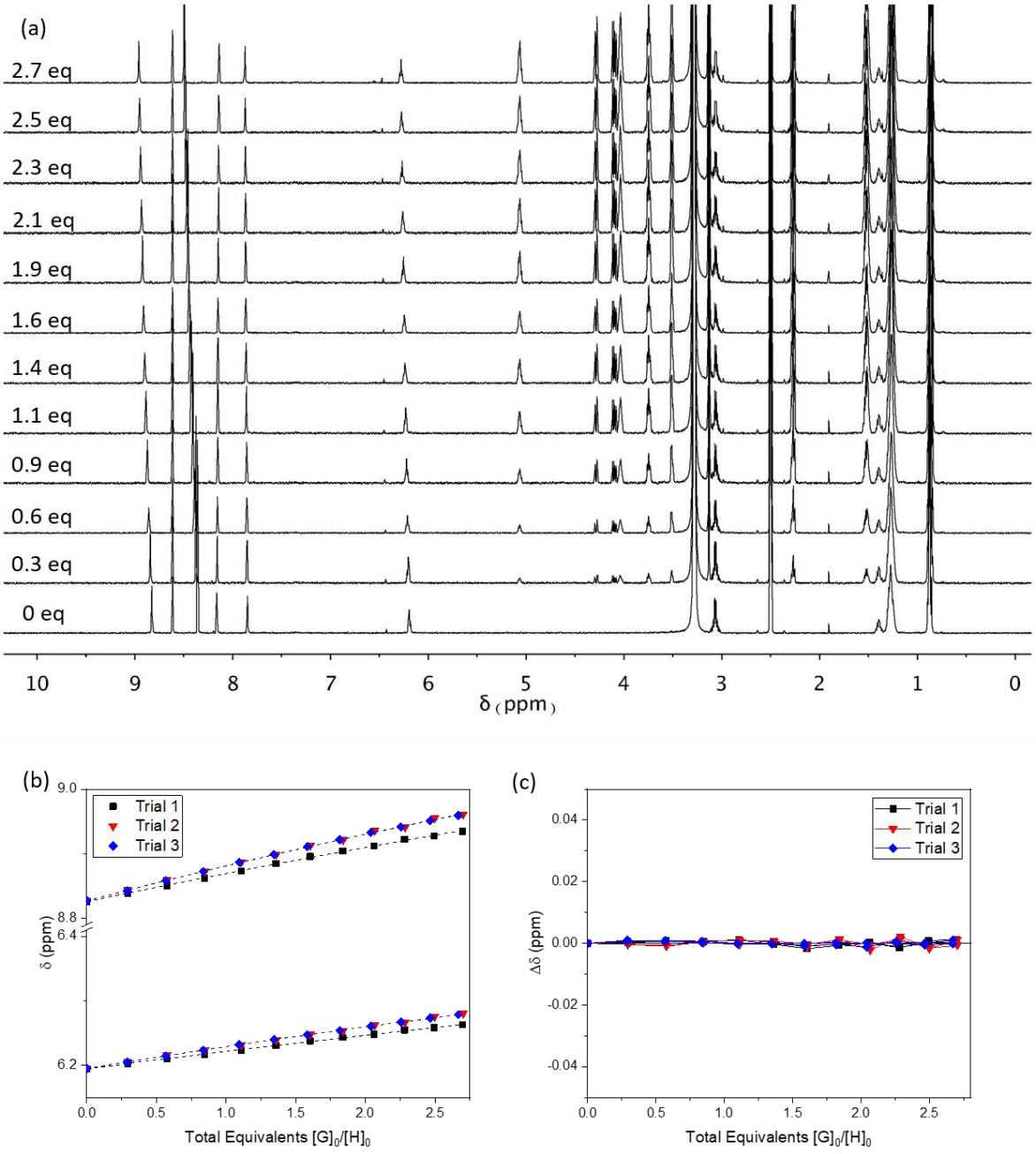

Figure S35. ^{1}H NMR titration of **8** with DHPC in 99.5% DMSO-d_6:0.5% Milli-Q H_2O at 310 K. (a) Stacked spectra plot of a representative titration. (b) Fitplot for the urea NHs at δ_A = 6.29 ppm and δ_B= 6.03 ppm using global analysis and 1:1 binding stoichiometry. The symbols of each trial report the chemical shift in ppm and the dashed lines represent the calculated fit of each curve. Data from 3 independent repeats are overlaid. (c) Plot of the residuals for urea NHs at δ_A = 8.84 ppm and δ_B= 6.21 ppm using global analysis and 1:1 binding stoichiometry. Data from 3 independent repeats are overlaid.

S4.3. DDPG-TMA ^{1}H NMR titration results

Below are the results of the ^{1}H NMR titrations of boronic acids **1-8** with the phosphatidylglycerol lipid DDPG-TMA. When the change in chemical shift was < 0.1 ppm, the data was not fitted and very weak binding was assumed. When slow exchange occurred, the obtained integrations are indicated on the spectra.

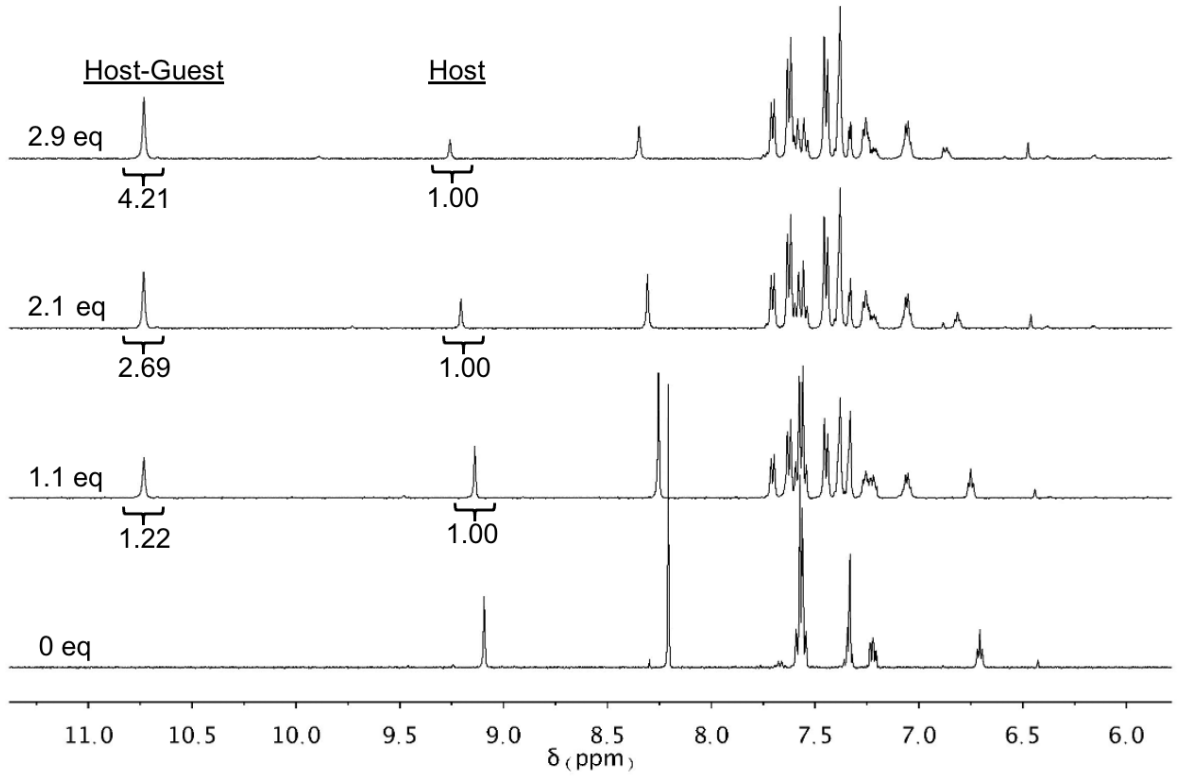

Figure S36. ^{1}H NMR titration of **1** with DDPG-TMA in 99.5% DMSO-d_6:0.5% Milli-Q H_2O at 310 K (stacked spectra plot of a representative titration). Due to slow chemical exchange on the 500 MHz NMR timescale, the binding constants were calculated by comparing integration ratios of host and host-guest complex with total concentrations of host and guest in a mass balance equation. Data was collected from three independent repeats, each consisting of three measurements of increasing guest concentration. The samples were incubated for one hour between measurements.

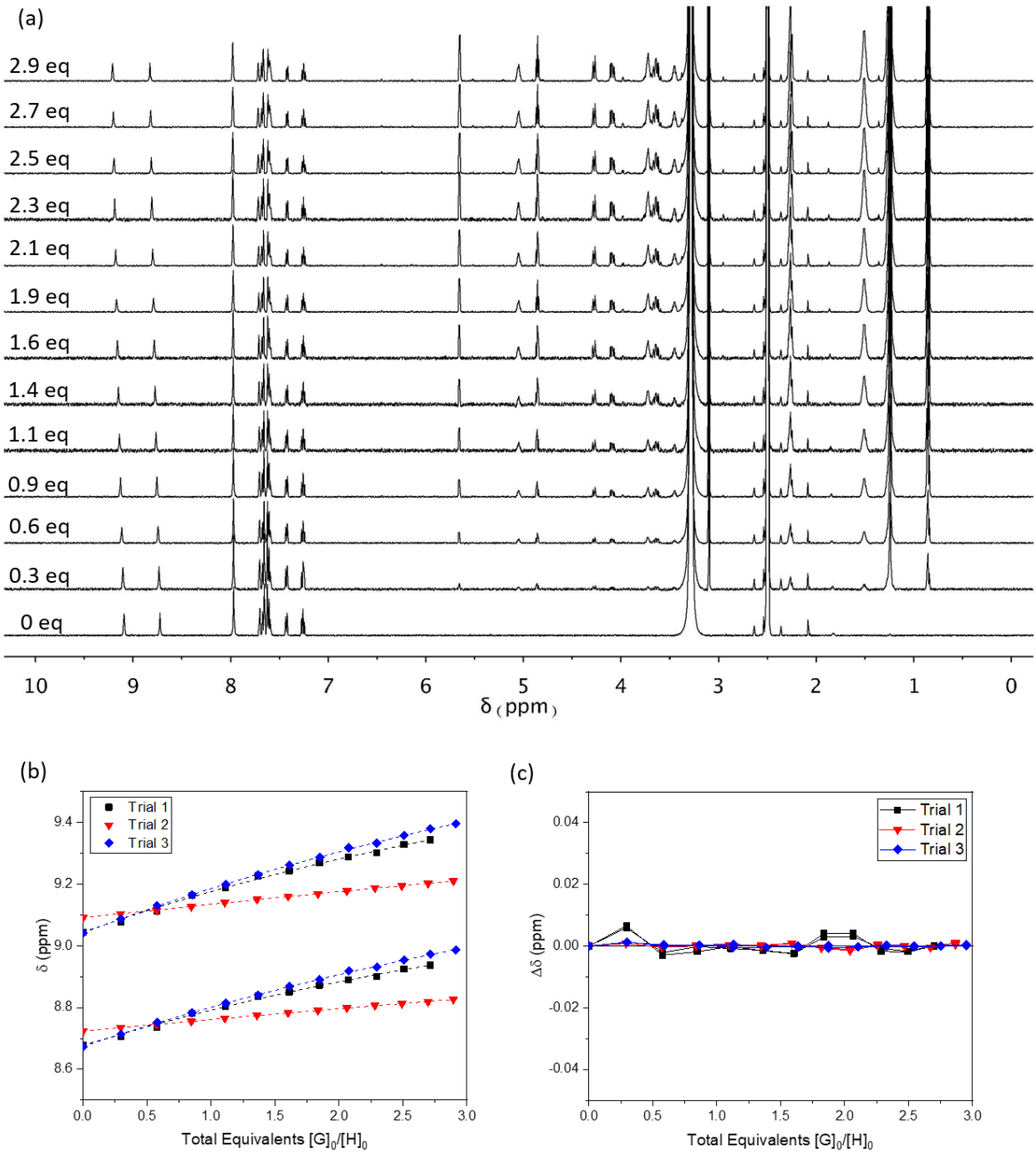

Figure S37. ^{1}H NMR titration of **2** with DDPG-TMA in 99.5% DMSO-*d*$_6$:0.5% Milli-Q H_2O at 310 K. (a) Stacked spectra plot of a representative titration. (b) Fitplot for the urea NHs at δ_A = 9.06 ppm and δ_B= 8.69 ppm using global analysis and 1:1 binding stoichiometry. The symbols of each trial report the chemical shift in ppm and the dashed lines represent the calculated fit of each curve. Data from 3 independent repeats are overlaid. (c) Plot of the residuals for urea NHs at δ_A = 9.06 ppm and δ_B= 8.69 ppm using global analysis and 1:1 binding stoichiometry. Data from 3 independent repeats are overlaid.

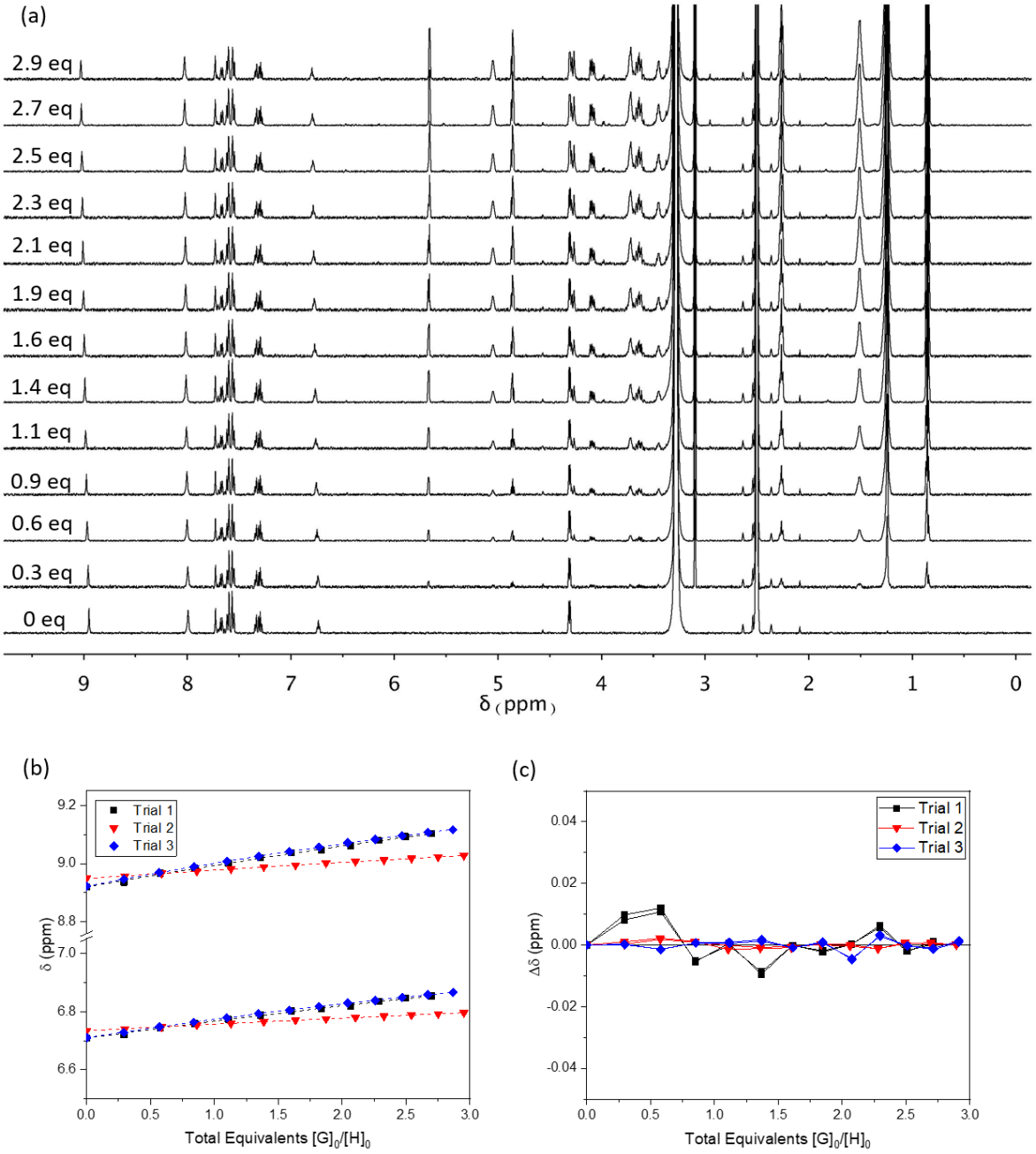

Figure S38. ^{1}H NMR titration of **3** with DDPG-TMA in 99.5% DMSO-d_6:0.5% Milli-Q H_2O at 310 K. (a) Stacked spectra plot of a representative titration. (b) Fitplot for the urea NHs at δ_A = 8.94 ppm and δ_B= 6.73 ppm using global analysis and 1:1 binding stoichiometry. The symbols of each trial report the chemical shift in ppm and the dashed lines represent the calculated fit of each curve. Data from 3 independent repeats are overlaid. (c) Plot of the residuals for urea NHs at δ_A = 8.94 ppm and δ_B= 6.73 ppm using global analysis and 1:1 binding stoichiometry. Data from 3 independent repeats are overlaid.

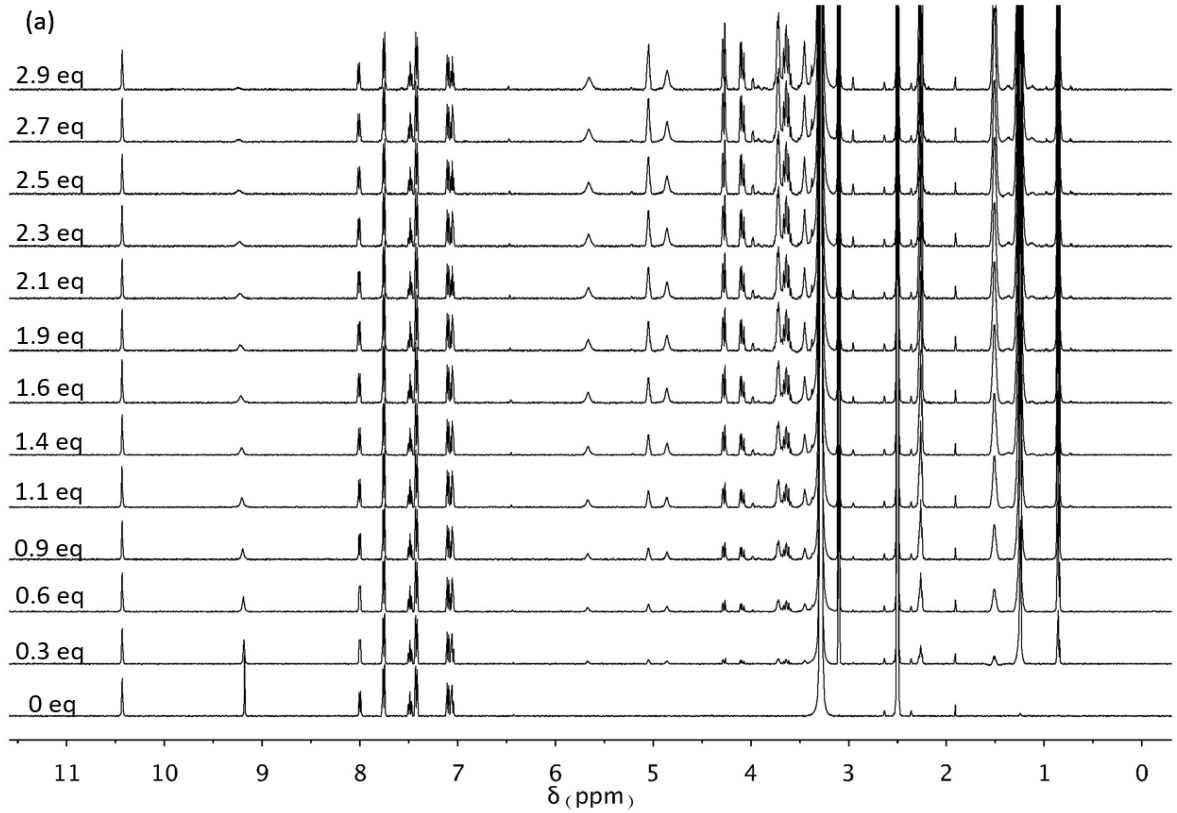

Figure S39. ^{1}H NMR titration of **4** with DDPG-TMA in 99.5% DMSO-d_6:0.5% Milli-Q H_2O at 310 K. (a) Stacked spectra plot of a representative titration. The resultant chemical shift due to the host and guest complexation was too small to quantify (<0.03 ppm).

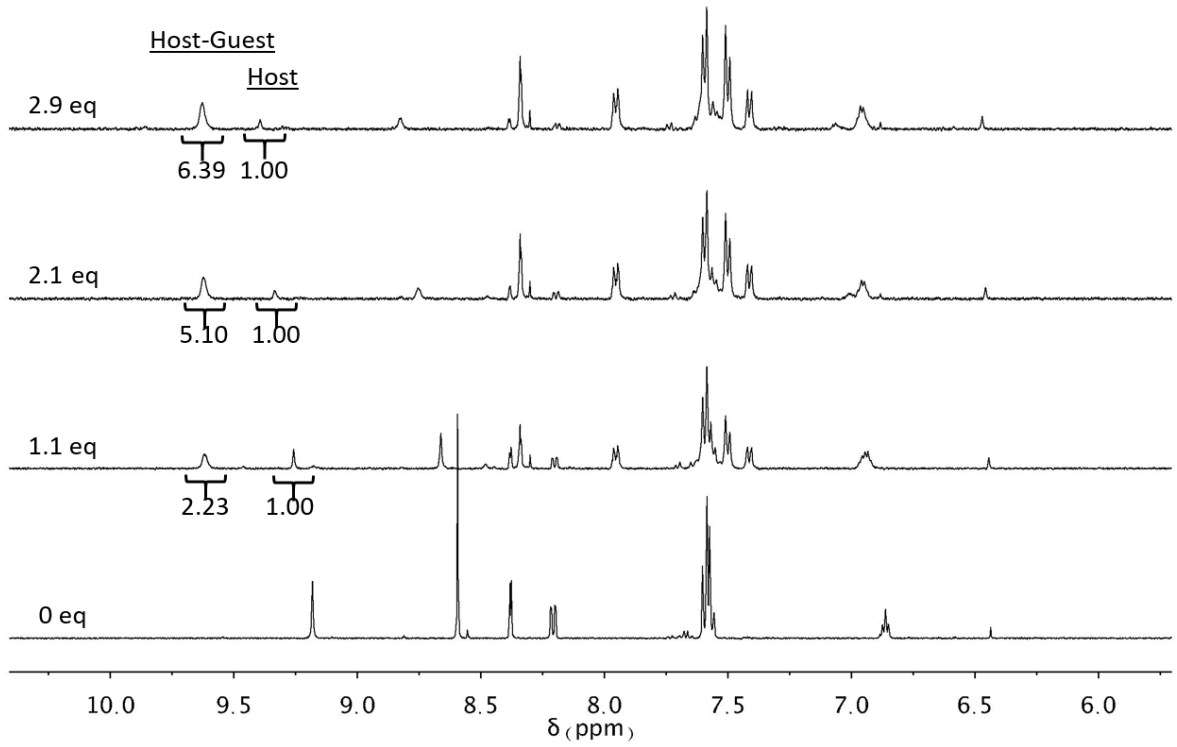

Figure S40. ^{1}H NMR titration of **5** with DDPG-TMA in 99.5% DMSO-d_6:0.5% Milli-Q H_2O at 310 K (stacked spectra plot of a representative titration). Due to slow chemical exchange on the 500 MHz NMR timescale, the binding constant was calculated by comparing integration ratios of host and host-guest complex with total concentrations of host and guest in a mass balance equation. Data was collected from three independent repeats, each consisting of three measurements of increasing guest concentration. The samples were incubated for one hour between measurements.

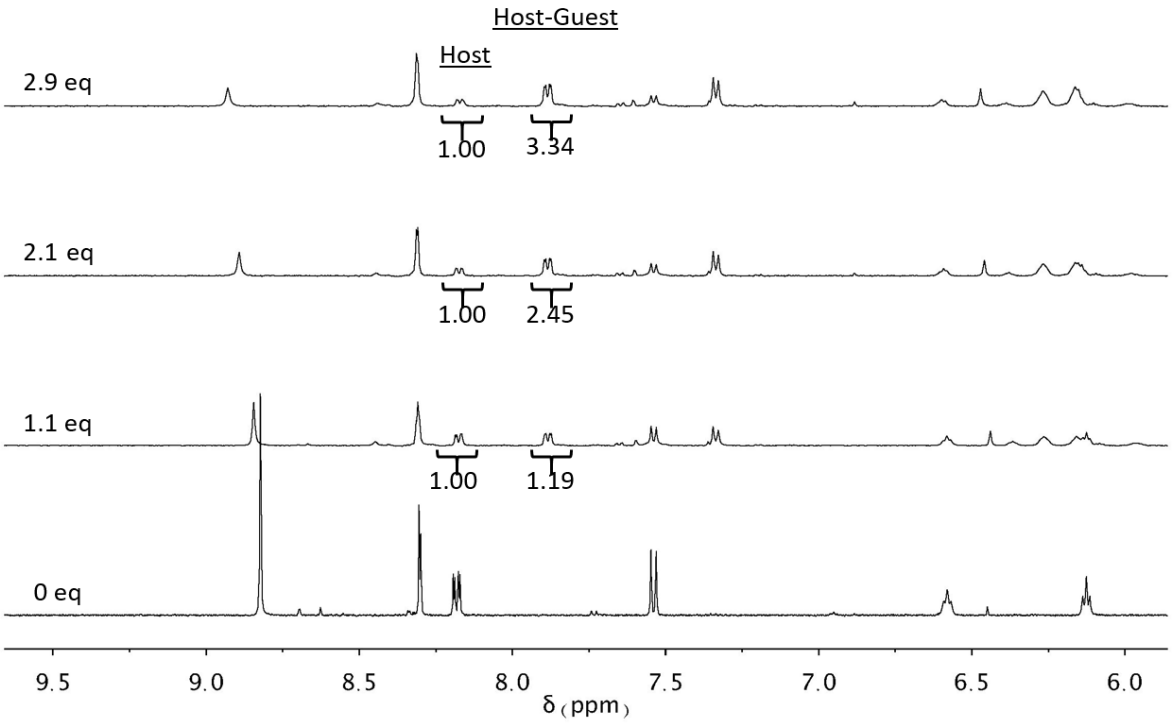

Figure S41. ^{1}H NMR titration of **6** with DDPG-TMA in 99.5% DMSO-d_6:0.5% Milli-Q H_2O at 310 K (stacked spectra plot of a representative titration). Due to slow chemical exchange on the 500 MHz NMR timescale, the binding constant was calculated by comparing integration ratios of host and host-guest complex with total concentrations of host and guest in a mass balance equation. Data was collected from three independent repeats, each consisting of three measurements of increasing guest concentration. The samples were incubated for one hour between measurements.

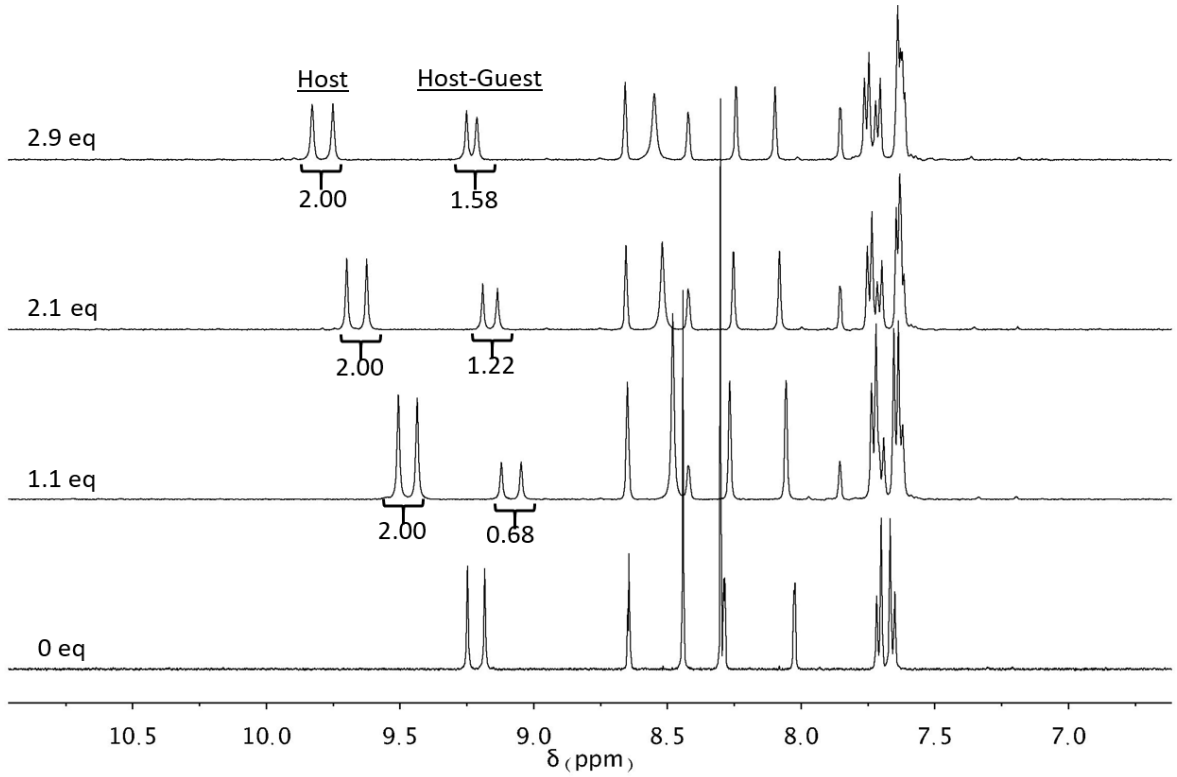

Figure S42. ^{1}H NMR titration of **7** with DDPG-TMA in 99.5% DMSO-d_6:0.5% Milli-Q H_2O at 310 K (stacked spectra plot of a representative titration). Due to slow chemical exchange on the 500 MHz NMR timescale, the binding constant was calculated by comparing integration ratios of host and host-guest complex with total concentrations of host and guest in a mass balance equation. Data was collected from three independent repeats each consisting of three measurements of increasing guest concentration. The samples were incubated for one hour between measurements.

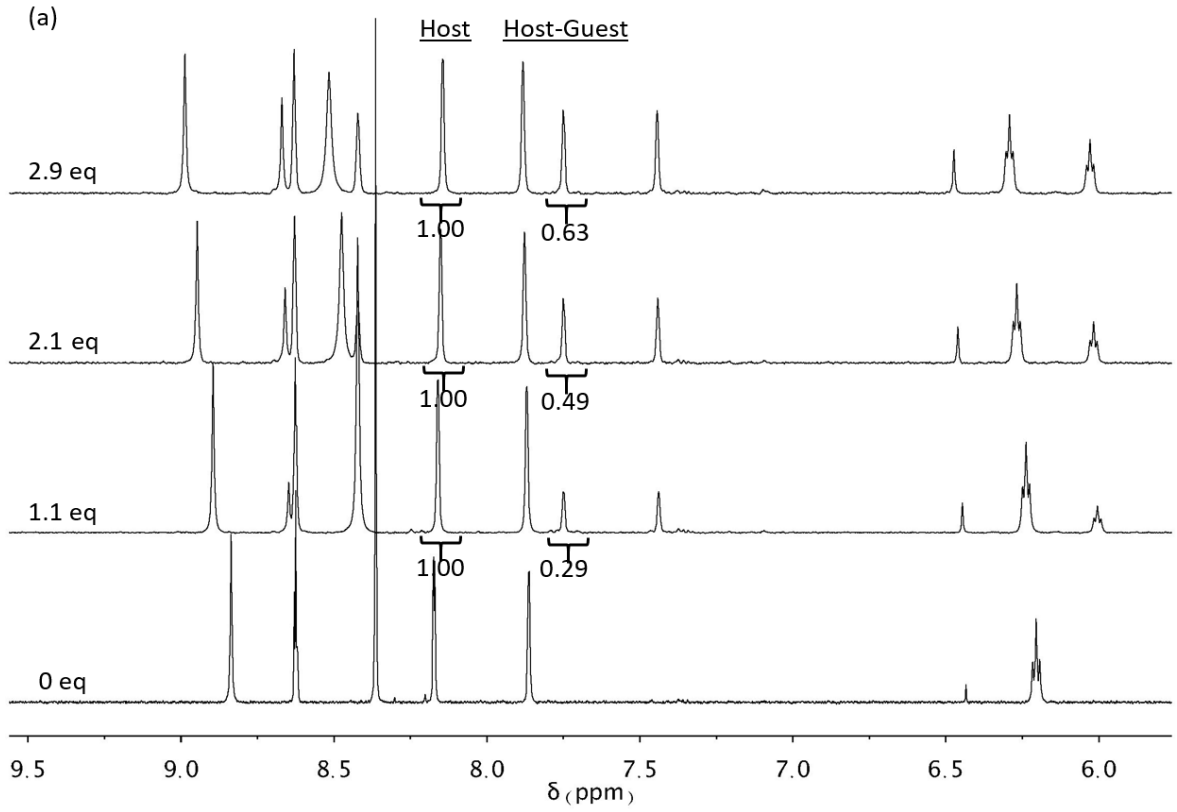

Figure S43. ^{1}H NMR titration of **8** with DDPG-TMA in 99.5% DMSO-d_6:0.5% Milli-Q H_2O at 310 K (stacked spectra plot of a representative titration). Due to slow chemical exchange on the 500 MHz NMR timescale, the binding constant was calculated by comparing integration ratios of host and host-guest complex with total concentrations of host and guest in a mass balance equation. Data was collected from three independent repeats each consisting of three measurements of increasing guest concentration. The samples were incubated for one hour between measurements.

S5. Fluorescent Alizarin Red S Assay

S5.1. Experimental procedure of the ARS assay

To measure the K_a of BA with POPG, a dye displacement assay was used whereby the PG lipids can displace the ARS dye bound to the boronic acids. First, the association constant between boronic acids **1-8** or **PBA** and Alizarin Red S (K_{ars}) had to be obtained. This titration used three separate solutions: a reference solution of HEPES buffer (10 mM HEPES, 150 mM NaCl, 1% DMSO, pH 7.4), a host solution of 35 µM ARS in HEPES buffer, and a host-guest solution which contained 35 µM ARS and 200 µM BA in HEPES buffer. To start the titration, 2 mL of the ARS solution was added to a 65 mm tall cuvette with 10 mm pathlength containing a stir bar. The cuvette was placed in an Agilent Cary 100 UV-Vis spectrophotometer, zeroed, and the absorbance spectrum was obtained at 25˚C with background correction (buffer only). Aliquots of the host-guest solution were added, and the mixture was allowed to incubate for 3 minutes before the resulting change in absorbance was measured. This was repeated 13 times until a final volume of 3.4 mL was reached. The absorbance at λ =514 nm of each run was then plotted against the concentrations of ARS and BA and analyzed using Bindfit to determine the K_{ars}. The reported results are the average of three repeats with the error representing the standard deviation. Due to the limited solubility of compound **1**, the titration was performed using 100 µM BA. Due to complete insolubility of **2** in this solvent system, compound **2** was not measured. The results are shown in section S5.2. The obtained K_{ars} values are given in the main manuscript. Interestingly, the natural logarithm of the obtained K_{ars} values shows a parabolic relationship with the pK_a of the BAs (**Figure S44**), confirming the importance of an optimal pK_a for the binding of BAs to a specific diol.

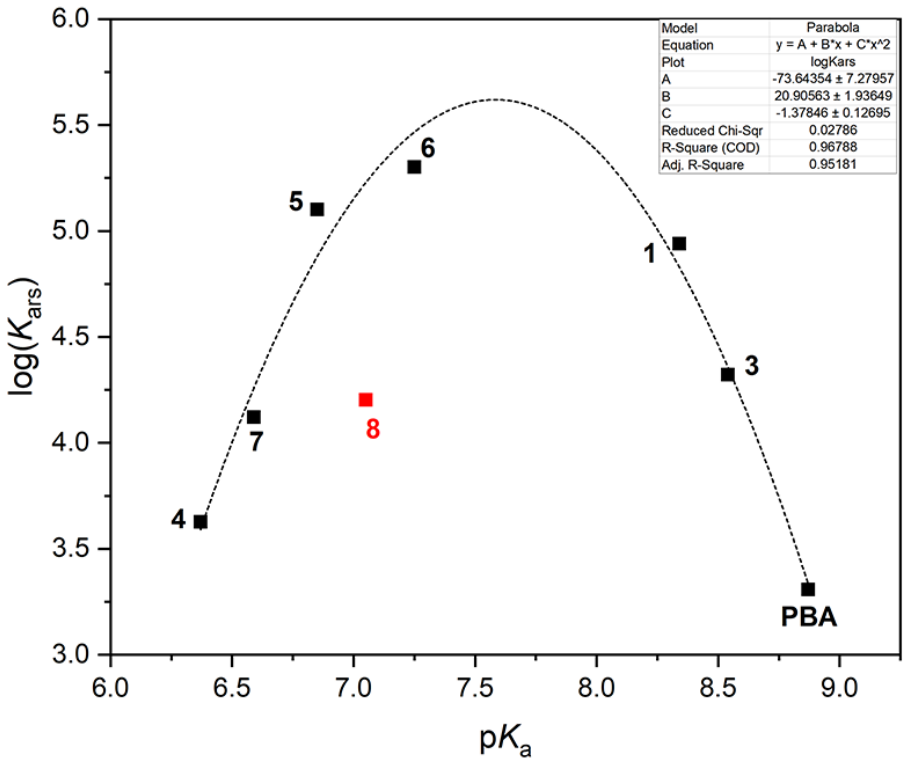

Figure S44. Relationship between the logarithm of the equilibrium constant between the BA and the ARS dye (logK_{ars}) and the pK_a of the boronic acids. Compound **2** was not soluble enough to measure K_{ars}.

Once the K_{ars} values were obtained, the association constant of the boronic acids with PG lipids could be determined using an ARS displacement assay. This assay also required three solutions and the same buffer conditions were used as the K_{ars} determination, to ensure the results were accurate. The first solution contained 10 µM ARS in HEPES buffer (10 mM HEPES, 150 mM NaCl, 1% DMSO, pH 7.4). The second solution contained 10 µM ARS and 125 µM BA in HEPES Buffer (100 µM for compound **1**). The third solution contained 20 mM POPG or POPC small unilamellar vesicles (SUVs) in HEPES buffer. To prepare the SUVs, lipid from a chloroform stock solution (25 mg/mL POPC or POPG) was transferred to a pre-weighed vial. The chloroform was evaporated by a gentle stream of nitrogen gas and the lipid formed a film on the glass. The vial was then dried overnight under high vacuum. The next day, the dried lipid film was weighed and hydrated in HEPES buffer to achieve a final concentration of 20 mM lipid. The lipid solution was sonicated for 30 minutes, followed by extrusion through a 50 nm polycarbonate membrane (*Nucleopore*) using a mini-extruder set (*Avanti Polar Lipids, Inc*.) for a total of 21 times. For the experiment, 2 mL of the BA and ARS solution was added to a clean fluorescence cuvette containing a stir bar. The baseline fluorescence was scanned with an excitation wavelength of λ = 478 nm. Then, 20 µL of liposomes (20 mM) was added and allowed to mix for 3 minutes before measuring the change in fluorescence. This was repeated 10 times. A control whereby the liposomes were added to a solution of only ARS in HEPES buffer (no boronic acid) was also measured and the obtained spectra were subtracted from each liposome addition to account for the scattering of light due to the liposomes and potential partitioning of free ARS into the liposomes. The relative fluorescence at λ = 582 nm was recorded and processed with the formulas (6) and (7), adapted Wang *et al*.[6]

$$Q = \frac{I_{f*BAARS} - I_{f*}}{I_{f*}} \qquad (6)$$

$$P = [BA]_0 - \frac{1}{QK_{ARS}} - \frac{[ARS]_0}{1+Q} \qquad (7)$$

Formula (6) describes Q which is obtained from the fluorescence intensities at λ = 582 nm. $I_{f*BAARS}$ is the initial fluorescence in the absence of competing diol, with background subtracted (background was measured from a solution of free ARS (no boronic acid or liposomes present) in HEPES buffer). I_{f*} is the fluorescence intensity in the presence of lipid, with liposomes scattering subtracted. For the liposome scattering, a parallel titration was performed whereby a matching aliquot of 50 nm POPG (or POPC) liposomes was added to a solution containing free ARS in HEPES buffer (no boronic acid). This correction factor is therefore different for each data point and takes into account both liposome scattering and partitioning of free ARS into the liposome membrane (if any). From Q, we can calculate value P according to formula (7). A plot of [Lipid]/P vs Q allows the determination of the association constant between BA and the lipid (K_a) from the slope, as given by formula (8). Ultimately, only the last five lipid additions (120-200 µL) were used to calculate the slope. In theory, the intercept should be 1, but this is usually not the case.[7] The obtained K_a values are given in main manuscript, and the graphs are shown in section S5.3 and S5.4.

$$\frac{[Lipid]_0}{P} = \frac{K_{ars}}{K_a}Q + 1 \qquad (8)$$

S5.2. Determination of K_a between ARS and the boronic acids

The results of the UV-Vis titrations to determine the association constant between the boronic acids and ARS are shown below. A clear, single isosbestic point is observed in all cases, confirming a 1:1 stoichiometry of the interaction. Compound **2** was not soluble enough for the conditions of the titration.

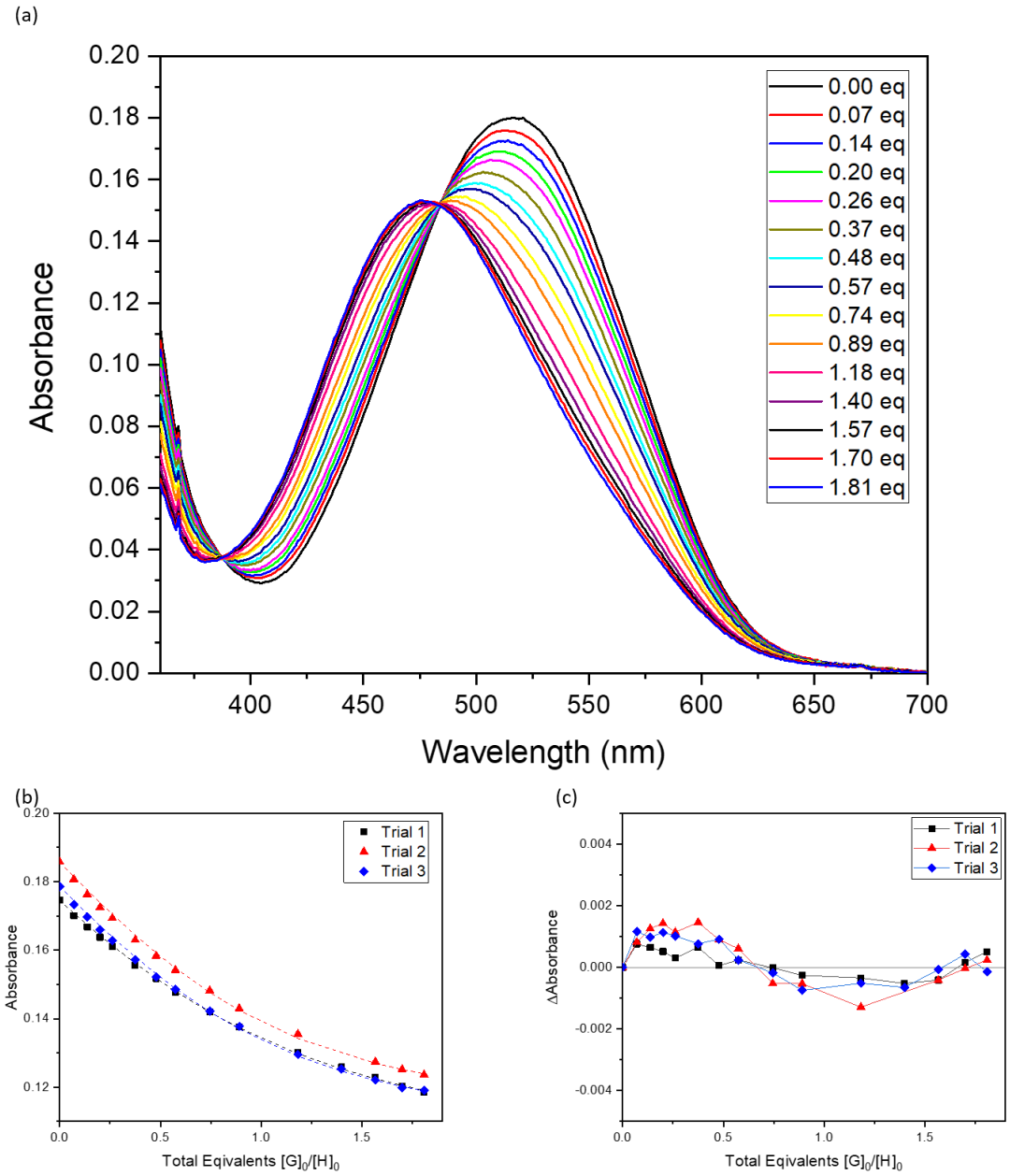

Figure S45. UV-Vis titration of ARS with **1** in 10 mM HEPES, 150 mM NaCl, 1% DMSO, pH 7.4 at 298 K. (a) Stacked spectra plot of a representative titration. (b) Fitplot using global analysis and 1:1 binding stoichiometry. The symbols of each trial report the absorbance at λ =514 nm and the dashed lines represent the calculated fit of each curve. Data from 3 independent repeats are overlaid. (c) Plot of the residuals using global analysis and 1:1 binding stoichiometry. Data from 3 independent repeats are overlaid.

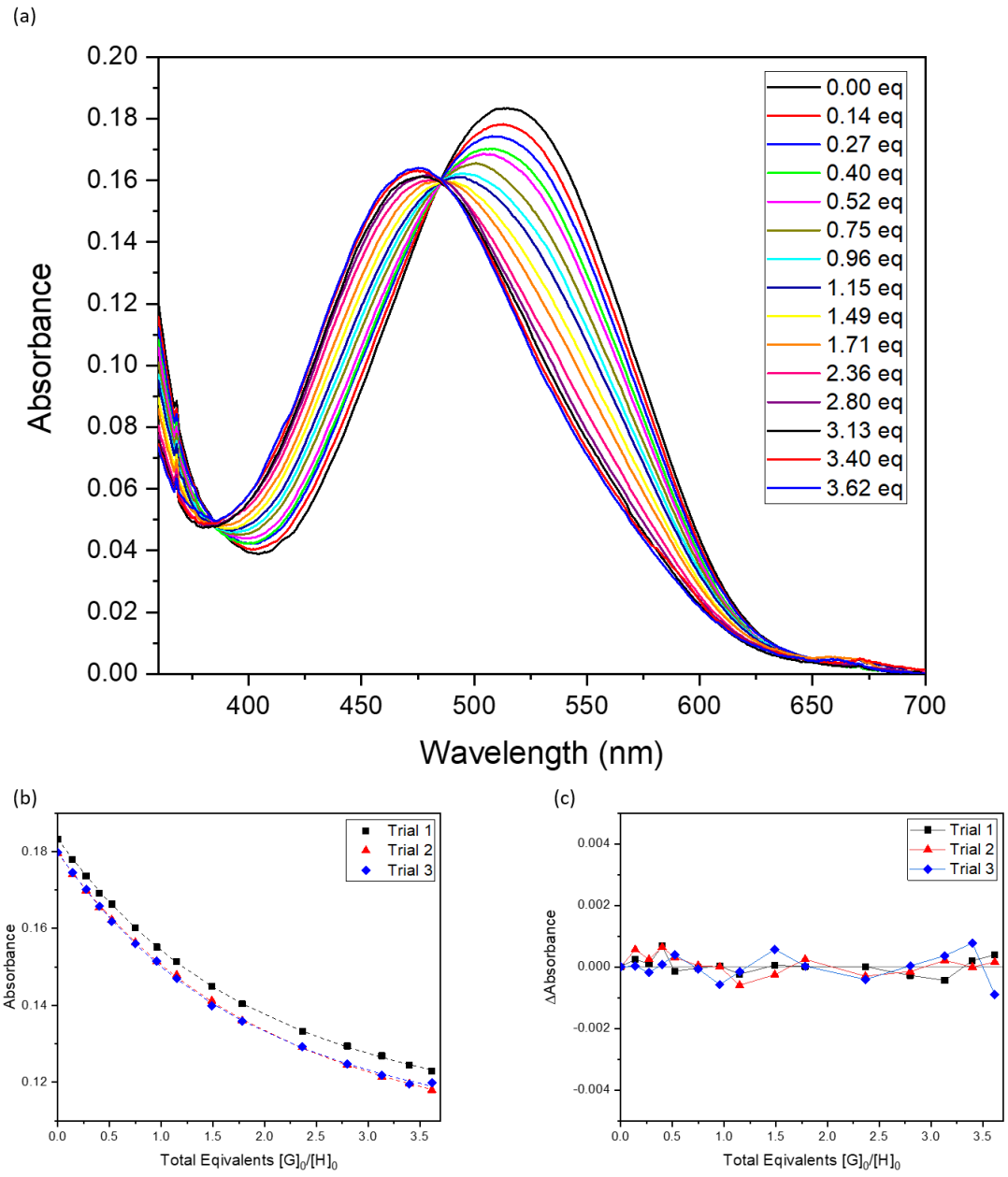

Figure S46. UV-Vis titration of ARS with **3** in 10 mM HEPES, 150 mM NaCl, 1% DMSO, pH 7.4 at 298 K. (a) Stacked spectra plot of a representative titration. (b) Fitplot using global analysis and 1:1 binding stoichiometry. The symbols of each trial report the absorbance at λ = 514 nm and the dashed lines represent the calculated fit of each curve. Data from 3 independent repeats are overlaid. (c) Plot of the residuals using global analysis and 1:1 binding stoichiometry. Data from 3 independent repeats are overlaid.

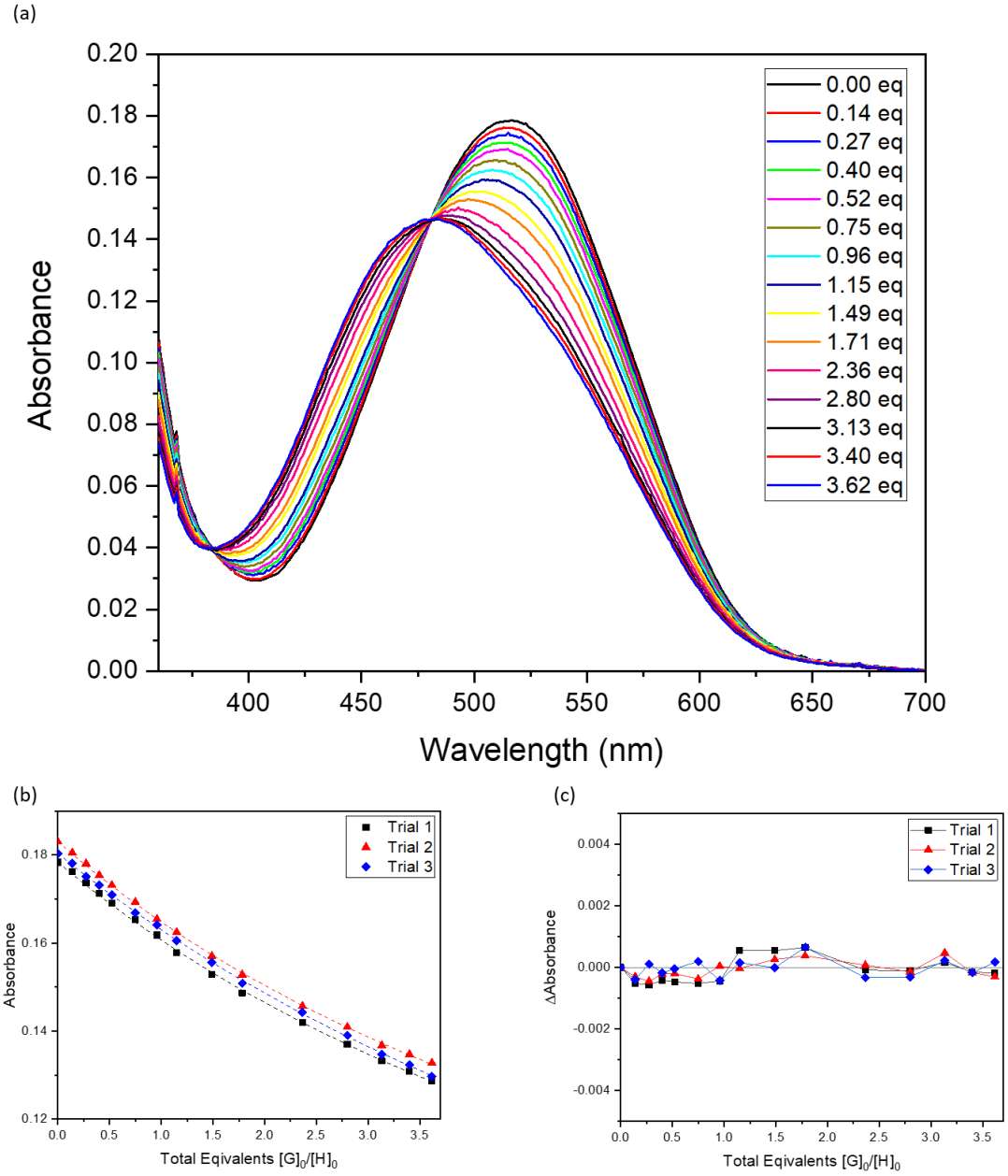

Figure S47. UV-Vis titration of ARS with **4** in 10 mM HEPES, 150 mM NaCl, 1% DMSO, pH 7.4 at 298 K. (a) Stacked spectra plot of a representative titration. (b) Fitplot using global analysis and 1:1 binding stoichiometry. The symbols of each trial report the absorbance at λ = 514 nm and the dashed lines represent the calculated fit of each curve. Data from 3 independent repeats are overlaid. (c) Plot of the residuals using global analysis and 1:1 binding stoichiometry. Data from 3 independent repeats are overlaid.

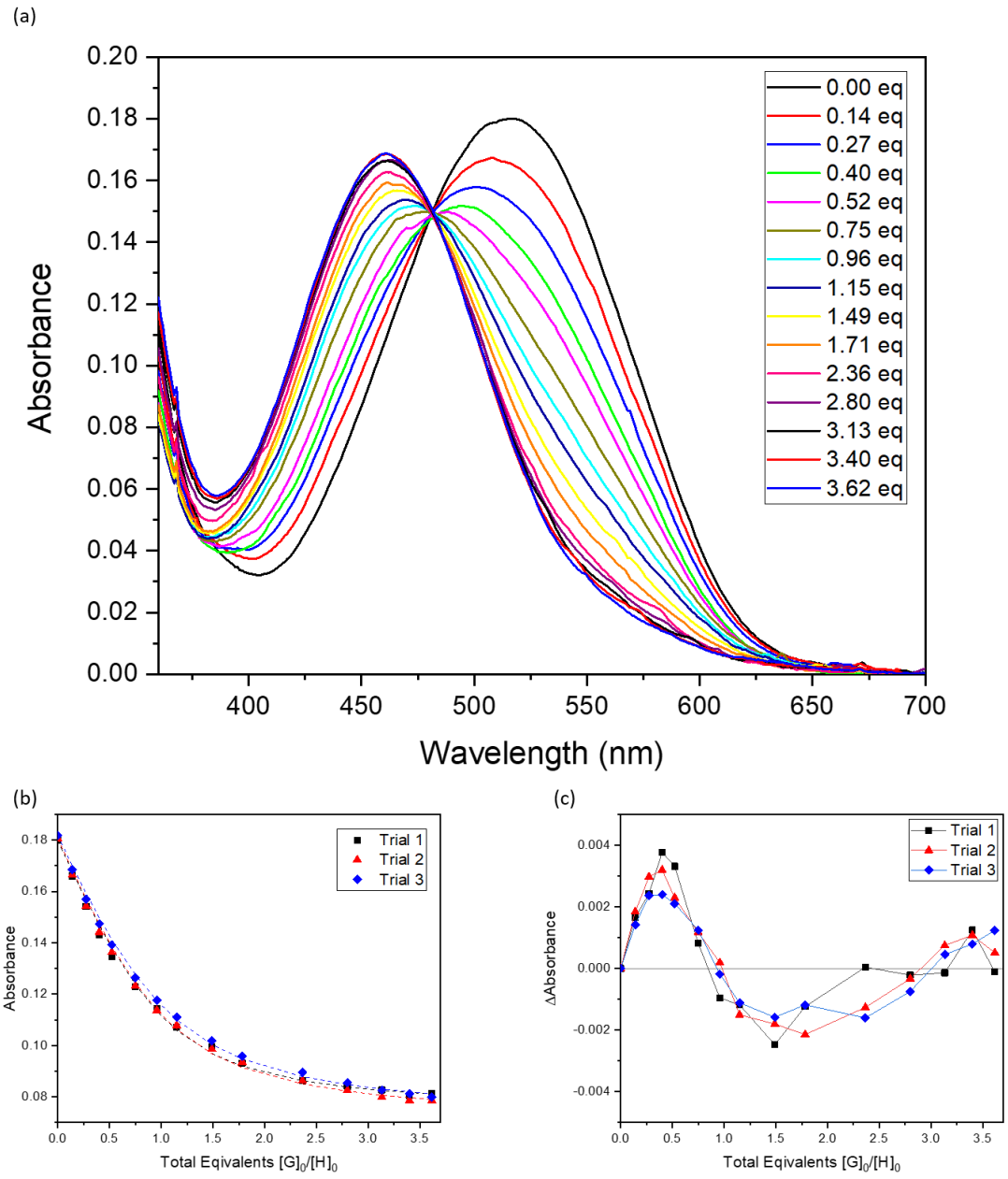

Figure S48. UV-Vis titration of ARS with **5** in 10 mM HEPES, 150 mM NaCl, 1% DMSO, pH 7.4 at 298 K. (a) Stacked spectra plot of a representative titration. (b) Fitplot using global analysis and 1:1 binding stoichiometry. The symbols of each trial report the absorbance at λ = 514 nm and the dashed lines represent the calculated fit of each curve. Data from 3 independent repeats are overlaid. (c) Plot of the residuals using global analysis and 1:1 binding stoichiometry. Data from 3 independent repeats are overlaid.

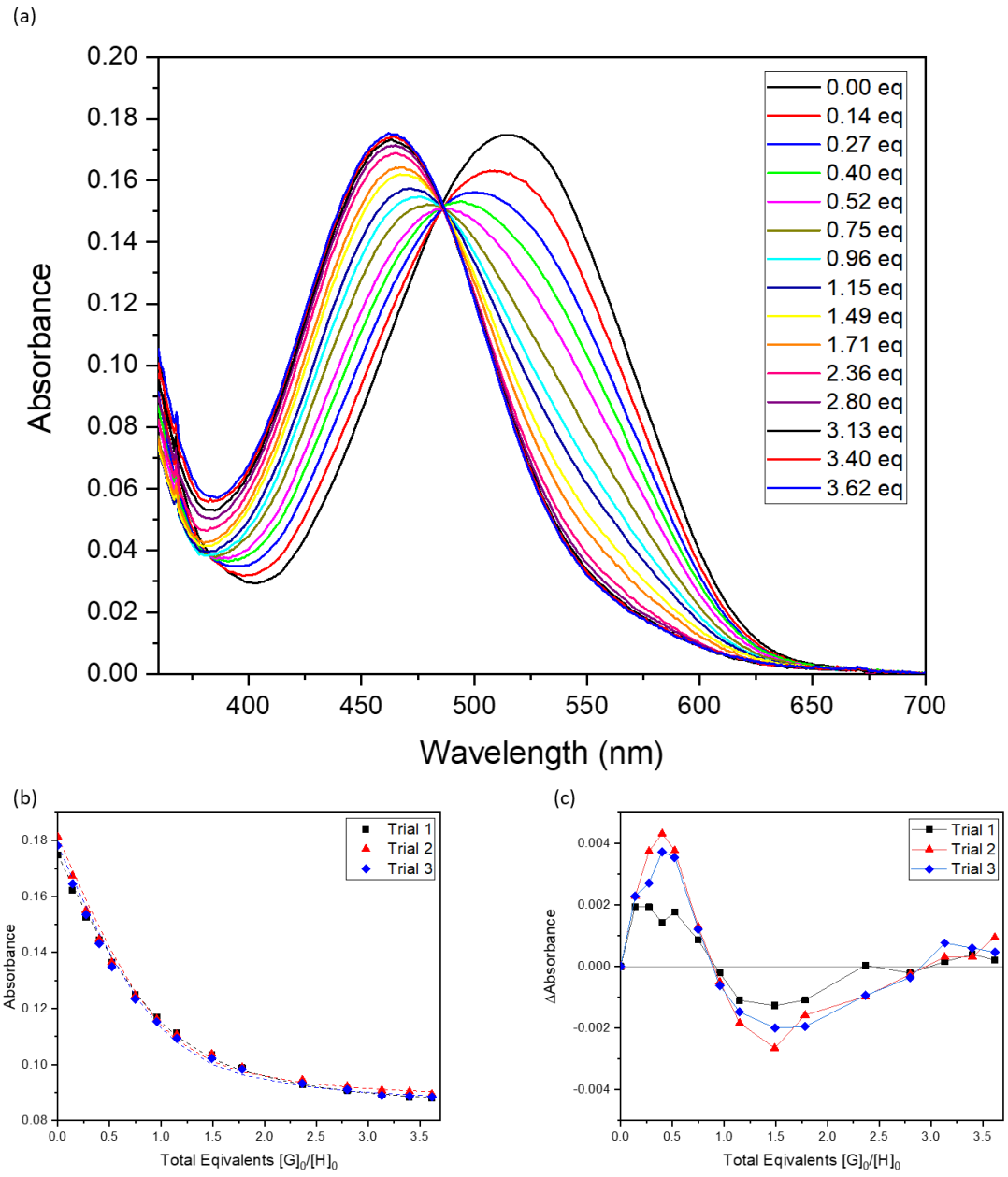

Figure S49. UV-Vis titration of ARS with **6** in 10 mM HEPES, 150 mM NaCl, 1% DMSO, pH 7.4 at 298 K. (a) Stacked spectra plot of a representative titration. (b) Fitplot using global analysis and 1:1 binding stoichiometry. The symbols of each trial report the absorbance at λ = 514 nm and the dashed lines represent the calculated fit of each curve. Data from 3 independent repeats are overlaid. (c) Plot of the residuals using global analysis and 1:1 binding stoichiometry. Data from 3 independent repeats are overlaid.

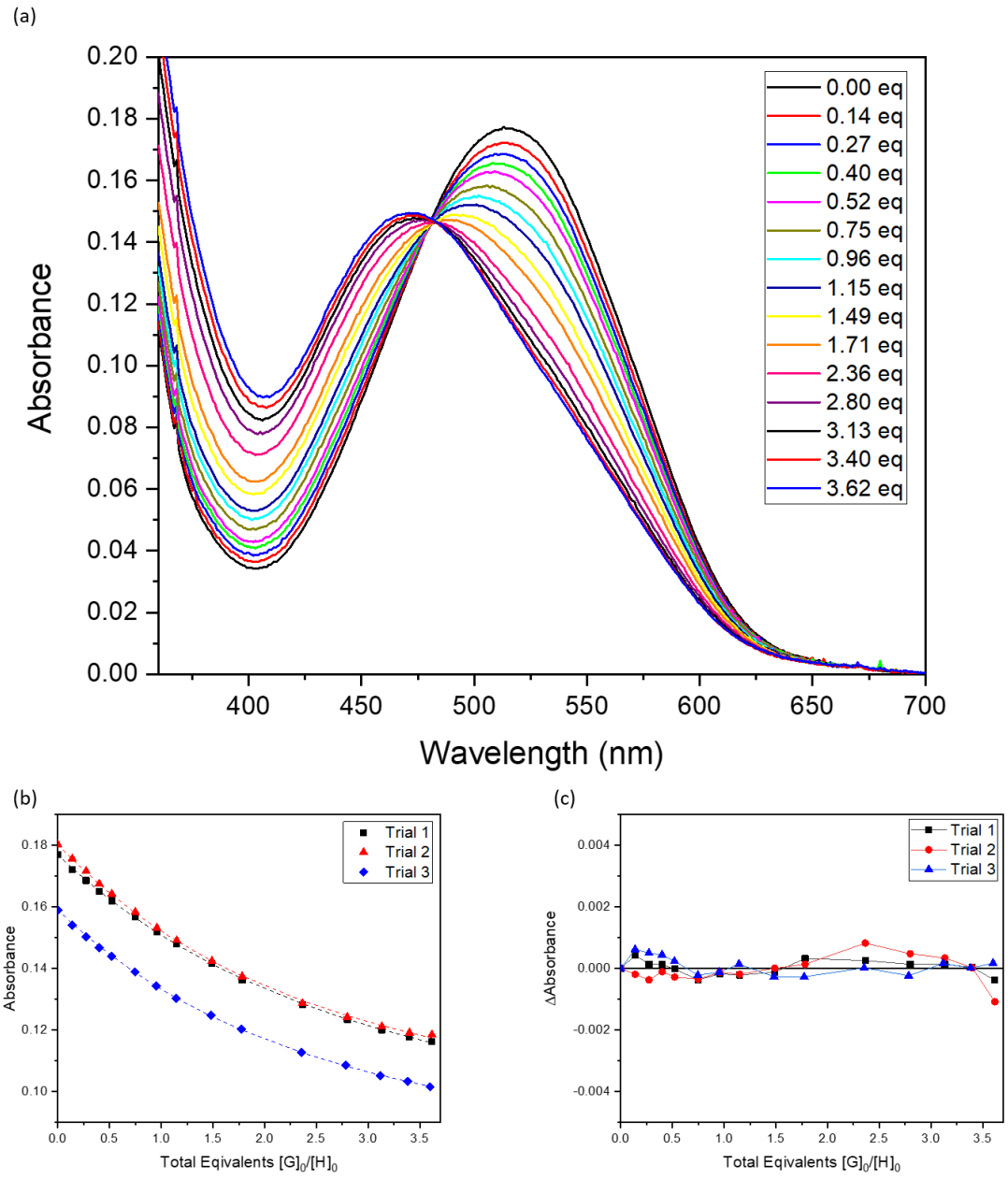

Figure S50. UV-Vis titration of ARS with **7** in 10 mM HEPES, 150 mM NaCl, 1% DMSO, pH 7.4 at 298 K. (a) Stacked spectra plot of a representative titration. (b) Fitplot using global analysis and 1:1 binding stoichiometry. The symbols of each trial report the absorbance at λ = 514 nm and the dashed lines represent the calculated fit of each curve. Data from 3 independent repeats are overlaid. (c) Plot of the residuals using global analysis and 1:1 binding stoichiometry. Data from 3 independent repeats are overlaid.

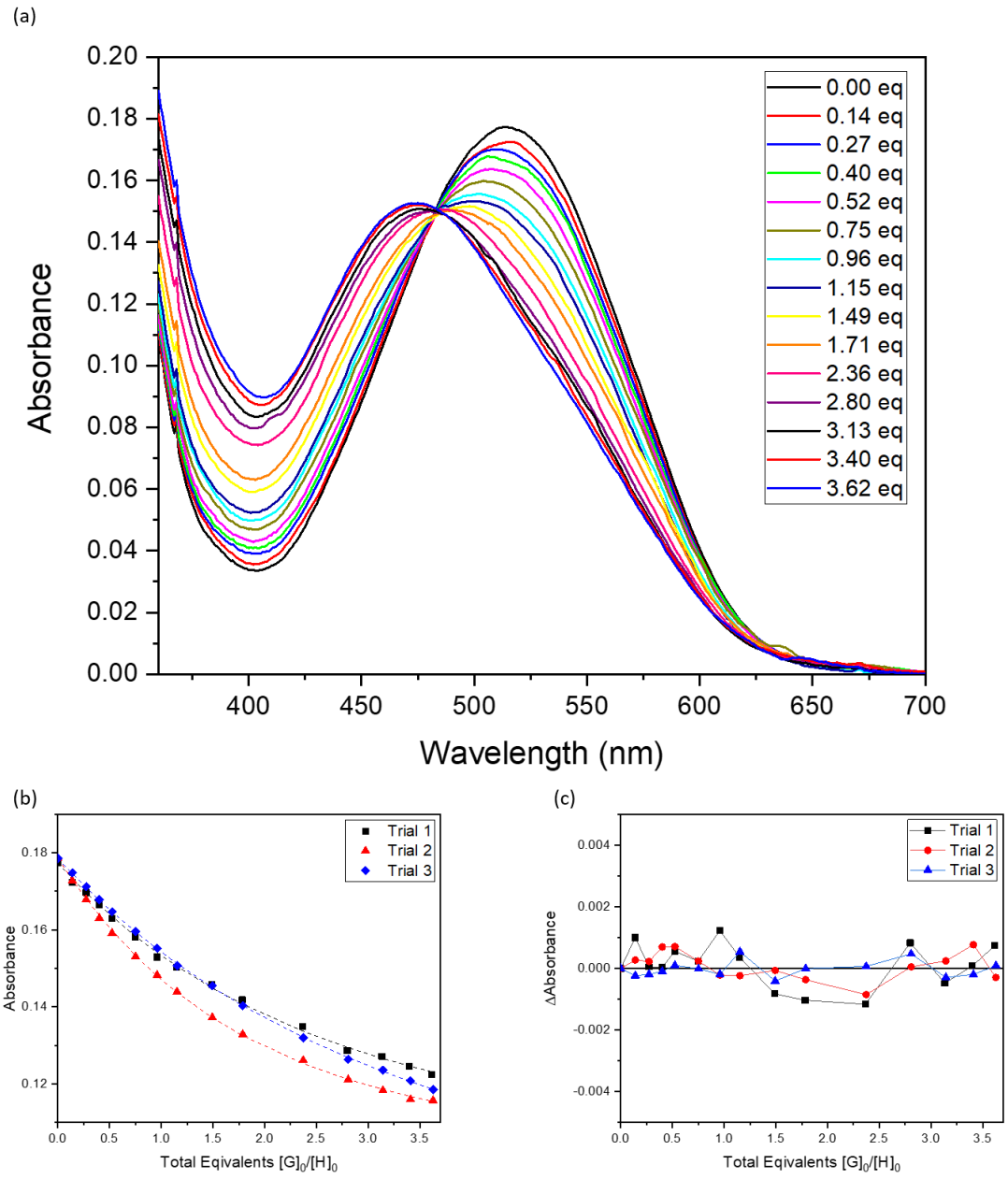

Figure S51. UV-Vis titration of ARS with **8** in 10 mM HEPES, 150 mM NaCl, 1% DMSO, pH 7.4 at 298 K. (a) Stacked spectra plot of a representative titration. (b) Fitplot using global analysis and 1:1 binding stoichiometry. The symbols of each trial report the absorbance at λ = 514 nm and the dashed lines represent the calculated fit of each curve. Data from 3 independent repeats are overlaid. (c) Plot of the residuals using global analysis and 1:1 binding stoichiometry. Data from 3 independent repeats are overlaid.

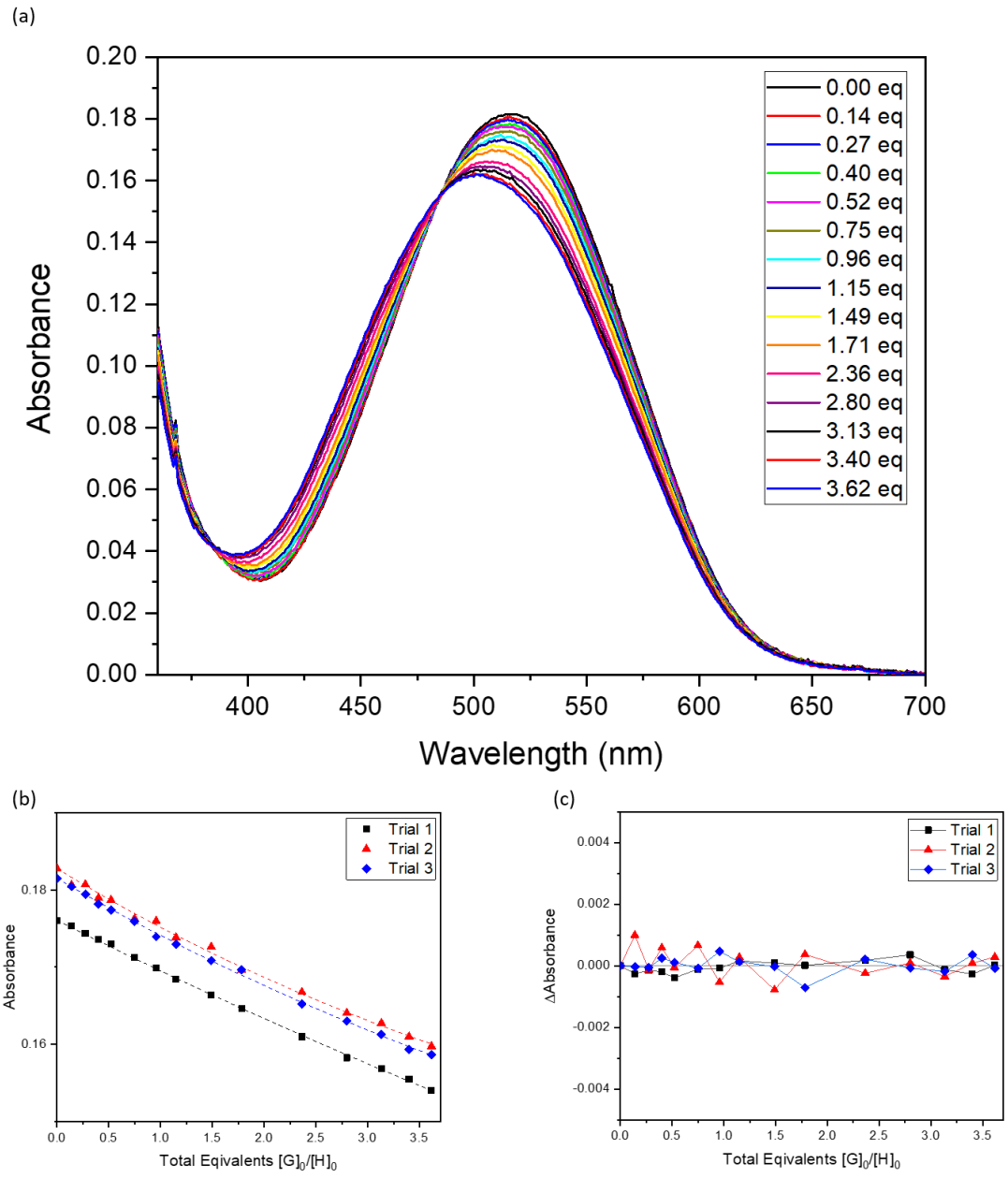

Figure S52. UV-Vis titration of ARS with **PBA** in 10 mM HEPES, 150 mM NaCl, 1% DMSO, pH 7.4 at 298 K. (a) Stacked spectra plot of a representative titration. (b) Fitplot using global analysis and 1:1 binding stoichiometry. The symbols of each trial report the absorbance at λ = 514 nm and the dashed lines represent the calculated fit of each curve. Data from 3 independent repeats are overlaid. (c) Plot of the residuals using global analysis and 1:1 binding stoichiometry. Data from 3 independent repeats are overlaid.

S5.3. Results of the ARS displacement assay with POPG liposomes

The ARS displacement assay described in section S5.1 was performed using 50 nm POPG liposomes to determine the binding of the boronic acids with PG lipids. Initially, ARS is bound to the boronic acid, giving rise to measurable fluorescence. When the PG liposomes are added, ARS is displaced from the boronic acid and the fluorescence intensity decreases. This decrease in fluorescence can be used to measure the association constant of the boronic acids with PG. In the conditions optimized for the experiment, compounds **2**, **4**, and **PBA** were unable to be analyzed. Compound **2** was not included due to insolubility in the solvent system. The ARS complex of compound **4** and **PBA** resulted in a fluorescence intensity that was too low to measure at the experimental concentrations. The fluorescence intensity of the **5**-ARS complex was much smaller than would be expected for the association constant between the two (K_{ars}). In theory, a higher K_{ars} value should result in a higher fluorescence intensity, as is seen for most of the other compounds (**Figure S53**). Compound **5**, on the other hand, had a lower fluorescence intensity than expected, potentially due to some quenching effect. It is possible that this low initial fluorescence intensity is the reason why no decrease in fluorescence is seen upon the addition of POPG liposomes to a solution of **5**-ARS (see **Figure S56**).

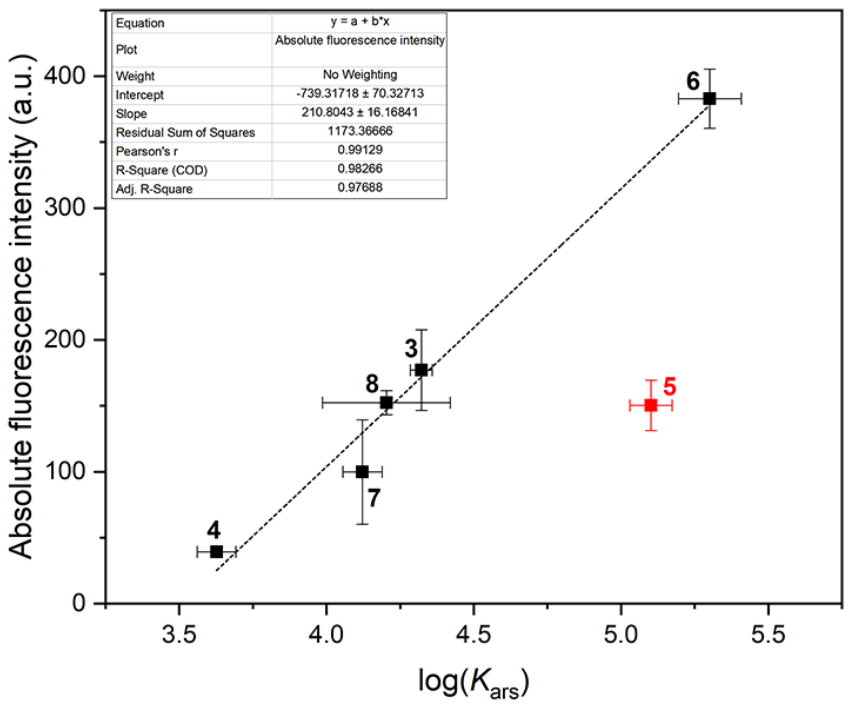

Figure S53. Plot of the absolute fluorescence intensity at λ = 582 nm upon excitation with 478 nm of a solution containing 10 µM ARS and 125 µM **1-8** in HEPES buffer (10 mM HEPES, 150 mM NaCl, 1% DMSO) at 298 K, against the log(K_{ars}) value of the given boronic acid. The settings of the fluorometer were identical for all experiments. A linear relationship is found for all compounds, except boronic acid **5**. BAs **1** and **2** were not soluble at the given conditions.

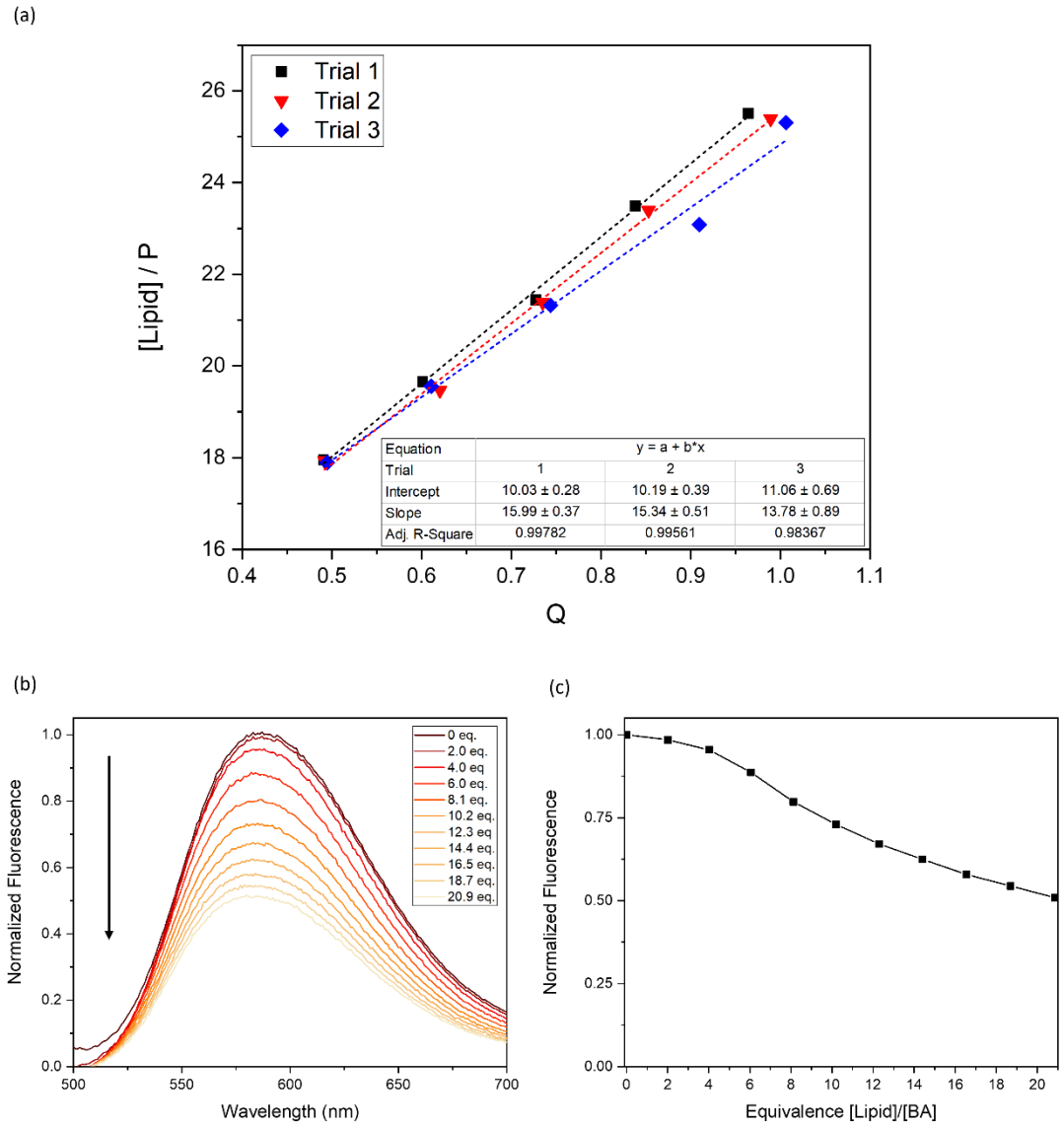

Figure S54. (a) Fluorescence competition assay of 10 µM ARS and 100 µM **1** with 50 nm POPG liposomes in HEPES buffer (10 mM HEPES, 150 mM NaCl, 1% DMSO) at 298 K. The last five liposome additions were processed with the approximation formula to derive an association constant between **1** and POPG. (b) Entire normalized fluorescence titration spectra. The relative fluorescence was normalized by dividing every value with the maxima value at λ = 582 nm of the first run containing 0 eq. POPG (c) Normalized fluorescence maxima at λ = 582 nm plotted against the equivalents of [Lipid]/[BA].

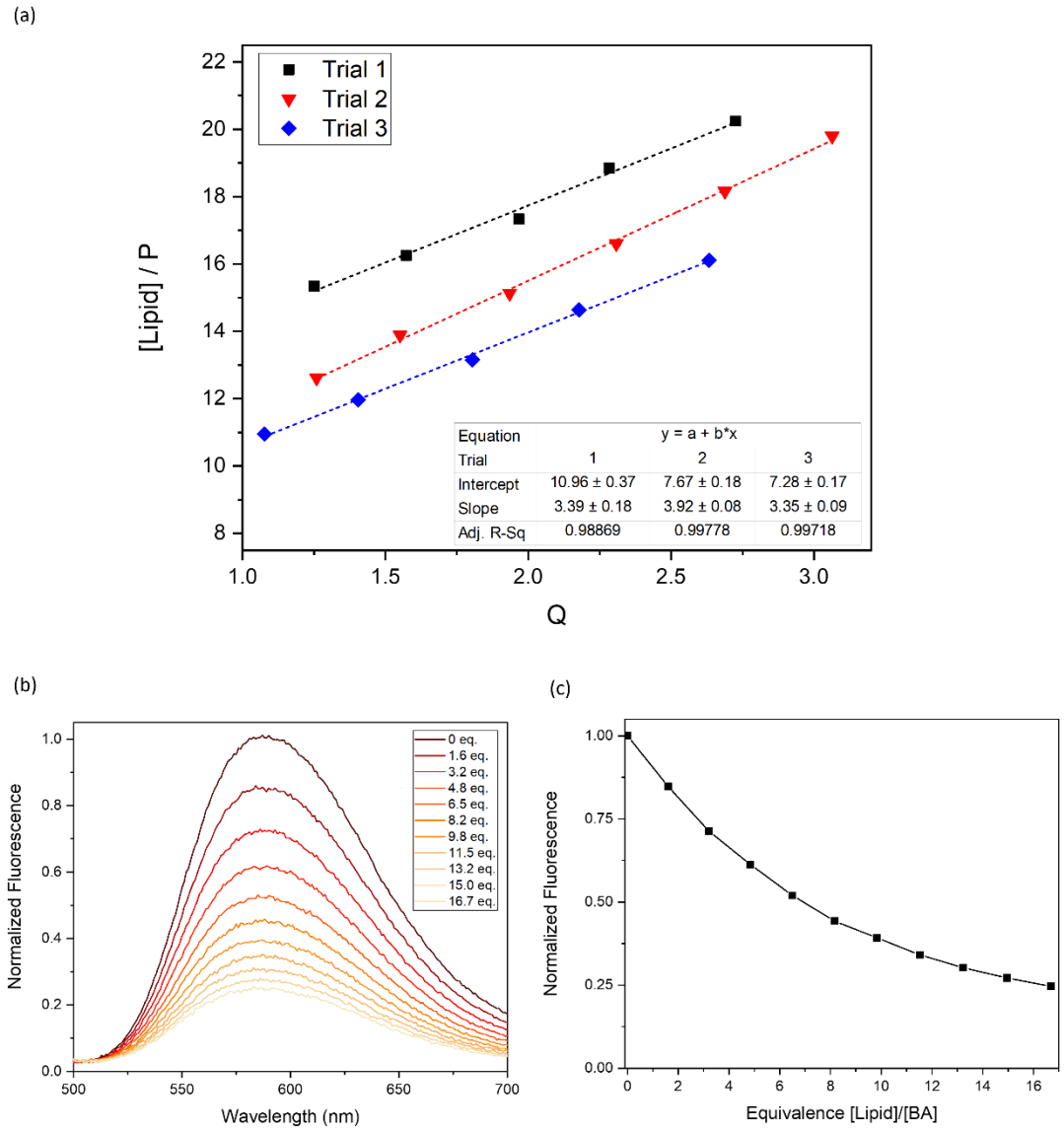

Figure S55. (a) Fluorescence competition assay of 10 μM ARS and 125 μM **3** with, 50 nm POPG liposomes in HEPES buffer (10 mM HEPES, 150 mM NaCl, 1% DMSO) at 298 K. The last five liposome additions were processed with the approximation formula to derive an association constant between **3** and POPG. (b) Entire normalized fluorescence titration spectra. The relative fluorescence was normalized by dividing every value with the maxima value at λ = 582 nm of the first run containing 0 eq. POPG (c) Normalized fluorescence maxima at λ = 582 nm plotted against the equivalents of [Lipid]/[BA].

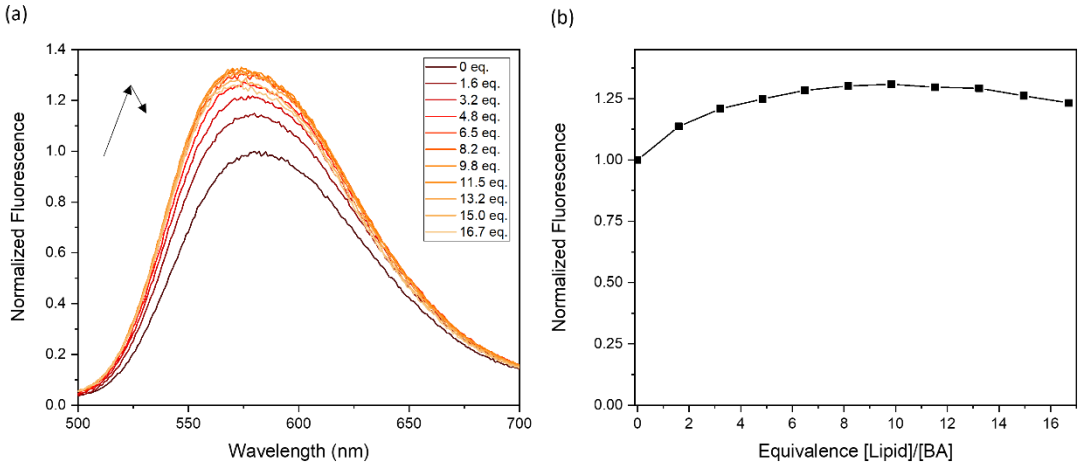

Figure S56. (a) Fluorescence competition assay of 10 µM ARS and 125 µM **5** with 50 nm POPG liposomes in HEPES buffer (10 mM HEPES, 150 mM NaCl, 1% DMSO) at 298 K. The relative fluorescence was normalized by dividing every value with the maxima value at λ = 582 nm of the first run containing 0 eq. POPG (c) Normalized fluorescence maxima at λ = 582 nm plotted against the equivalents of [Lipid]/[BA]. An increase in fluorescence intensity is seen, rather than the expected decrease.

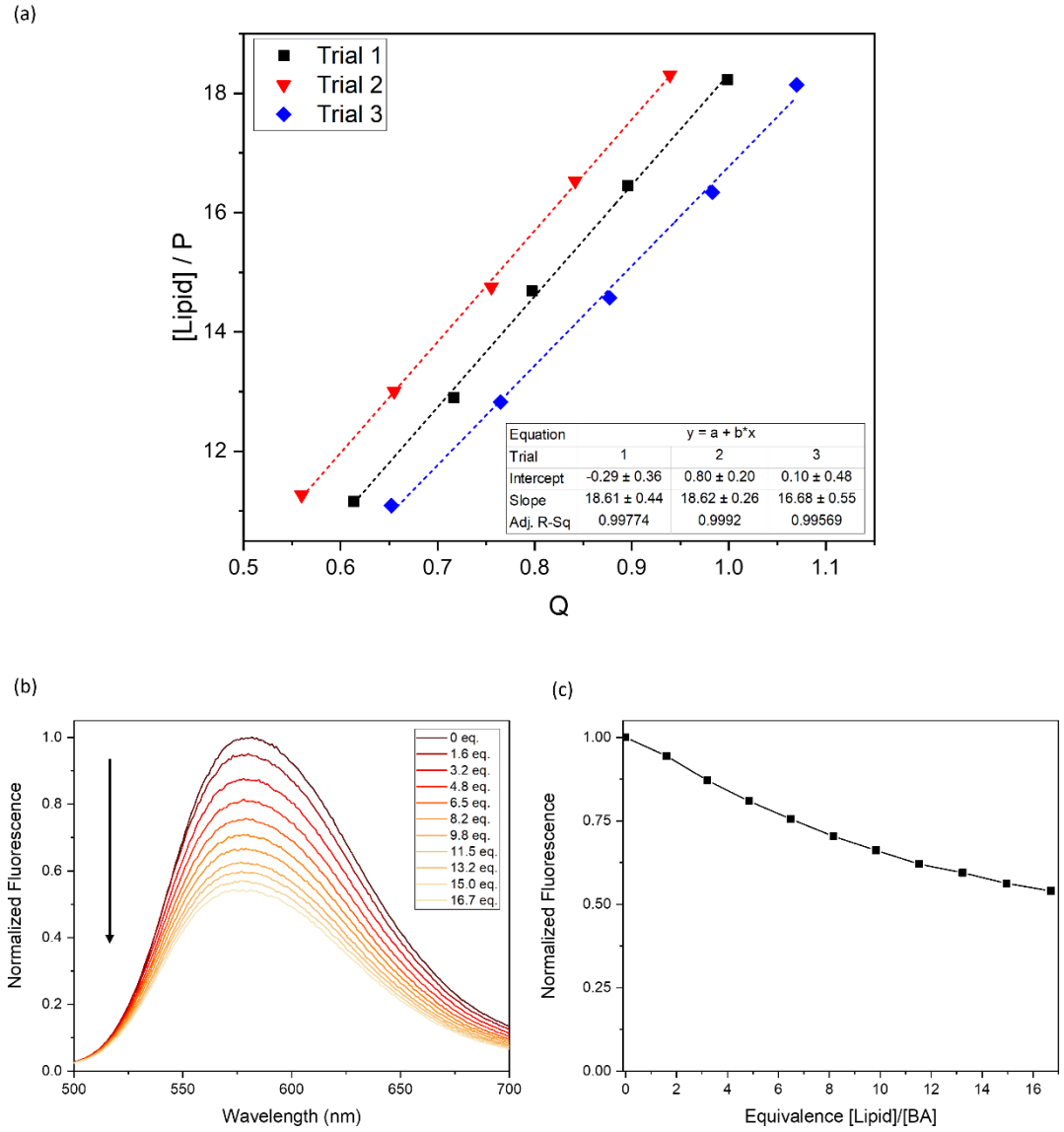

Figure S57. (a) Fluorescence competition assay of 10 µM ARS and 125 µM **6** with 50 nm POPG liposomes in HEPES buffer (10 mM HEPES, 150 mM NaCl, 1% DMSO) at 298 K. The last five liposome additions were processed with the approximation formula to derive an association constant between **6** and POPG. (b) Entire normalized fluorescence titration spectra. The relative fluorescence was normalized by dividing every value with the maxima value at λ = 582 nm of the first run containing 0 eq. POPG (c) Normalized fluorescence maxima at λ = 582 nm plotted against the equivalents of [Lipid]/[BA].

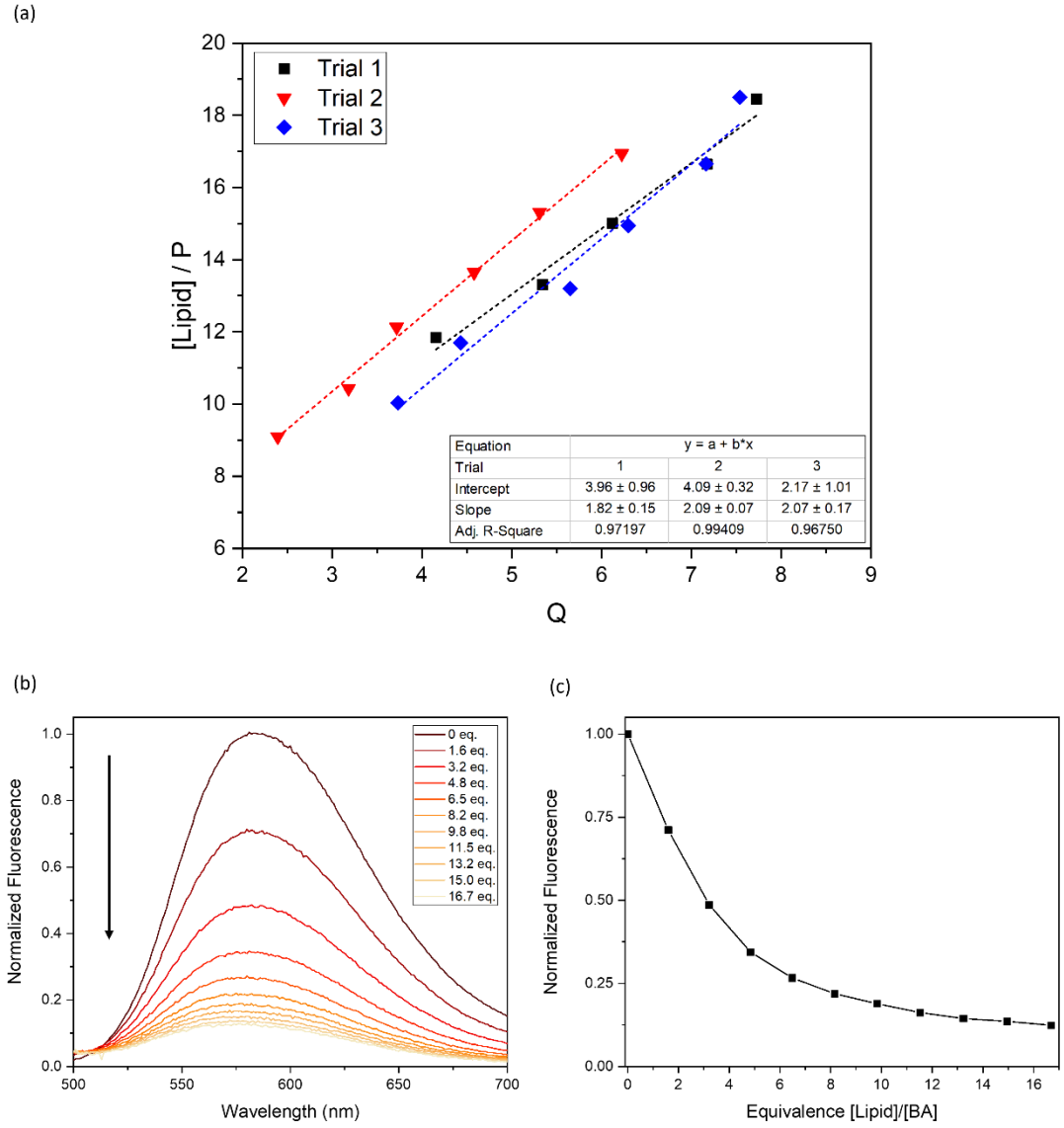

Figure S58 (a) Fluorescence competition assay of 10 µM ARS and 125 µM **7** with 20 mM, 50 nm POPG liposomes in HEPES buffer (10 mM HEPES, 150 mM NaCl, 1% DMSO) at 298 K. The last five liposome additions were processed with the approximation formula to derive an association constant between BA and POPG. (b) Entire normalized fluorescence titration spectra. The relative fluorescence was normalized by dividing every value with the maxima value at λ = 582 nm of the first run containing 0 eq. POPG (c) Normalized fluorescence maxima at λ = 582 nm plotted against the equivalents of [Lipid]/[BA].

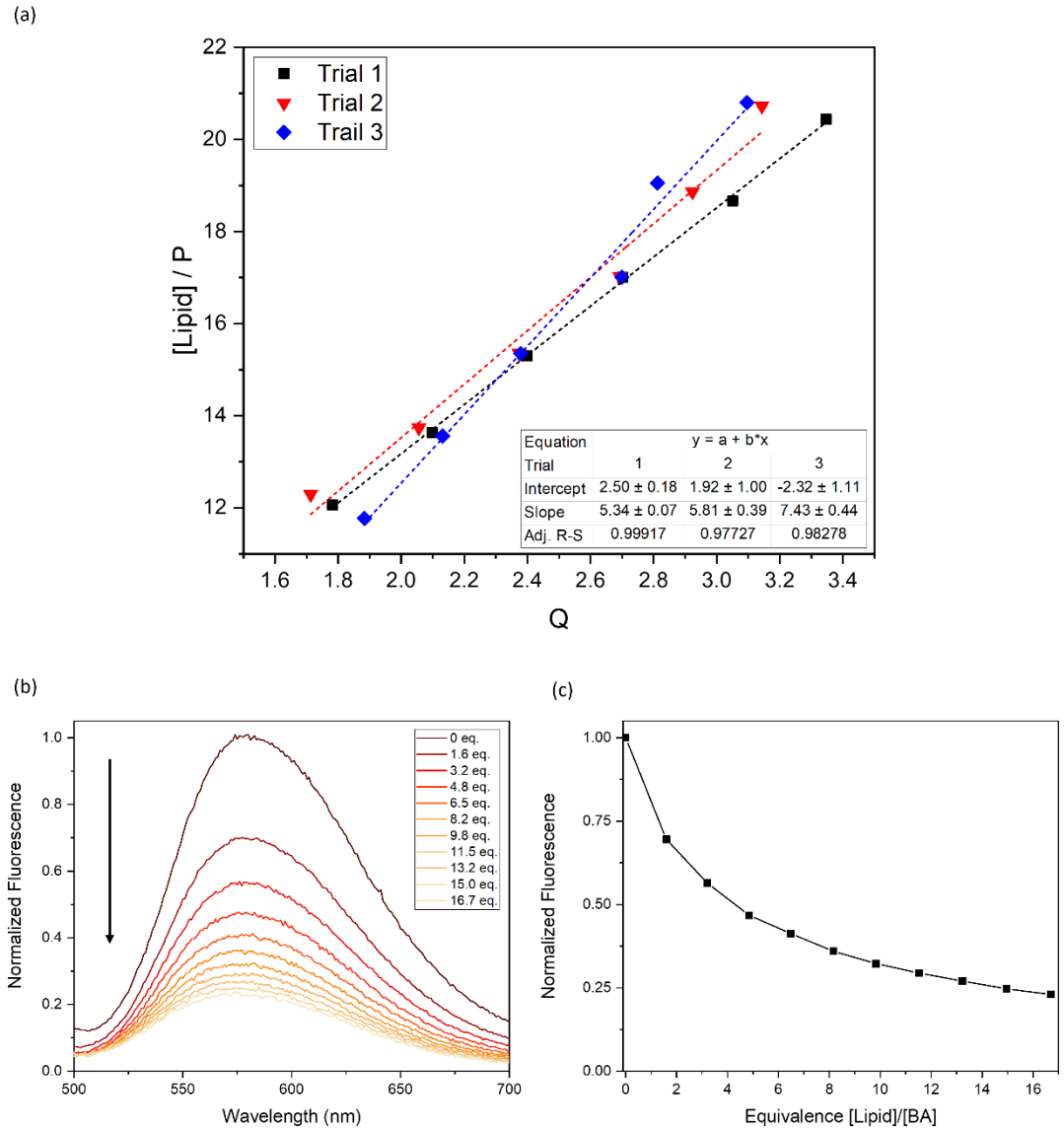

Figure S59. (a) Fluorescence competition assay of 10 µM ARS and 125 µM **8** with 20 mM, 50 nm POPG liposomes in HEPES buffer (10 mM HEPES, 150 mM NaCl, 1% DMSO) at 298 K. The last five liposome additions were processed with the approximation formula to derive an association constant between **8** and POPG. (b) Entire normalized fluorescence titration spectra. The relative fluorescence was normalized by dividing every value with the maxima value at λ = 582 nm of the first run containing 0 eq. POPG (c) Normalized fluorescence maxima at λ = 582 nm plotted against the equivalents of [Lipid]/[BA].

S5.4. Results of the ARS displacement assay with POPC liposomes

As a control, the ARS displacement assay was also performed using POPC liposomes. The boronic acids do not bind to PC lipids and ARS cannot be displaced. Therefore, there is no decrease in fluorescence intensity. Instead, the addition of POPC liposomes leads to an increase in fluorescence because the ARS-BA complex partitions into the non-polar environment of the liposome membrane, leading to a significant increase in fluorescence. The increase in fluorescence intensity is much more pronounced than when the liposomes are added to a solution of ARS only (no boronic acid), as shown in **Figure S60** and **Figure S61**, indicating that liposome scattering or partitioning of free ARS into liposome membranes is not the cause for the increase in fluorescence intensity. Instead, the increase is due to the partitioning of the BA-ARS complex, without displacement of the ARS dye.

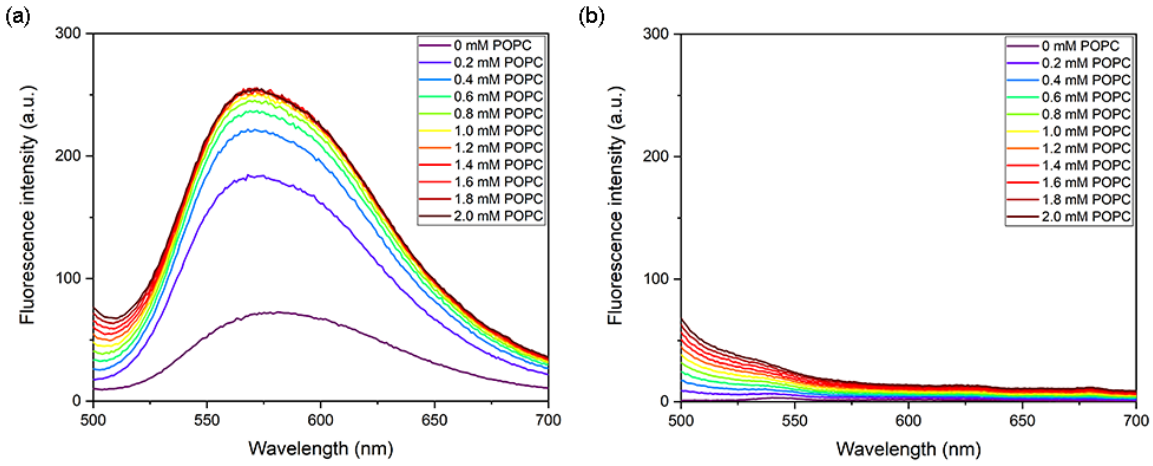

Figure S60. Limited scattering by POPC liposomes. (a) Absolute fluorescence intensity of a titration of 50 nm POPC liposomes into a solution of 10 µM ARS and 125 µM **6** in HEPES buffer (10 mM HEPES, 150 mM NaCl, 1% DMSO, pH 7.4) at 298 K, showing large increase in fluorescence due to partitioning of **6**-ARS complex into the POPC membranes. (b) Parallel titration of 50 nm POPC liposomes into a solution of 10 µM ARS in HEPES buffer (10 mM HEPES, 150 mM NaCl, 1% DMSO, pH 7.4) at 298 K, showing limited effect of liposome scattering and partitioning of free ARS into the liposomes.

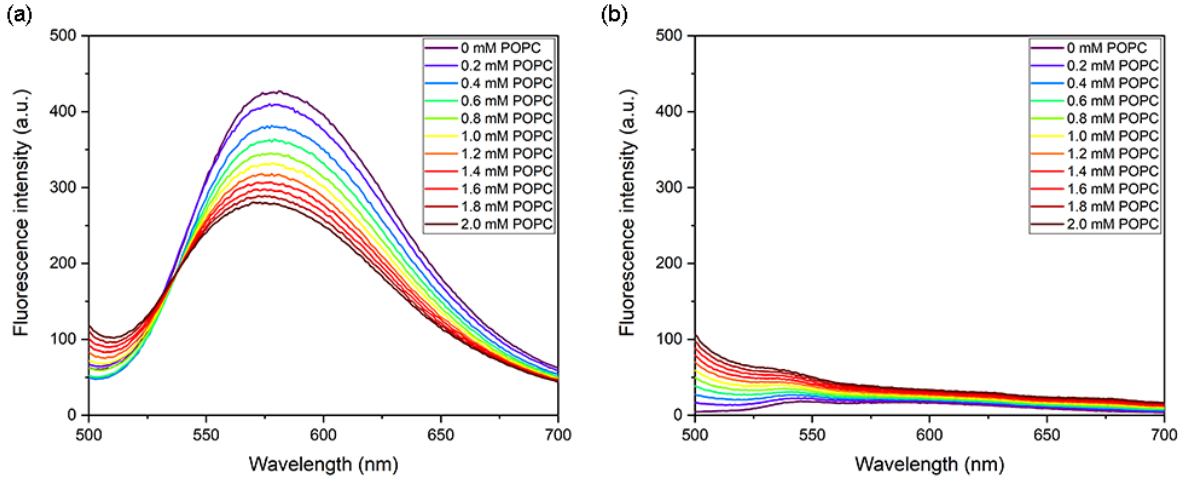

Figure S61. Limited scattering by POPG liposomes. (a) Absolute fluorescence intensity of a titration of 50 nm POPG liposomes into a solution of 10 µM ARS and 125 µM **6** in HEPES buffer (10 mM HEPES, 150 mM NaCl, 1% DMSO, pH 7.4) at 298 K, showing a decrease in fluorescence due to binding of **6** to the PG headgroup and displacement of ARS. (b) Parallel titration of 50 nm POPG liposomes into a solution of 10 µM ARS in HEPES buffer (10 mM HEPES, 150 mM NaCl, 1% DMSO, pH 7.4) at 298 K, showing limited effect of liposome scattering and partitioning of free ARS into the liposomes.

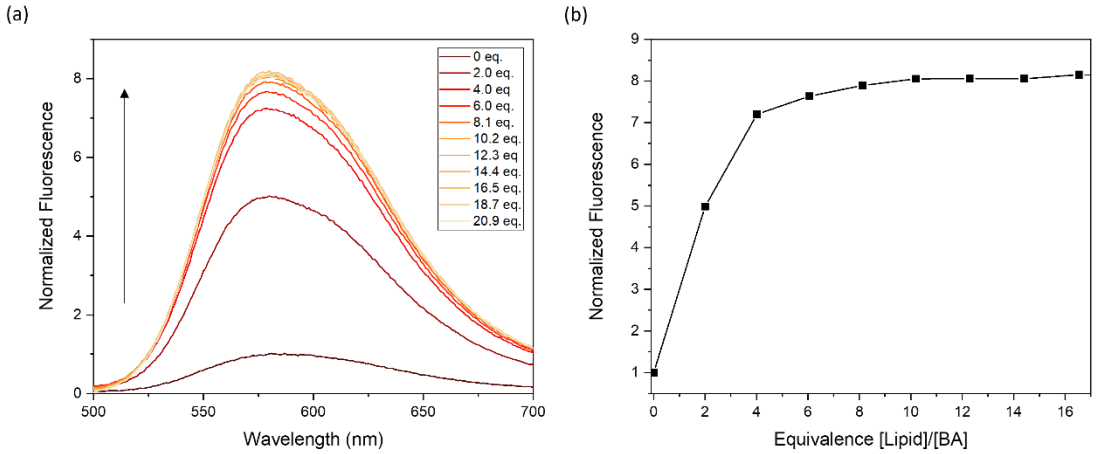

Figure S62. (a) Fluorescence titration of 10 µM ARS and 100 µM **1** with 20 mM POPC liposomes (50 nm diameter) in HEPES buffer (10 mM HEPES, 150 mM NaCl, 1% DMSO, pH 7.4) at 298 K. Fluorescence values were normalized by dividing each value with the maxima value λ = 582 nm of the first run containing 0 eq. POPC. (b) Normalized fluorescence maxima at λ = 582 nm plotted against the equivalents of lipid.

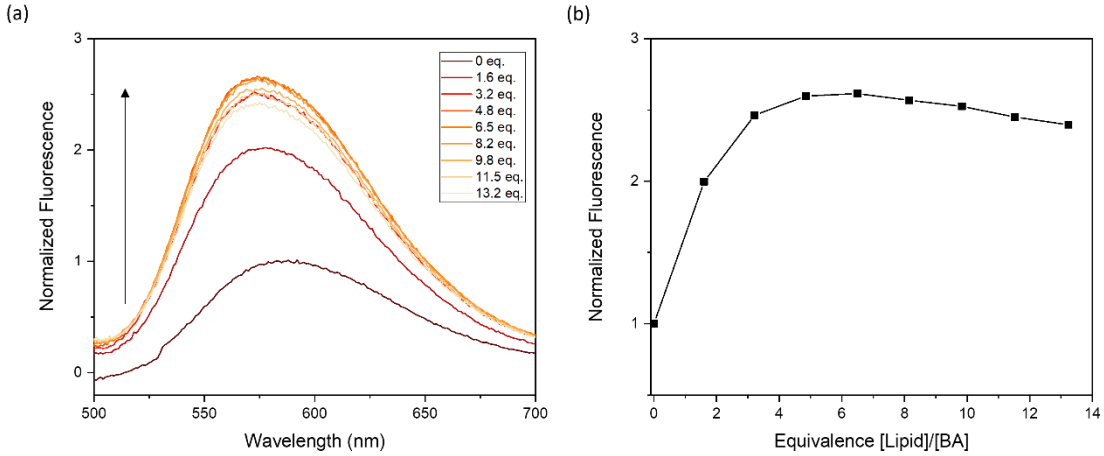

Figure S63. (a) Fluorescence titration of 10 µM ARS and 125 µM **3** with 20 mM POPC liposomes (50 nm diameter) in HEPES buffer (10 mM HEPES, 150 mM NaCl, 1% DMSO, pH 7.4) at 298 K. Fluorescence values were normalized by dividing each value with the maxima value λ = 582 nm of the first run containing 0 eq. POPC. (b) Normalized fluorescence maxima at λ = 582 nm plotted against the equivalents of lipid.

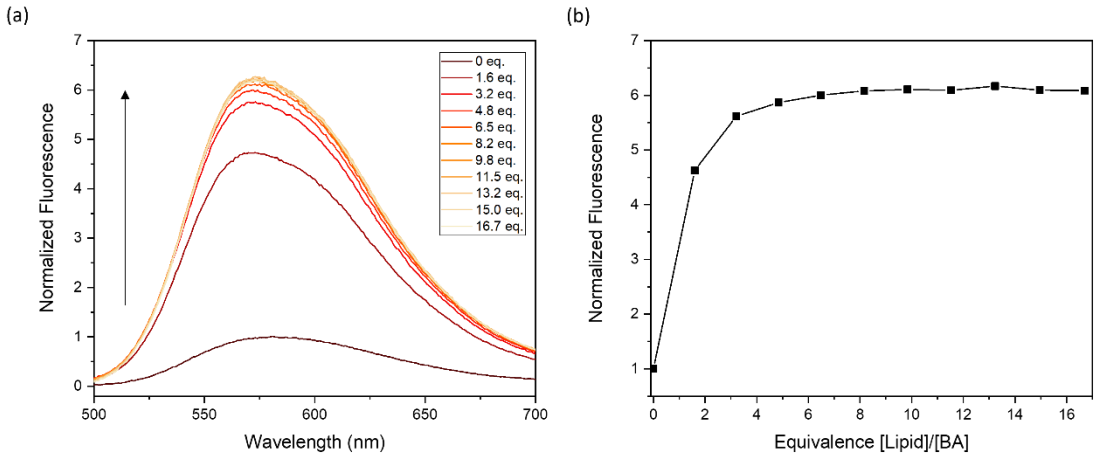

Figure S64. (a) Fluorescence titration of 10 µM ARS and 125 µM **5** with 20 mM POPC liposomes (50 nm diameter) in HEPES buffer (10 mM HEPES, 150 mM NaCl, 1% DMSO, pH 7.4) at 298 K. Fluorescence values were normalized by dividing each value with the maxima value λ = 582 nm of the first run containing 0 eq. POPC. (b) Normalized fluorescence maxima at λ = 582 nm plotted against the equivalents of lipid.

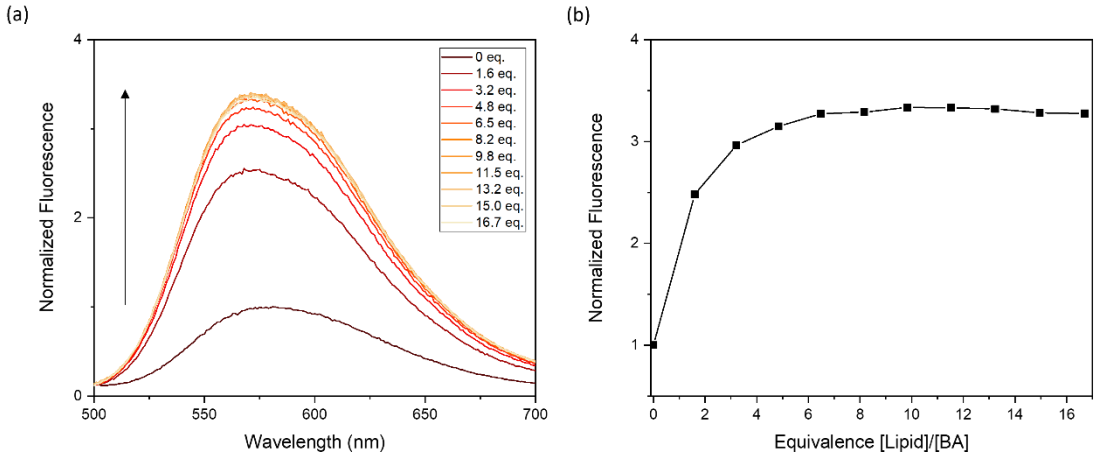

Figure S65. (a) Fluorescence titration of 10 µM ARS and 125 µM **6** with 20 mM POPC liposomes (50 nm diameter) in HEPES buffer (10 mM HEPES, 150 mM NaCl, 1% DMSO, pH 7.4) at 298 K. Fluorescence values were normalized by dividing each value with the maxima value λ = 582 nm of the first run containing 0 eq. POPC. (b) Normalized fluorescence maxima at λ = 582 nm plotted against the equivalents of lipid.

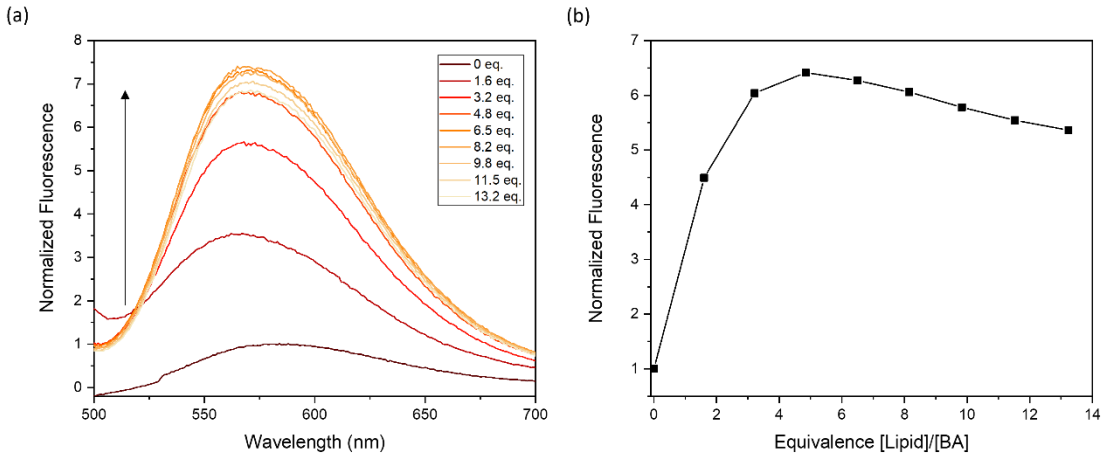

Figure S66. (a) Fluorescence titration of 10 µM ARS and 125 µM **7** with 20 mM POPC liposomes (50 nm diameter) in HEPES buffer (10 mM HEPES, 150 mM NaCl, 1% DMSO, pH 7.4) at 298 K. Fluorescence values were normalized by dividing each value with the maxima value λ = 582 nm of the first run containing 0 eq. POPC. (b) Normalized fluorescence maxima at λ = 582 nm plotted against the equivalents of lipid.

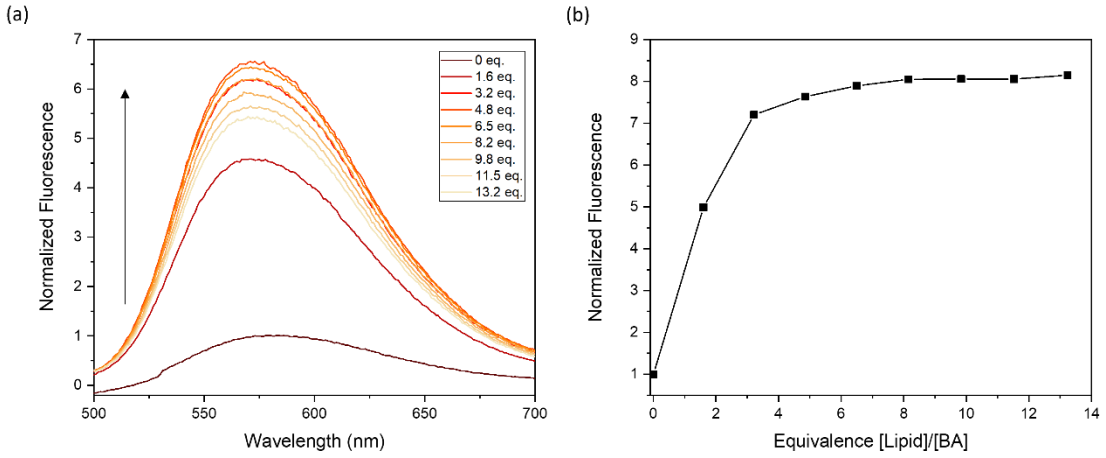

Figure S67. (a) Fluorescence titration of 10 µM ARS and 125 µM **8** with 20 mM POPC liposomes (50 nm diameter) in HEPES buffer (10 mM HEPES, 150 mM NaCl, 1% DMSO, pH 7.4) at 298 K. Fluorescence values were normalized by dividing each value with the maxima value λ = 582 nm of the first run containing 0 eq. POPC. (b) Normalized fluorescence maxima at λ = 582 nm plotted against the equivalents of lipid.

S6. Antibacterial activity

S6.1. MIC determination

The minimum inhibitory concentration (MIC) against the Gram-positive bacteria *B. subtilis, S. aureus* and *E. faecalis,* and the Gram-negative bacterium *E. coli,* was determined using the broth microdilution method recommended by the Clinical and Laboratory Standards Institute.[8] All bacteria were obtained from the American Type Culture Collection (*B. subtilis* -ATCC 6051 *, S. aureus* – ATCC 25923, *E. faecalis* – ATCC 29212, and *E. coli* – ATCC 25922) and stored in glycerol stocks at -80 °C.

For each experiment, a small amount of the glycerol stock was streaked onto a Müller-Hinton agar plate (Sigma-Aldrich #70191) and the agar plate was incubated for 18-24 hours at 35 °C. The obtained colonies were aseptically transferred into sterile cation-adjusted Müller-Hinton broth (Sigma-Aldrich #90922) and vortexed briefly. Colonies were added until the inoculum solution achieved an OD_{600} value corresponding to 1 x 10^8 CFU/mL. OD_{600} values were determined using a Biowave CO8000 Cell Density meter and 17x100 mm polystyrene culture tubes (VWR #60818-703). The inoculum was subsequently diluted to 5 x 10^5 CFU/mL in sterile cation-adjusted Müller-Hinton broth. 192 µL of this inoculum was transferred to the wells of a sterile flat-bottom polystyrene non-tissue culture treated 96-well plate (Falcon #351172) and 8 µL of a DMSO stock solution of compounds **1-8, PBA** or **indolicidin** was added to each well (final DMSO concentration 4%) and the 96-well plate was covered with a Breathe-Easy sealing membrane (Sigma-Aldrich # Z380059). The optical density at 600 nm (OD_{600}) was subsequently measured for 24 hours using a BioTek Cytation 5 Cell Imaging Multi-Mode Reader (35 °C, absorbance measurement at 600 nm, orbital shaking (shaking every 10 minutes, for 1 min at 548 rpm (2 mm)). The MIC value was defined as the minimum concentration of compound that resulted in complete inhibition of bacterial growth over the full 24 hours (OD_{600} = 0.1 after 24 hours). Ampicillin and clindamycin were used for quality control reasons (experiments were considered valid if the MIC for clindamycin was 1-2 µg/mL against *B. subtilis*, and 0.06-0.25 µg/mL against S. aureus, and the MIC for ampicillin was 0.25-2.0 µg/mL against *E. faecalis* and 2-8 µg/mL against *E. coli*).

A table of the obtained MIC values is given in the main manuscript, and the obtained optical densities after 24 hour incubation are shown in **Figure S68** -**Figure S98**. P-values were calculated (two-sample t-test) comparing to the blank and concentrations where the p-value < 0.001 are annotated with ***. The MIC value was taken as the lowest concentration resulting in an average OD_{600} = 0.10-0.15 (no growth) and a p-value < 0.001 compared to the blank. In most cases, a statistically relevant delay or reduction in bacterial growth was also observed at concentrations below the MIC, but not full inhibition of bacterial growth. These lower concentrations of BAs were therefore not considered MIC, but still have some effect on the bacteria. The highest antibacterial activity against Gram-positive bacteria was seen for compounds **1** and **3** (MIC of 12.5-25 µM against all 3 Gram-positive bacteria). None of the compounds showed any antibacterial activity against the Gram-negative bacterium *E. coli.* Indolicidin was chosen as a control antimicrobial peptide that has been proposed to bind to PG lipids.[9] However, high concentrations of indolicidin (>25 µM) caused erratic readings of the OD_{600}, possibly due to solubility issues. The MIC of indolicidin was determined to be 6.25 µM against *B. subtilis,* but the MIC against the other bacteria could not be determined (>25 µM).

S6.1.1. MIC against B. subtilis

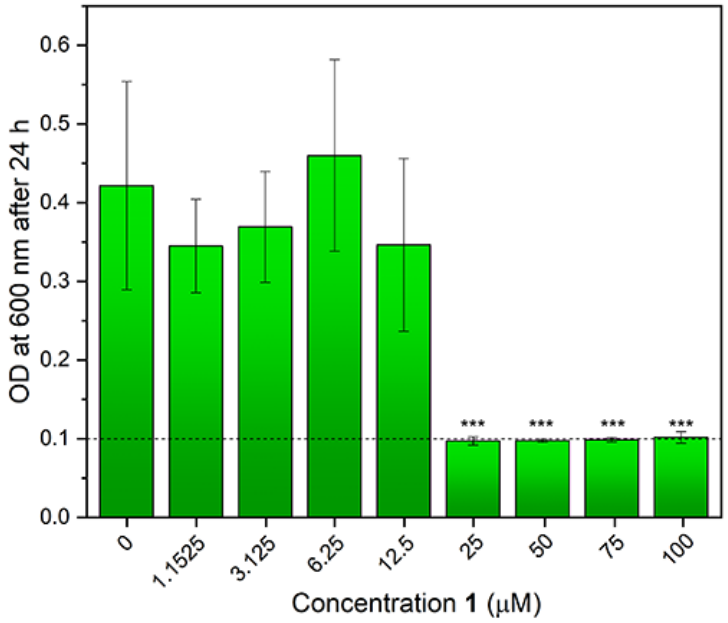

Figure S68. MIC determination for compound **1** against *B. subtilis*. The optical density at 600 nm after 24 h incubation at 35 °C was measured for a solution of *B. subtilis* (starting point 5 x 10^5 CFU/mL) in Müller-Hinton broth containing 4% DMSO and various concentrations of compound **1**. DMSO was used as a negative control. The results are the average of minimum 2 biological x 2 technical repeats and the error bars represent standard deviations. The dashed line at OD_{600} = 0.1 indicates the OD expected when bacterial growth is completely inhibited. The obtained MIC is 25 µM.

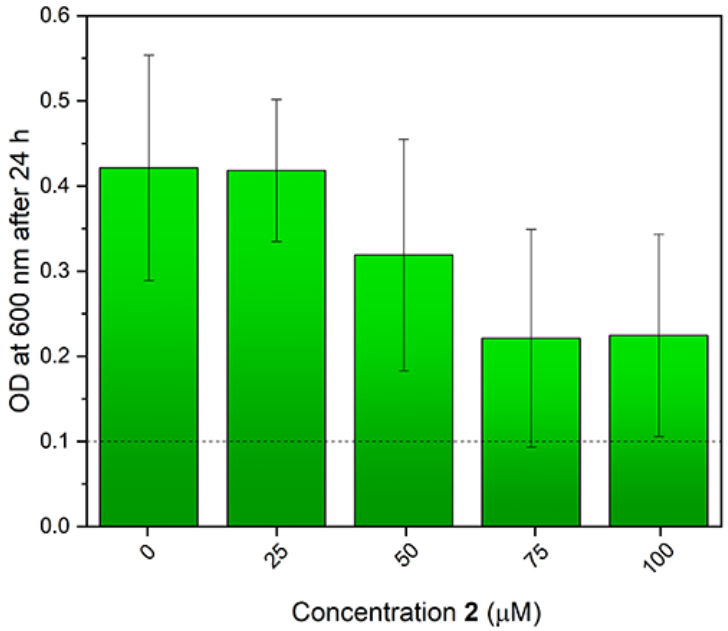

Figure S69. MIC determination for compound **2** against *B. subtilis*. The optical density at 600 nm after 24 h incubation at 35 °C was measured of a solution of *B. subtilis* (starting point 5 x 10^5 CFU/mL) in Müller-Hinton broth containing 4% DMSO and various concentrations of compound **2**. DMSO was used as a negative control. The results are the average of minimum 2 biological x 2 technical repeats and the error bars represent standard deviations. The dashed line at OD_{600} = 0.1 indicates the OD expected when bacterial growth is completely inhibited. The obtained MIC is >100 µM (although some delay in growth is observed at 75 µM and 100 µM).

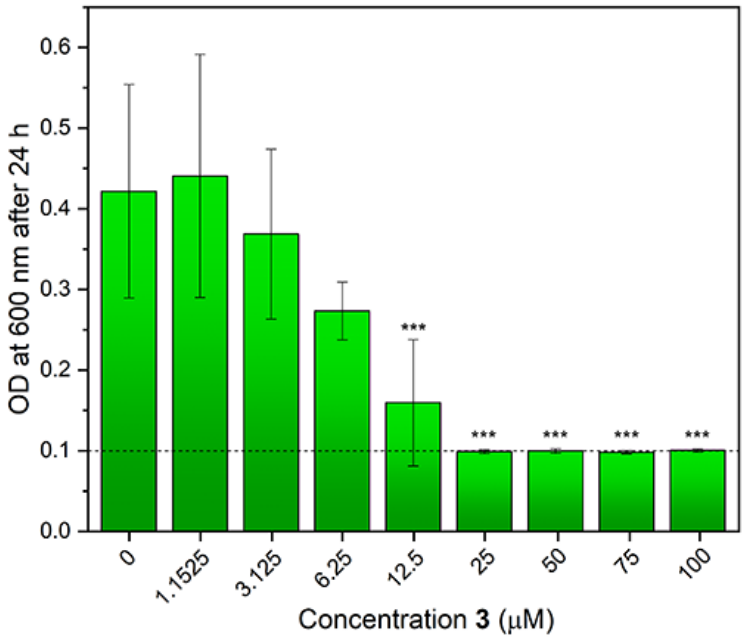

Figure S70. MIC determination for compound **3** against *B. subtilis*. The optical density at 600 nm after 24 h incubation at 35 °C was measured for a solution of *B. subtilis* (starting point 5 x 10^5 CFU/mL) in Müller-Hinton broth containing 4% DMSO and various concentrations of compound **3**. DMSO was used as a negative control. The results are the average of minimum 2 biological x 2 technical repeats and the error bars represent standard deviations. The dashed line at OD_{600} = 0.1 indicates the OD expected when bacterial growth is completely inhibited. The obtained MIC is 25 µM.

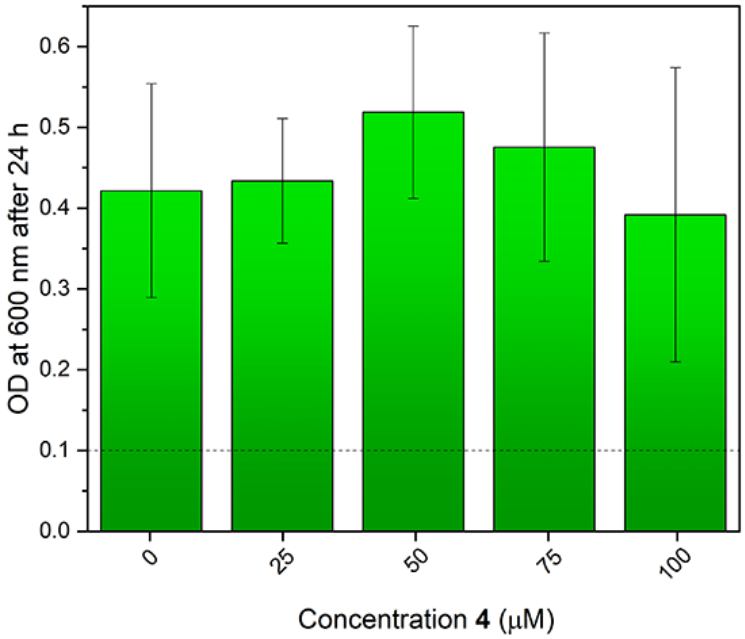

Figure S71. MIC determination for compound **4** against *B. subtilis*. The optical density at 600 nm after 24 h incubation at 35 °C was measured for a solution of *B. subtilis* (starting point 5 x 10^5 CFU/mL) in Müller-Hinton broth containing 4% DMSO and various concentrations of compound **4**. DMSO was used as a negative control. The results are the average of minimum 2 biological x 2 technical repeats and the error bars represent standard deviations. (a) Full growth curves. The dashed line at OD_{600} = 0.1 indicates the OD expected when bacterial growth is completely inhibited. The obtained MIC is >100 µM (no statistical difference with blank for any concentration).

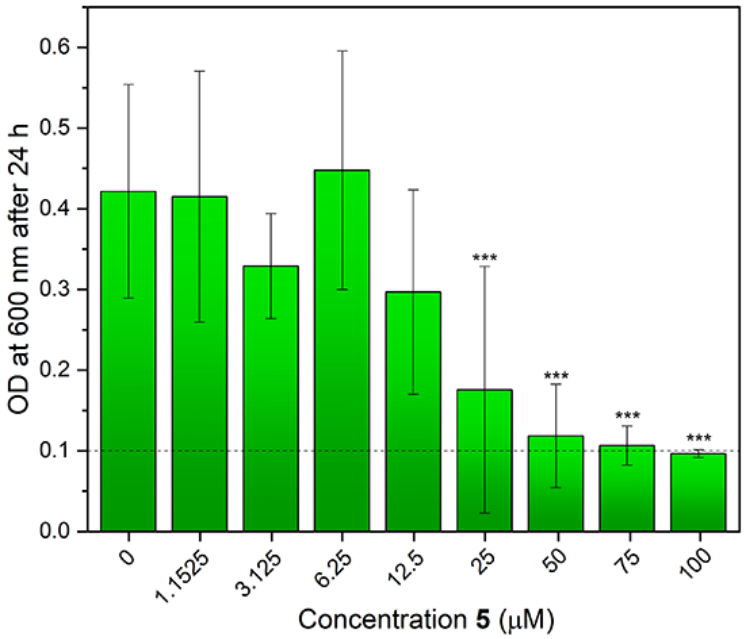

Figure S72. MIC determination for compound **5** against *B. subtilis*. The optical density at 600 nm after 24 h incubation at 35 °C was measured for a solution of *B. subtilis* (starting point 5 x 10^5 CFU/mL) in Müller-Hinton broth containing 4% DMSO and various concentrations of compound **5**. DMSO was used as a negative control. The results are the average of minimum 2 biological x 2 technical repeats and the error bars represent standard deviations. The dashed line at OD_{600} = 0.1 indicates the OD expected when bacterial growth is completely inhibited. The obtained MIC is 50 µM.

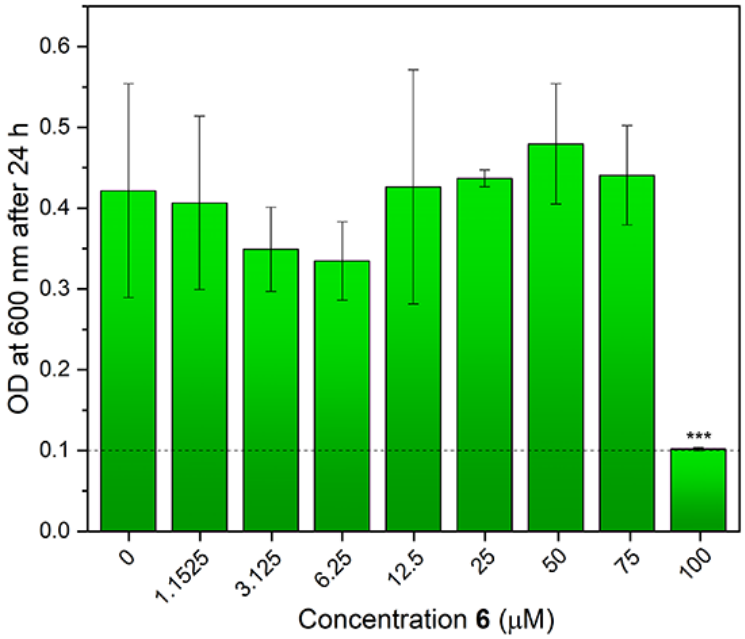

Figure S73. MIC determination for compound **6** against *B. subtilis*. The optical density at 600 nm after 24 h incubation at 35 °C was measured for a solution of *B. subtilis* (starting point 5 x 10^5 CFU/mL) in Müller-Hinton broth containing 4% DMSO and various concentrations of compound **6**. DMSO was used as a negative control. The results are the average of minimum 2 biological x 2 technical repeats and the error bars represent standard deviations. The dashed line at OD_{600} = 0.1 indicates the OD expected when bacterial growth is completely inhibited. The obtained MIC is 100 µM.

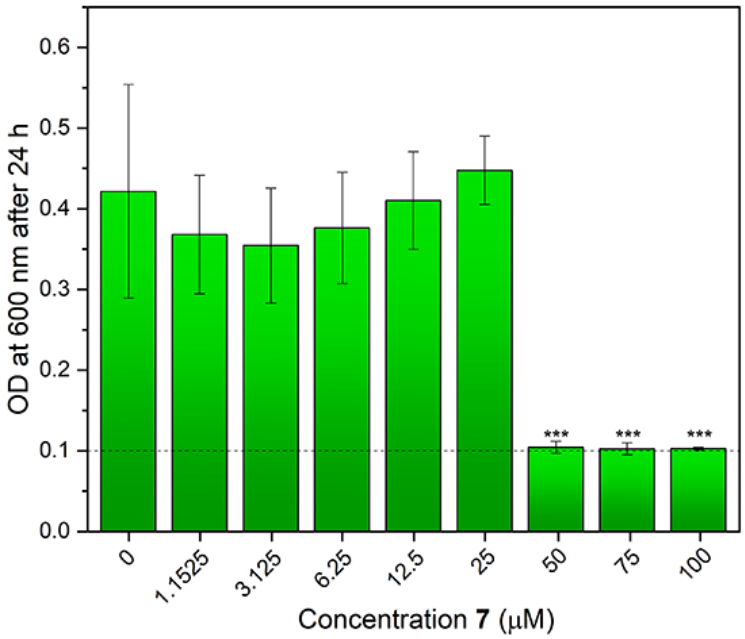

Figure S74. MIC determination for compound **7** against *B. subtilis*. The optical density at 600 nm after 24 h incubation at 35 °C was measured for a solution of *B. subtilis* (starting point 5 x 10^5 CFU/mL) in Müller-Hinton broth containing 4% DMSO and various concentrations of compound **7**. DMSO was used as a negative control. The results are the average of minimum 2 biological x 2 technical repeats and the error bars represent standard deviations. The dashed line at OD_{600} = 0.1 indicates the OD expected when bacterial growth is completely inhibited. The obtained MIC is 50 µM.

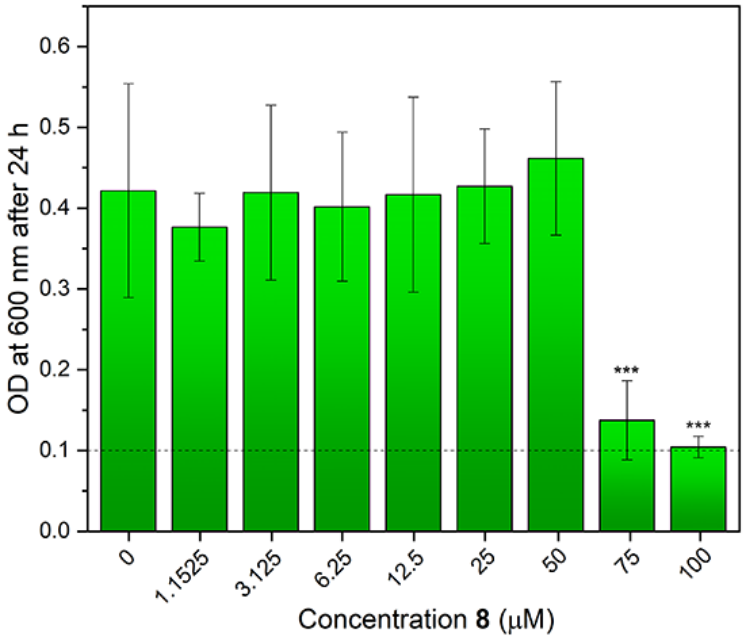

Figure S75. MIC determination for compound **8** against *B. subtilis.* The optical density at 600 nm after 24 h incubation at 35 °C was measured for a solution of *B. subtilis* (starting point 5 x 10^5 CFU/mL) in Müller-Hinton broth containing 4% DMSO and various concentrations of compound **8**. DMSO was used as a negative control. The results are the average of minimum 2 biological x 2 technical repeats and the error bars represent standard deviations. The dashed line at OD_{600} = 0.1 indicates the OD expected when bacterial growth is completely inhibited. The obtained MIC is 75 µM.

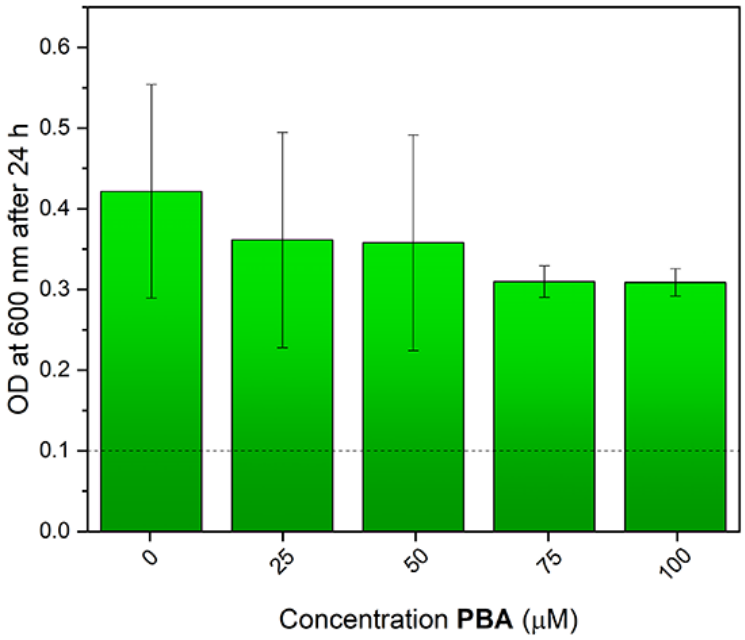

Figure S76. MIC determination for **PBA** against *B. subtilis*. The optical density at 600 nm after 24 h incubation at 35 °C was measured for a solution of *B. subtilis* (starting point 5 x 10^5 CFU/mL) in Müller-Hinton broth containing 4% DMSO and various concentrations of **PBA**. DMSO was used as a negative control. The results are the average of minimum 2 biological x 2 technical repeats and the error bars represent standard deviations. The dashed line at OD_{600} = 0.1 indicates the OD expected when bacterial growth is completely inhibited. The obtained MIC is >100 µM (no statistical difference with blank for any concentration).

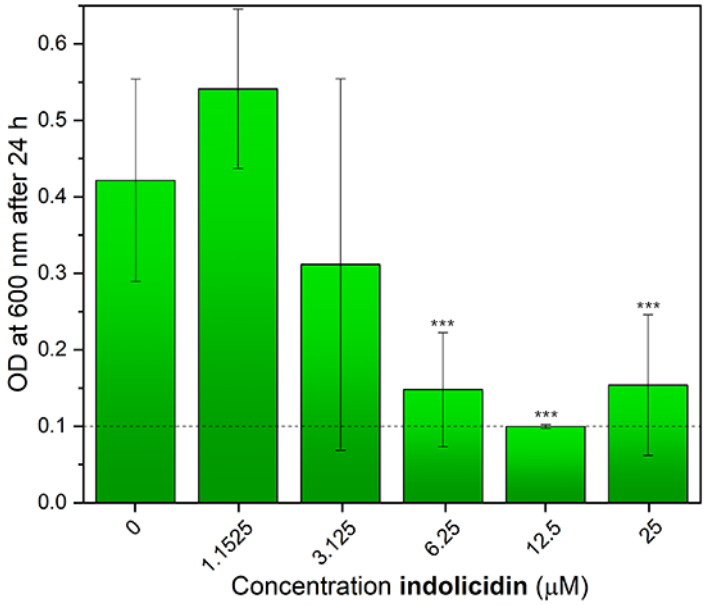

Figure S77. MIC determination for **indolicidin** against *B. subtilis*. The optical density at 600 nm after 24 h incubation at 35 °C was measured for a solution of *B. subtilis* (starting point 5 x 10^5 CFU/mL) in Müller-Hinton broth containing 4% DMSO and various concentrations of **indolicidin**. DMSO was used as a negative control. The results are the average of minimum 2 biological x 2 technical repeats and the error bars represent standard deviations. The dashed line at OD_{600} = 0.1 indicates the OD expected when bacterial growth is completely inhibited. The obtained MIC is 6.25 µM.

S6.1.2. MIC against S. aureus

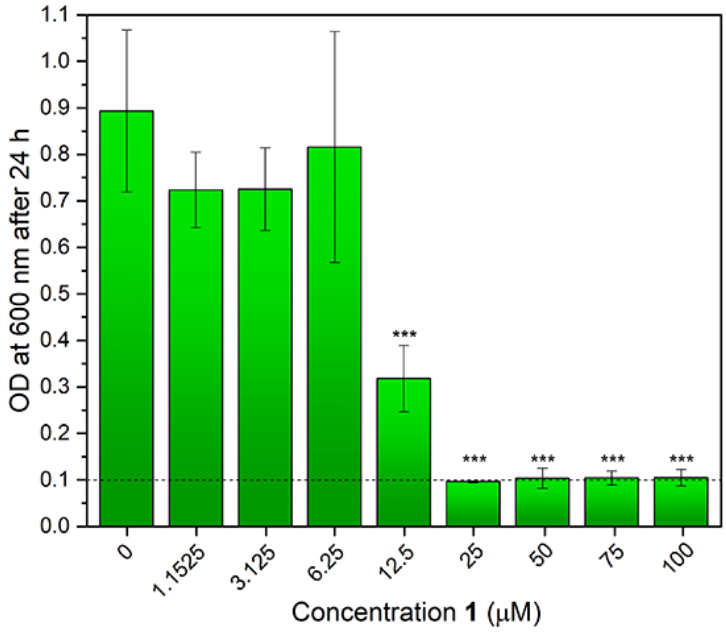

Figure S78. MIC determination for compound **1** against *S. aureus*. The optical density at 600 nm after 24 h incubation at 35 °C was measured for a solution of *S. aureus* (starting point 5 x 10^5 CFU/mL) in Müller-Hinton broth containing 4% DMSO and various concentrations of compound **1**. DMSO was used as a negative control. The results are the average of minimum 2 biological x 2 technical repeats and the error bars represent standard deviations. The dashed line at OD_{600} = 0.1 indicates the OD expected when bacterial growth is completely inhibited. The obtained MIC is 25 µM µM.

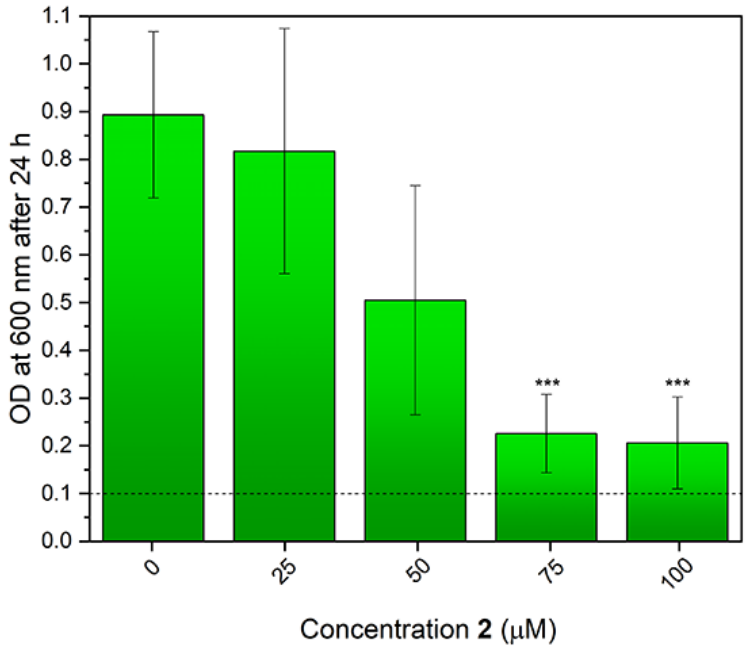

Figure S79. MIC determination for compound **2** against *S. aureus*. The optical density at 600 nm after 24 h incubation at 35 °C was measured for a solution of *S. aureus* (starting point 5 x 10^5 CFU/mL) in Müller-Hinton broth containing 4% DMSO and various concentrations of compound **2**. DMSO was used as a negative control. The results are the average of minimum 2 biological x 2 technical repeats and the error bars represent standard deviations. The dashed line at OD_{600} = 0.1 indicates the OD expected when bacterial growth is completely inhibited. The obtained MIC is >100 µM (some delay in growth is observed at 75 µM and 100 µM).

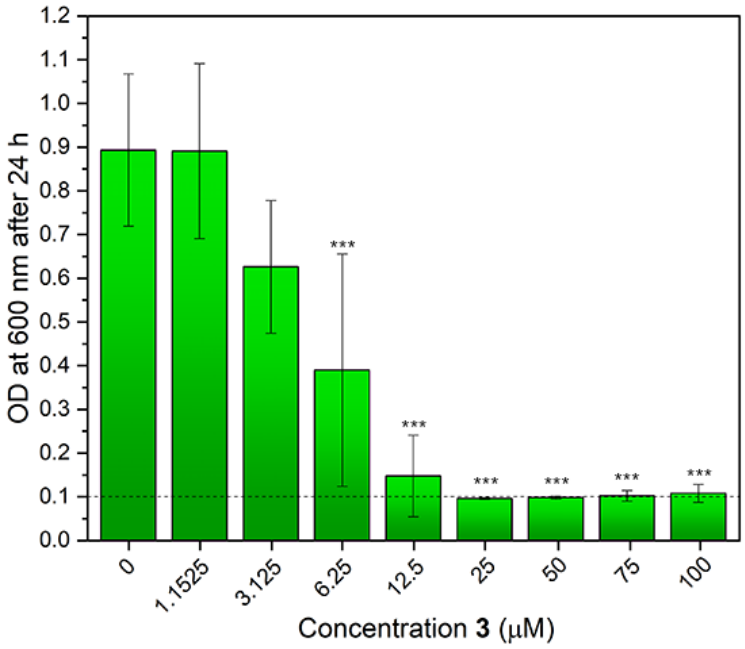

Figure S80. MIC determination for compound **3** against *S. aureus*. The optical density at 600 nm after 24 h incubation at 35 °C was measured for a solution of *S. aureus* (starting point 5 x 10^5 CFU/mL) in Müller-Hinton broth containing 4% DMSO and various concentrations of compound **3**. DMSO was used as a negative control. The results are the average of minimum 2 biological x 2 technical repeats and the error bars represent standard deviations. The dashed line at OD_{600} = 0.1 indicates the OD expected when bacterial growth is completely inhibited. The obtained MIC is 12.5 µM.

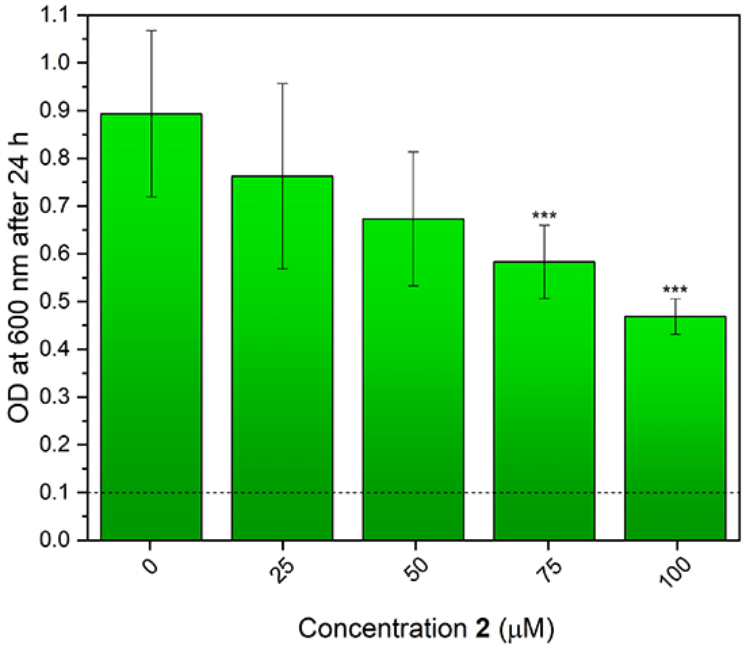

Figure S81. MIC determination for compound **4** against *S. aureus*. The optical density at 600 nm after 24 h incubation at 35 °C was measured for a solution of *S. aureus* (starting point 5 x 10^5 CFU/mL) in Müller-Hinton broth containing 4% DMSO and various concentrations of compound **4**. DMSO was used as a negative control. The results are the average of minimum 2 biological x 2 technical repeats and the error bars represent standard deviations. The dashed line at OD_{600} = 0.1 indicates the OD expected when bacterial growth is completely inhibited. The obtained MIC is >100 µM (some delay in growth is observed for most concentrations).

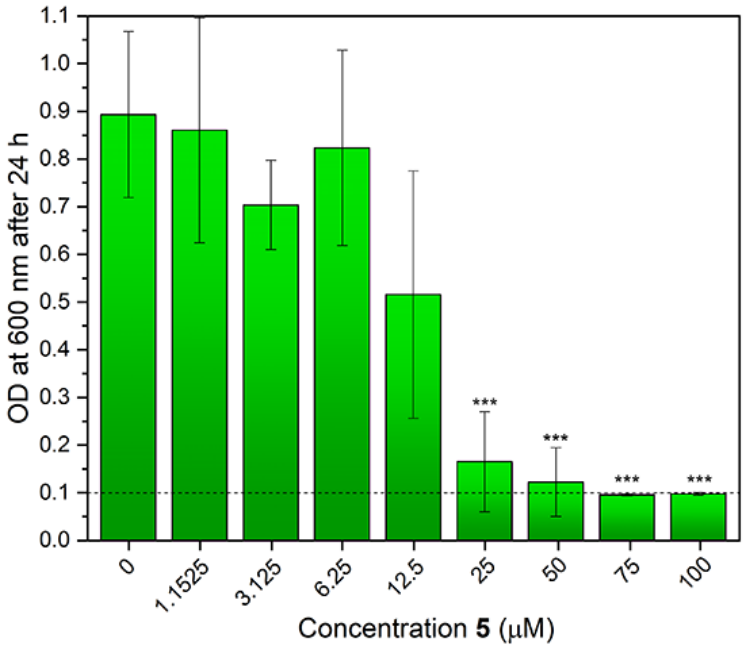

Figure S82. MIC determination for compound **5** against *S. aureus*. The optical density at 600 nm after 24 h incubation at 35 °C was measured for a solution of *S. aureus* (starting point 5 x 10^5 CFU/mL) in Müller-Hinton broth containing 4% DMSO and various concentrations of compound **5**. DMSO was used as a negative control. The results are the average of minimum 2 biological x 2 technical repeats and the error bars represent standard deviations. The dashed line at OD_{600} = 0.1 indicates the OD expected when bacterial growth is completely inhibited. The obtained MIC is 50 μM.

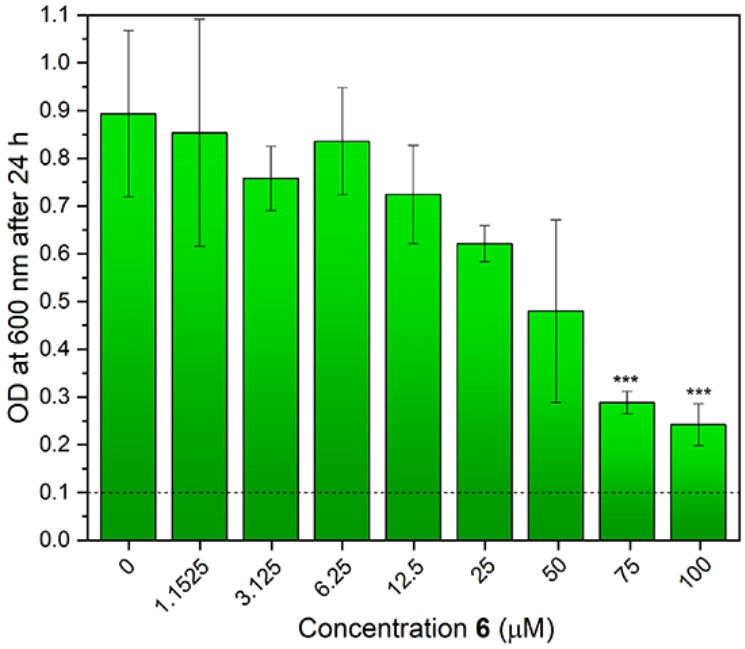

Figure S83. MIC determination for compound **6** against *S. aureus*. The optical density at 600 nm after 24 h incubation at 35 °C was measured for a solution of *S. aureus* (starting point 5 x 10^5 CFU/mL) in Müller-Hinton broth containing 4% DMSO and various concentrations of compound **6**. DMSO was used as a negative control. The results are the average of minimum 2 biological x 2 technical repeats and the error bars represent standard deviations. The dashed line at OD_{600} = 0.1 indicates the OD expected when bacterial growth is completely inhibited. The obtained MIC is >100 μM (although significant delay in growth is observed at 75 μM and 100 μM).

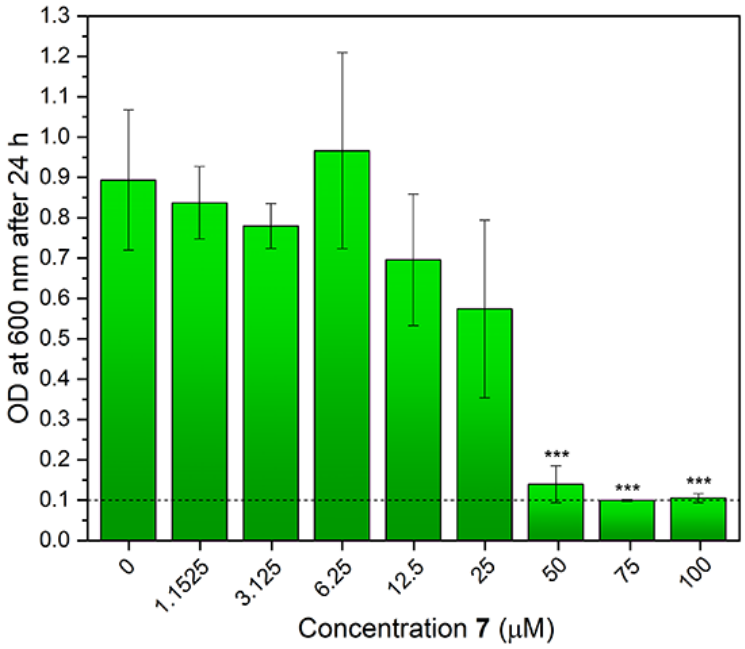

Figure S84. MIC determination for compound **7** against *S. aureus*. The optical density at 600 nm after 24 h incubation at 35 °C was measured for a solution of *S. aureus* (starting point 5 x 10^5 CFU/mL) in Müller-Hinton broth containing 4% DMSO and various concentrations of compound **7**. DMSO was used as a negative control. The results are the average of minimum 2 biological x 2 technical repeats and the error bars represent standard deviations. The dashed line at OD_{600} = 0.1 indicates the OD expected when bacterial growth is completely inhibited. The obtained MIC is 50 µM.

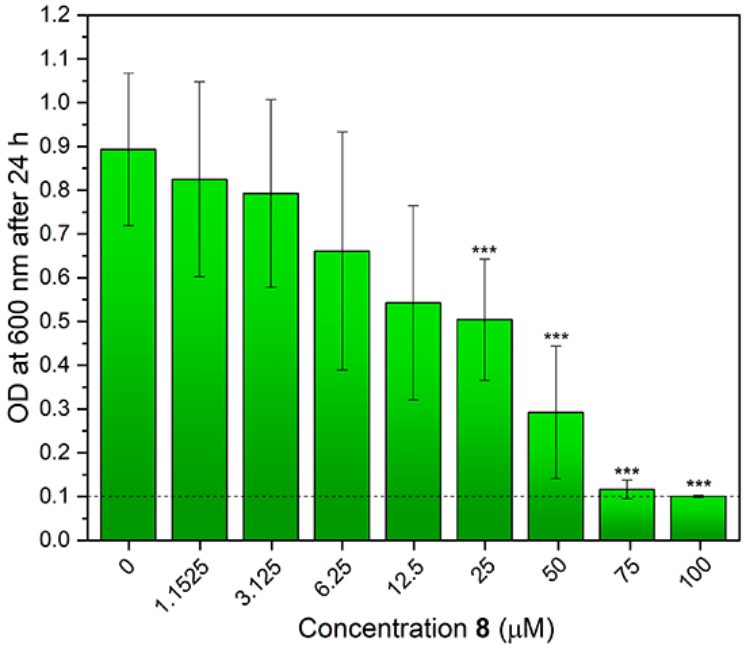

Figure S85. MIC determination for compound **8** against *S. aureus*. The optical density at 600 nm after 24 h incubation at 35 °C was measured for a solution of *S. aureus* (starting point 5 x 10^5 CFU/mL) in Müller-Hinton broth containing 4% DMSO and various concentrations of compound **8**. DMSO was used as a negative control. The results are the average of minimum 2 biological x 2 technical repeats and the error bars represent standard deviations. The dashed line at OD_{600} = 0.1 indicates the OD expected when bacterial growth is completely inhibited. The obtained MIC is 75 µM.

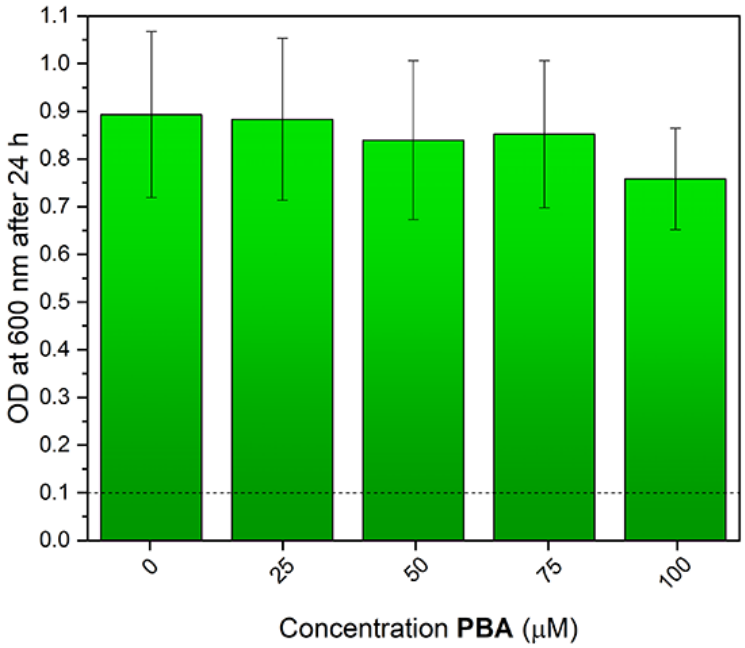

Figure S86. MIC determination for **PBA** against *S. aureus*. The optical density at 600 nm after 24 h incubation at 35 °C was measured for a solution of *S. aureus* (starting point 5 x 10^5 CFU/mL) in Müller-Hinton broth containing 4% DMSO and various concentrations of **PBA**. DMSO was used as a negative control. The results are the average of minimum 2 biological x 2 technical repeats and the error bars represent standard deviations. The dashed line at OD_{600} = 0.1 indicates the OD expected when bacterial growth is completely inhibited. The obtained MIC is >100 µM (no significant difference with blank for all concentrations).

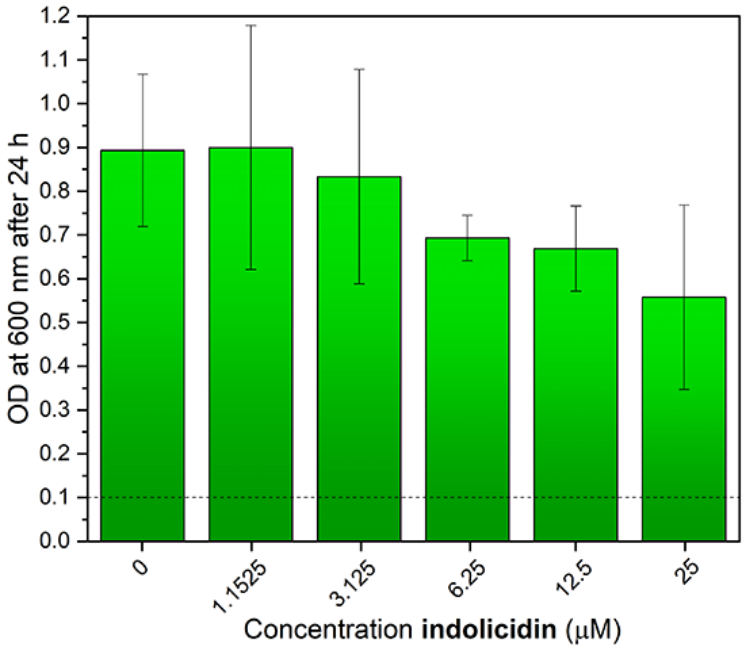

Figure S87. MIC determination for **indolicidin** against *S. aureus*. The optical density at 600 nm after 24 h incubation at 35 °C was measured for a solution of *S. aureus* (starting point 5 x 10^5 CFU/mL) in Müller-Hinton broth containing 4% DMSO and various concentrations of **indolicidin**. DMSO was used as a negative control. The results are the average of minimum 2 biological x 2 technical repeats and the error bars represent standard deviations. The dashed line at OD_{600} = 0.1 indicates the OD expected when bacterial growth is completely inhibited. The obtained MIC is >25 µM (higher concentrations precipitated out or caused other interference).

S6.1.3. MIC against E. faecalis

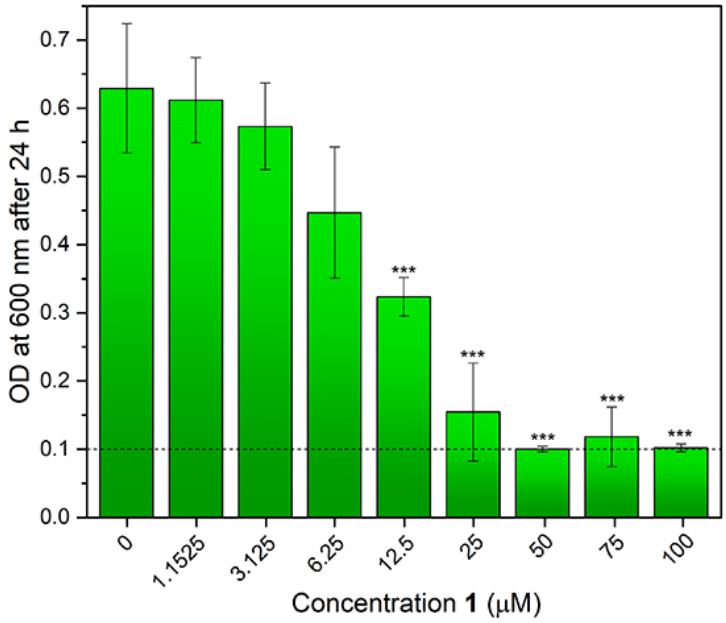

Figure S88. MIC determination for compound **1** against *E. faecalis*. The optical density at 600 nm after 24 h incubation at 35 °C was measured for a solution of *E. faecalis* (starting point 5 x 10^5 CFU/mL) in Müller-Hinton broth containing 4% DMSO and various concentrations of compound **1**. DMSO was used as a negative control. The results are the average of minimum 2 biological x 2 technical repeats and the error bars represent standard deviations. The dashed line at OD_{600} = 0.1 indicates the OD expected when bacterial growth is completely inhibited. The obtained MIC is 50 µM.

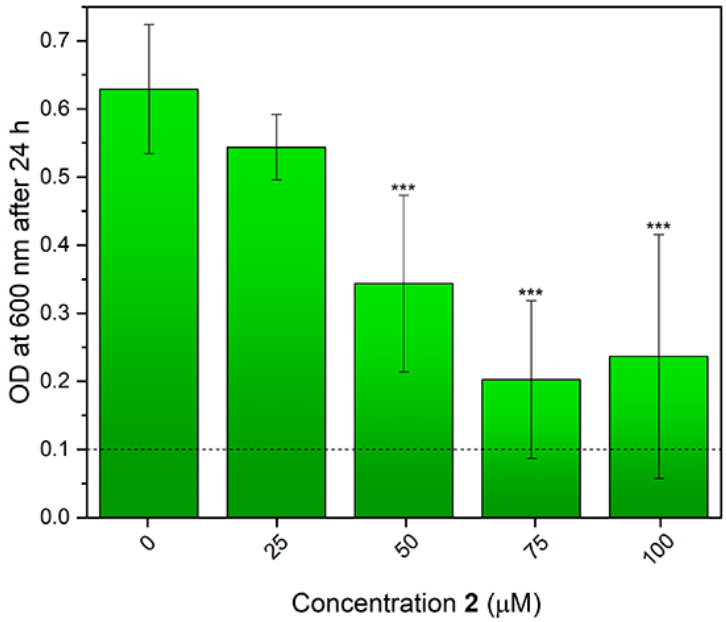

Figure S89. MIC determination for compound **2** against *E. faecalis*. The optical density at 600 nm after 24 h incubation at 35 °C was measured for a solution of *E. faecalis* (starting point 5 x 10^5 CFU/mL) in Müller-Hinton broth containing 4% DMSO and various concentrations of compound **2**. DMSO was used as a negative control. The results are the average of minimum 2 biological x 2 technical repeats and the error bars represent standard deviations. The dashed line at OD_{600} = 0.1 indicates the OD expected when bacterial growth is completely inhibited. The obtained MIC is >100 µM (although significant delay in growth is observed at 75 µM and 100 µM).

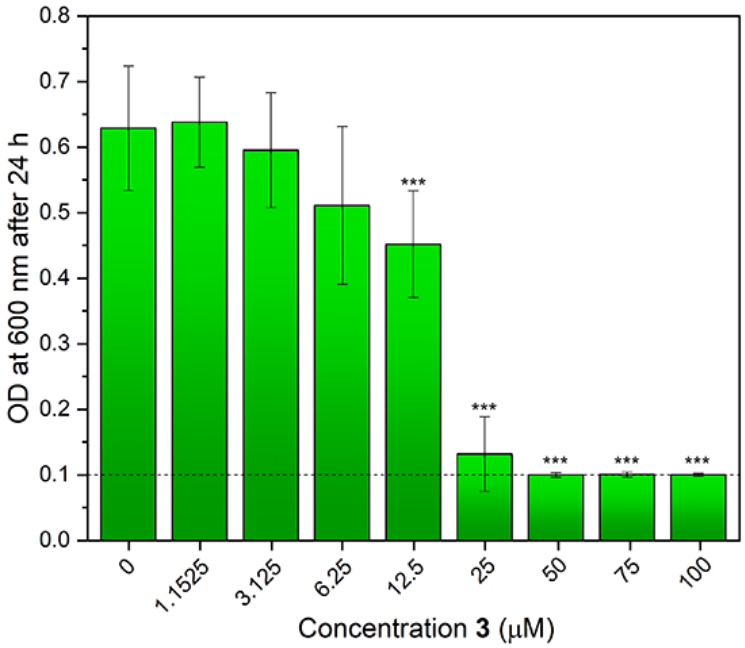

Figure S90. MIC determination for compound **3** against *E. faecalis*. The optical density at 600 nm after 24 h incubation at 35 °C was measured for a solution of *E. faecalis* (starting point 5 x 10^5 CFU/mL) in Müller-Hinton broth containing 4% DMSO and various concentrations of compound **3**. DMSO was used as a negative control. The results are the average of minimum 2 biological x 2 technical repeats and the error bars represent standard deviations. The dashed line at OD_{600} = 0.1 indicates the OD expected when bacterial growth is completely inhibited. The obtained MIC is 25 μM.

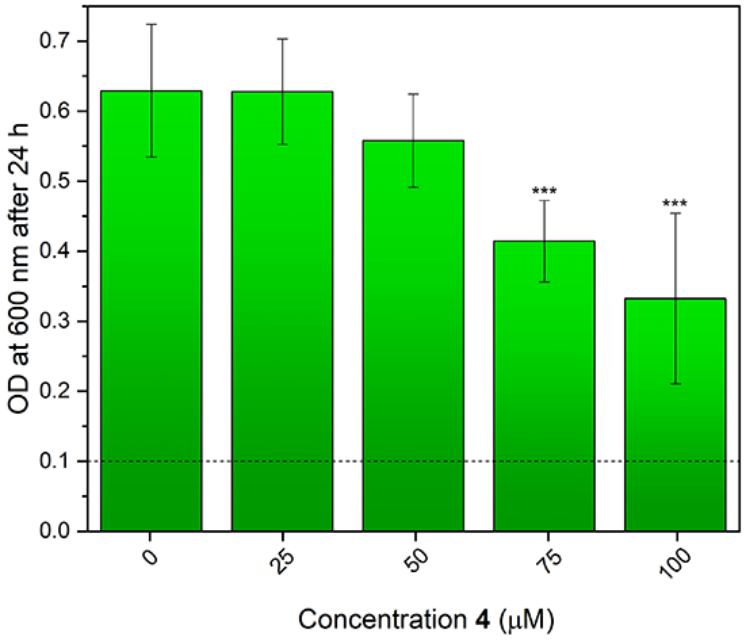

Figure S91. MIC determination for compound **4** against *E. faecalis*. The optical density at 600 nm after 24 h incubation at 35 °C was measured for a solution of *E. faecalis* (starting point 5 x 10^5 CFU/mL) in Müller-Hinton broth containing 4% DMSO and various concentrations of compound **4**. DMSO was used as a negative control. The results are the average of minimum 2 biological x 2 technical repeats and the error bars represent standard deviations. The dashed line at OD_{600} = 0.1 indicates the OD expected when bacterial growth is completely inhibited. The obtained MIC is >100 μM (although significant delay in growth is observed at 75 μM and 100 μM).

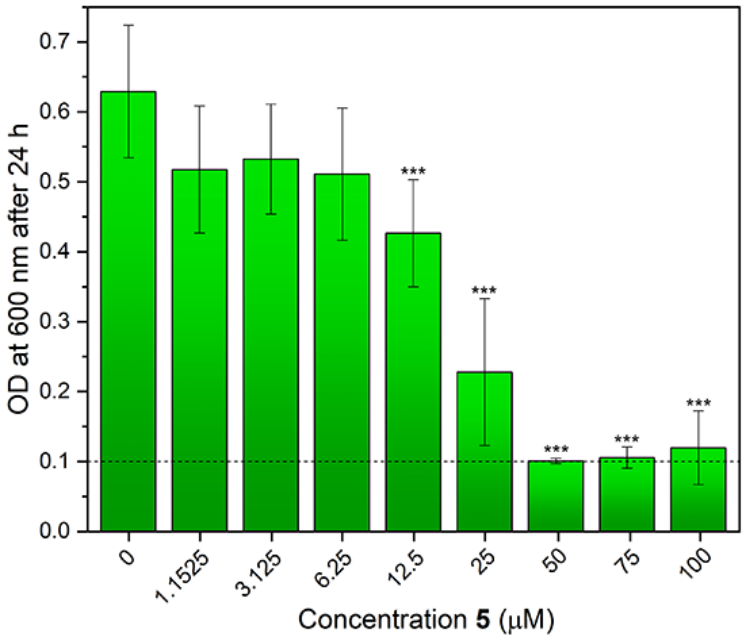

Figure S92. MIC determination for compound **5** against *E. faecalis*. The optical density at 600 nm after 24 h incubation at 35 °C was measured for a solution of *E. faecalis* (starting point 5 x 10^5 CFU/mL) in Müller-Hinton broth containing 4% DMSO and various concentrations of compound **5**. DMSO was used as a negative control. The results are the average of minimum 2 biological x 2 technical repeats and the error bars represent standard deviations. The dashed line at OD_{600} = 0.1 indicates the OD expected when bacterial growth is completely inhibited. The obtained MIC is 50 µM.

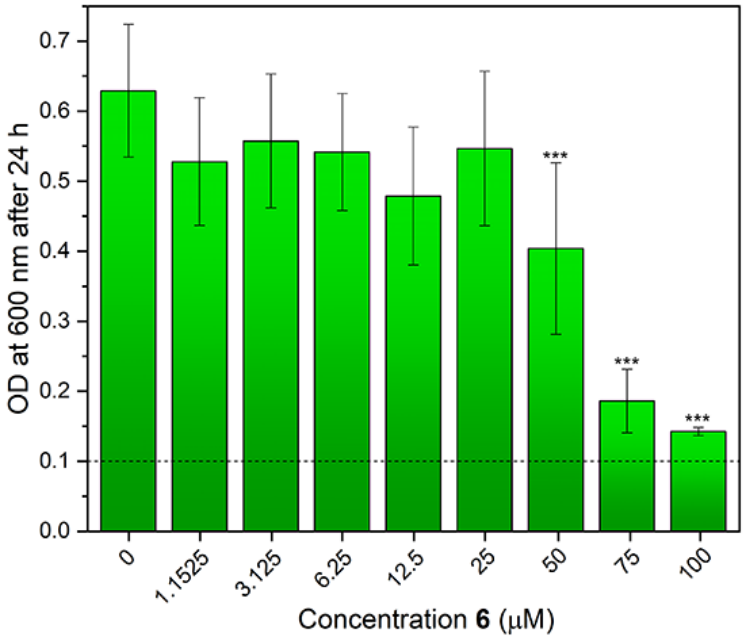

Figure S93. MIC determination for compound **6** against *E. faecalis*. The optical density at 600 nm after 24 h incubation at 35 °C was measured for a solution of *E. faecalis* (starting point 5 x 10^5 CFU/mL) in Müller-Hinton broth containing 4% DMSO and various concentrations of compound **6**. DMSO was used as a negative control. The results are the average of minimum 2 biological x 2 technical repeats and the error bars represent standard deviations. The dashed line at OD_{600} = 0.1 indicates the OD expected when bacterial growth is completely inhibited. The obtained MIC is 100 µM.

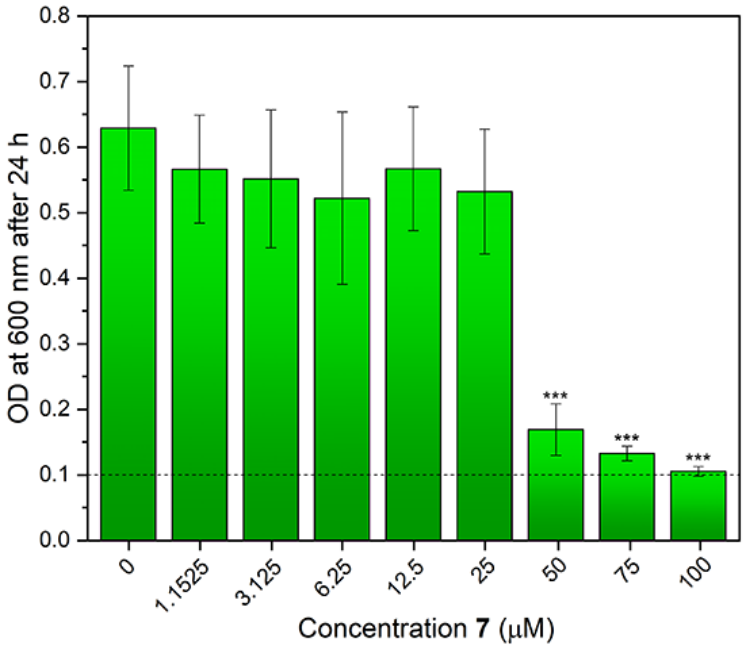

Figure S94. MIC determination for compound **7** against *E. faecalis*. The optical density at 600 nm after 24 h incubation at 35 °C was measured for a solution of *E. faecalis* (starting point 5 x 10^5 CFU/mL) in Müller-Hinton broth containing 4% DMSO and various concentrations of compound **7**. DMSO was used as a negative control. The results are the average of minimum 2 biological x 2 technical repeats and the error bars represent standard deviations. The dashed line at OD_{600} = 0.1 indicates the OD expected when bacterial growth is completely inhibited. The obtained MIC is 75 μM.

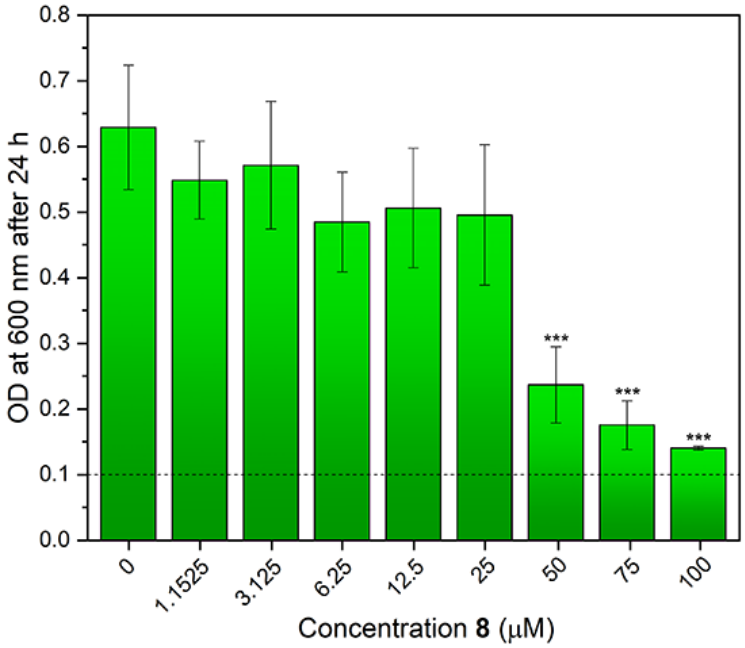

Figure S95. MIC determination for compound **8** against *E. faecalis*. The optical density at 600 nm after 24 h incubation at 35 °C was measured for a solution of *E. faecalis* (starting point 5 x 10^5 CFU/mL) in Müller-Hinton broth containing 4% DMSO and various concentrations of compound **8**. DMSO was used as a negative control. The results are the average of minimum 2 biological x 2 technical repeats and the error bars represent standard deviations. The dashed line at OD_{600} = 0.1 indicates the OD expected when bacterial growth is completely inhibited. The obtained MIC is 100 μM μM.

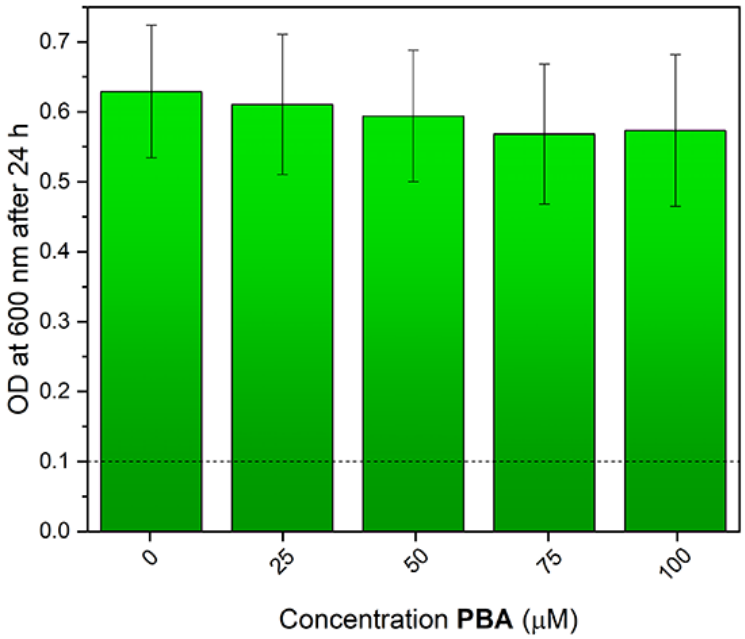

Figure S96. MIC determination for **PBA** against *E. faecalis*. The optical density at 600 nm after 24 h incubation at 35 °C was measured for a solution of *E. faecalis* (starting point 5 x 10^5 CFU/mL) in Müller-Hinton broth containing 4% DMSO and various concentrations of **PBA**. DMSO was used as a negative control. The results are the average of minimum 2 biological x 2 technical repeats and the error bars represent standard deviations. The dashed line at OD_{600} = 0.1 indicates the OD expected when bacterial growth is completely inhibited. The obtained MIC is >100 µM.

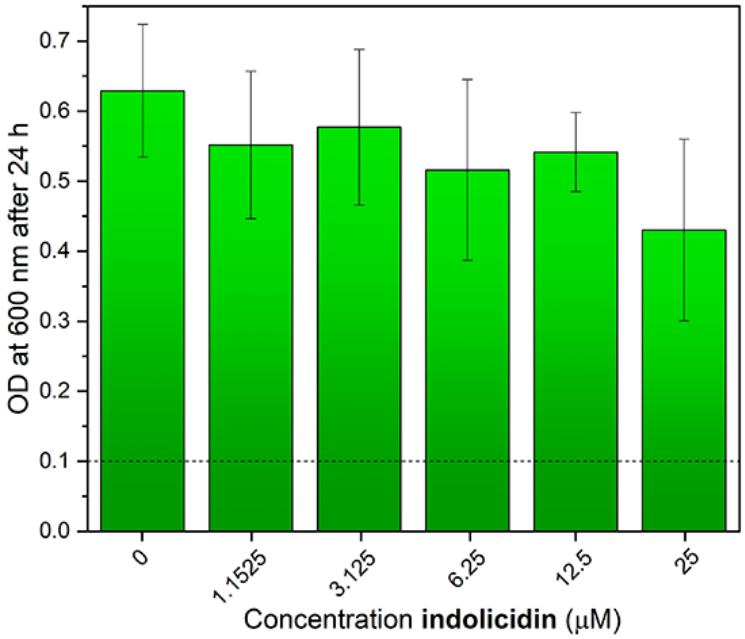

Figure S97. MIC determination for **indolicidin** against *E. faecalis*. The optical density at 600 nm after 24 h incubation at 35 °C was measured for a solution of *E. faecalis* (starting point 5 x 10^5 CFU/mL) in Müller-Hinton broth containing 4% DMSO and various concentrations of **indolicidin**. DMSO was used as a negative control. The results are the average of minimum 2 biological x 2 technical repeats and the error bars represent standard deviations. The dashed line at OD_{600} = 0.1 indicates the OD expected when bacterial growth is completely inhibited. The obtained MIC is >25 µM (higher concentrations precipitated out or caused other interference).

S6.1.4. MIC against E. coli

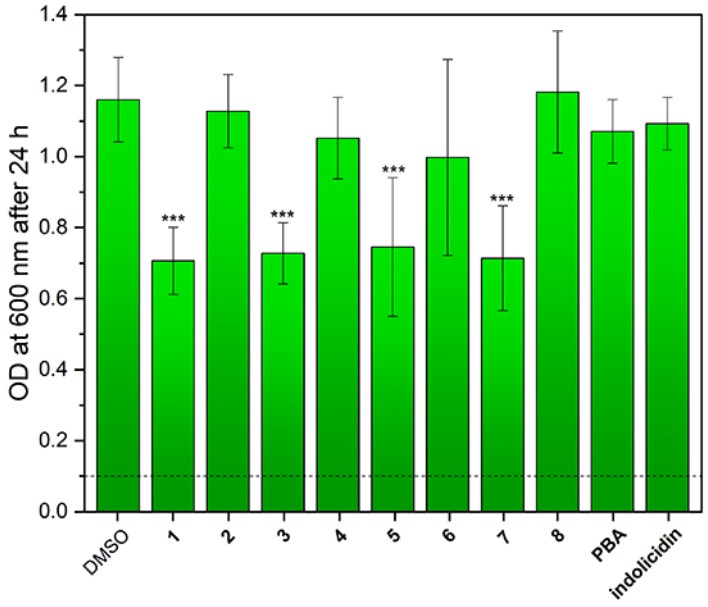

Figure S98. Potential antibacterial activity of 100 µM **1-8**, 100 µM **PBA** or 100 µM **indolicidin** against *E. coli*. The optical density at 600 nm after 24 h incubation at 35 °C was measured for a solution of *E. coli* (starting point 5 x 10^5 CFU/mL) in Müller-Hinton broth containing 4% DMSO and 100 µM **1-8**, 100 µM **PBA** or 100 µM **indolicidin**. DMSO was used as a negative control. The results are the average of minimum 2 biological x 2 technical repeats and the error bars represent standard deviations. The dashed line at OD_{600} = 0.1 indicates the OD expected when bacterial growth is completely inhibited. None of the compounds showed full inhibition of bacterial growth.

S6.2. $Disc_3(5)$ assay

A membrane depolarization assay was performed using the dye $Disc_3(5)$ (3,3'-dipropylthia-dicarbocyanine iodide), according to the method by te Winkel *et al.*[10] For each experiment, a small amount of the *B. subtilis* glycerol stock was streaked onto a Müller-Hinton agar plate and the agar plate was incubated for 18-24 hours at 35 °C. The obtained colonies were aseptically transferred into sterile cation-adjusted Müller-Hinton broth and diluted to OD_{600} = 0.2. The bacteria were subsequently incubated at 35 °C until they reached mid-logarithmic phase (typically OD_{600} of 0.7-0.9). The cultures were then centrifuged at 3000 rpm for 5 mins and the pellets were re-suspended and diluted in Müller-Hinton broth supplemented with 0.5 mg/mL BSA (bovine serum albumin) to an OD_{600} of 0.2. Then, 178 µL of the diluted cells were transferred to a fluorescence 96-well plate (sterile, black, flat-bottom, polystyrene microplate from Brand #7816668) and the fluorescence was followed for 3 minutes to obtain values for background fluorescence. After obtaining a baseline, 2 µL $DiSC_3(5)$ dissolved in DMSO was added to each well to a final concentration of 1 µM $DiSC_3(5)$ and 1% DMSO, and the fluorescence intensity was measured for another 15 minutes. At this point, 20 µL of stock solutions and control antibiotics (dissolved to 10x the desired concentration in Müller-Hinton broth with 1% DMSO) were added and the fluorescence was measured for 1 hour. All fluorescence measurements were preformed using a BioTek Cytation 5 Cell Imaging Multi-Mode Reader (35 °C, excitation at 610 nm and emission at 660 nm, time intervals of 23 seconds, orbital shaking (5 seconds at 548 rpm (2 mm) before each measurement). As a positive control, 10 µM gramicidin was used which

is known to cause membrane depolarization.[11] As a negative control, the ribosome-targeting antibiotic clindamycin was used (2 µg/mL), as well as a blank run (no antibiotic added). The kinetic traces are shown in the main manuscript, and a bar graph showing the fluorescence intensity after 10 minutes incubation with **1**, **3** or control compounds is shown in **Figure S99**. Compounds **1** and **3** clearly show depolarization of the membrane, giving rise to fluorescence intensities comparable to the positive control gramicidin.

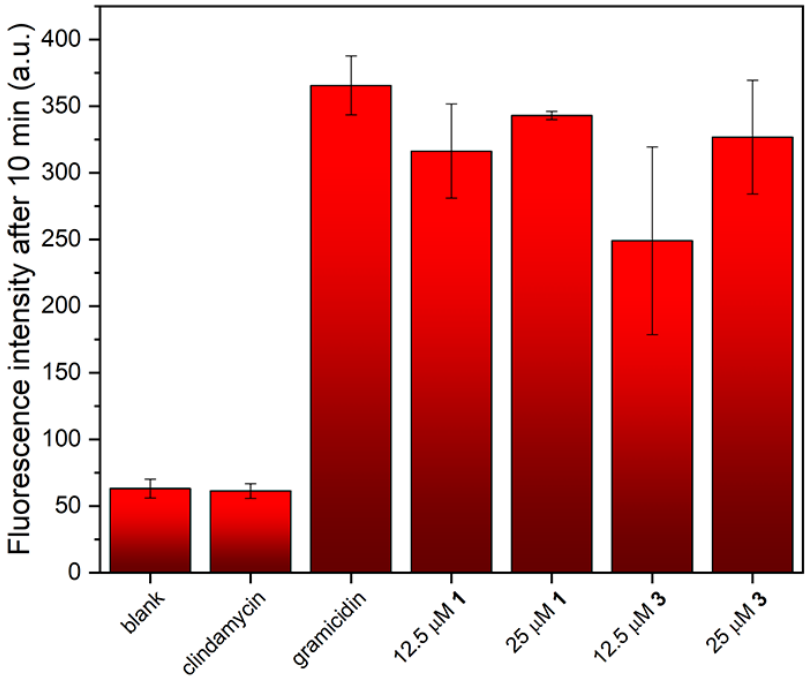

Figure S99. Membrane depolarization of *B. subtilis* induced by boronic acids **1** and **3.** Fluorescence intensity of $Disc_3(5)$ in *B. subtilis* after 10 minutes incubation with DMSO (1%, blank), clindamycin (2 µg/mL, negative control), gramicidin (10 µM, positive control), 12.5 µM **1**, 25 µM **1**, 12.5 µM **3**, or 25 µM **3**. Results are the average of at least 2 technical x 2 biological repeats and error bars represent standard deviations.

For the imaging, the membrane depolarization assay described above was stopped after 10-15 minutes, and 2 µL of the bacterial solution was transferred to a microscopy cover glass and a 1% agarose gel was put on top of the solution to immobilize the bacteria. Images were taken using a BioTek Cytation 5 Cell Imaging Multi-Mode Reader, with the Texas Red filter set for fluorescence images. All fluorescence images were taken using the same exposure settings (LED intensity = 3, Shutter Speed MS = 824, Camera Gain = 30). Overlays were generated using the software accompanying the BioTek Cytation 5 Cell Imaging Multi-Mode Reader. One biological repeat is shown in the main manuscript, additional biological repeats are shown in **Figure S100** - **Figure S101**. The imaging studies confirm the membrane depolarization activity of compounds **1** and **3**.

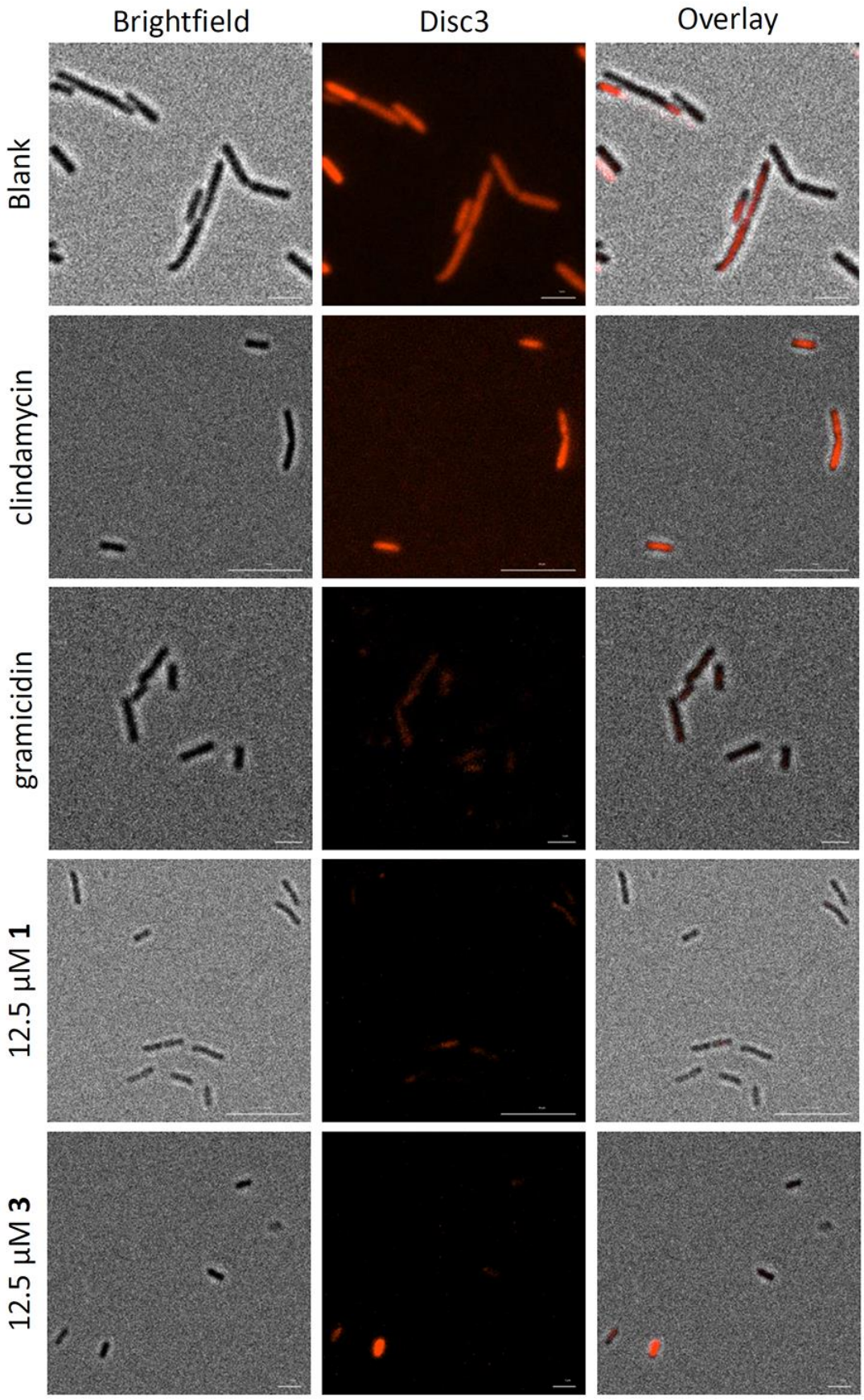

Figure S100. Images of membrane depolarization of *B. subtilis* by 1xMIC of clindamycin (negative control), gramicidin (positive control), **1** and **3**, using $Disc_3(5)$ as the voltage-dependent fluorophore. The *B. subtilis* cells were incubated for 10-15 minutes with 1% DMSO (blank), 2 µg/mL clindamycin, 10 µM gramicidin, 12.5 µM **1** or 12.5 µM **3**. Absence of fluorescence indicates that the cells are depolarized. Scale bars represent 10 µm.

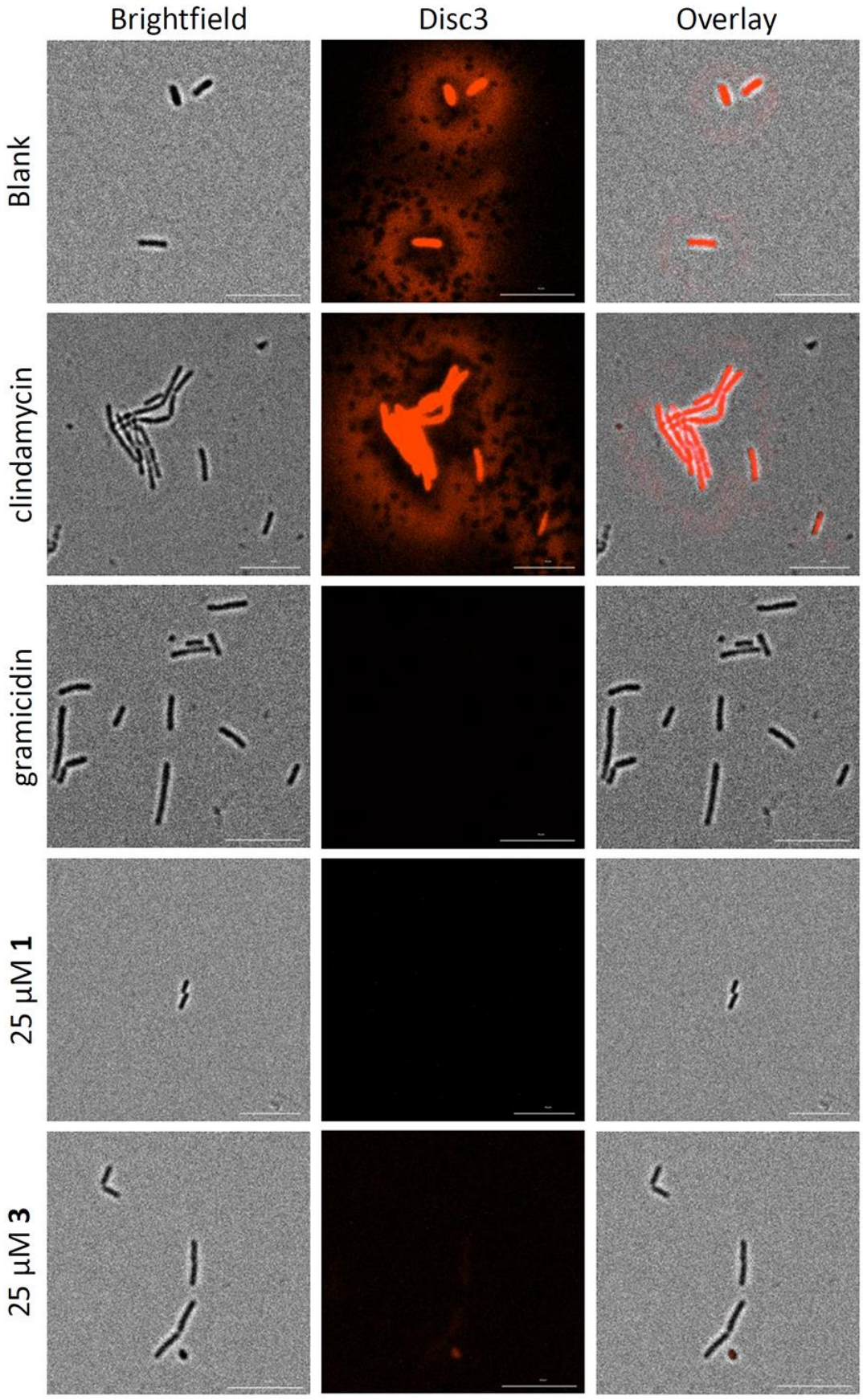

Figure S101. Images of membrane depolarization of *B. subtilis* by 2xMIC of clindamycin (negative control), gramicidin (positive control), **1** and **3**, using $Disc_3(5)$ as the voltage-dependent fluorophore. The *B. subtilis* cells were incubated for 10-15 minutes with 2% DMSO (blank), 4 µg/mL clindamycin, 2 µM gramicidin, 25 µM **1** or 25 µM **3**. Absence of fluorescence indicates that the cells are depolarized. Scale bars represent 10 µm.

S6.3. Sytox Green assay

To determine if the active compounds **1** and **3** cause the formation of large pores, or lead to other large defects or disruption of the membrane, we performed a fluorescence assay with Sytox Green.[12] For each experiment, a small amount of the *B. subtilis* glycerol stock was streaked onto a Müller-Hinton agar plate and the agar plate was incubated for 18-24 hours at 35 °C. The obtained colonies were aseptically transferred into sterile cation-adjusted Müller-Hinton broth and diluted to OD_{600} of 0.2. The bacteria were subsequently incubated at 35 °C until they reached mid-logarithmic phase (typically OD_{600} of 0.6). The cultures were then centrifuged at 3000 rpm for 5 mins and the pellets were washed twice with phosphate-buffered saline (PBS) and diluted in PBS to an OD_{600} of 0.2. Then, Sytox Green dissolved in DMSO was added to achieve a final Sytox Green concentration of 1 µM and 1% DMSO, and the bacteria were incubated at 35 °C for 15 minutes. Then, 180 µL of the bacteria suspension was transferred into the wells of a 96-well plate for fluorescence (sterile, black, flat-bottom, polystyrene microplate from Brand #7816668) and the fluorescence intensity was measured for 4 minutes. At this point, 20 µL of stock solutions and control antibiotics (dissolved to 10x the desired concentration in PBS buffer with 1% DMSO) were added and the fluorescence was measured for 2 hours. All fluorescence measurements were preformed using a BioTek Cytation 5 Cell Imaging Multi-Mode Reader (35 °C, excitation at 485 nm and emission at 520 nm, time intervals of 23 seconds, orbital shaking (5 seconds at 548 rpm (2 mm) before each measurement). As a positive control, 2.5 µM nisin was used, which is known to form large pores that allow Sytox Green to enter the bacterial cells.[10, 13, 14] As a negative control, the ribosome-targeting antibiotic clindamycin was used (2 µg/mL), as well as gramicidin (1 µM) and a blank run (no antibiotic added). The results are shown in **Figure S102**. Neither compound **1** nor **3** leads to an increase in fluorescence, indicating that they do not form large pores.

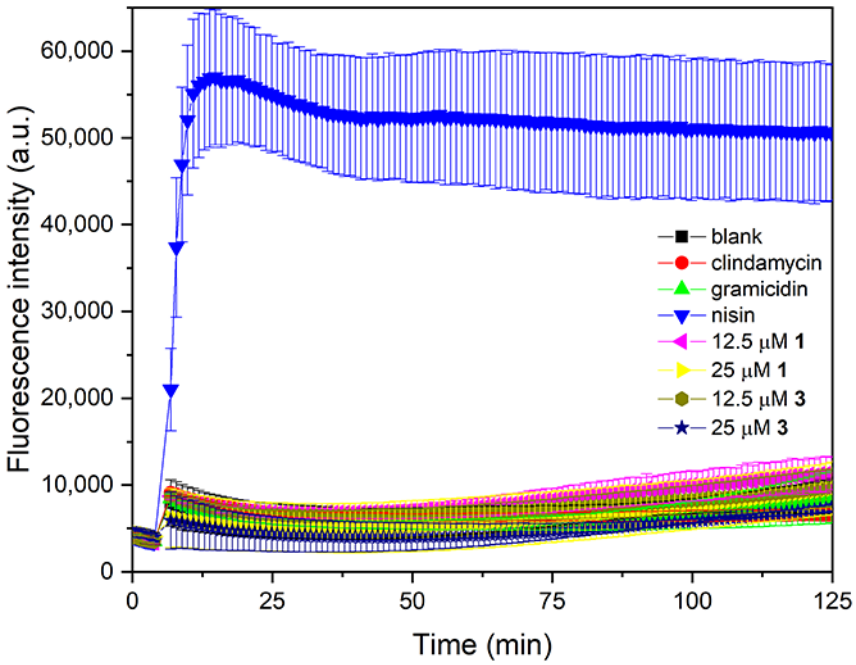

Figure S102. Fluorescence intensity of Sytox Green in *B. subtilis* in the presence of DMSO (1%, blank), clindamycin (2 µg/mL, negative control), gramicidin (1 µM, negative control), nisin (2.5 µM, positive control), 12.5 µM **1**, 25 µM **1**, 12.5 µM **3**, or 25 µM **3**. Results are the average of at least 2 technical x 2 biological repeats and error bars represent standard deviations.

S6.4. Laurdan assay

To investigate the effect of compounds **1** and **3** on the membrane fluidity of *B. subtilis*, we performed a Laurdan assay as described by Strahl and co-workers (this section)[15] and a DPH assay (next section). For each experiment, a small amount of the *B. subtilis* glycerol stock was streaked onto a Müller-Hinton agar plate and the agar plate was incubated for 18-24 hours at 35 °C. The obtained colonies were aseptically transferred into sterile cation-adjusted Müller-Hinton broth supplemented with 0.1% glucose and diluted to OD_{600} of 0.2. The bacteria were subsequently incubated at 35 °C until OD_{600}.> 1.0. The cultures were then diluted in 17x100 mm polystyrene culture tubes with Müller-Hinton broth supplemented with 0.1% glucose to an OD_{600} of 0.20 or 0.45. Then, Laurdan dissolved in DMSO was added to achieve a final Laurdan concentration of 1 µM and 1% DMSO, and the bacteria were incubated at 35 °C for 5 minutes with shaking. The cultures were then centrifuged at 3000 rpm for 5 mins and the pellets were washed 4x with PBS buffer supplemented with 0.1% glucose and 1% DMSO. The supernatant of the last wash was kept for background fluorescence measurements (buffer+dye, no cells). The final pellets were re-suspended in PBS buffer supplemented with 0.1% glucose and 1% DMSO to an OD_{600} of 0.20 or 0.45, and 180 µL of this bacteria suspension was transferred into the wells of a 96-well plate for fluorescence (sterile, black, flat-bottom, polystyrene microplate from Brand #7816668) and the fluorescence intensity was measured for 5 minutes. At this point, 20 µL of stock solutions and control antibiotics (dissolved to 10x the desired concentration in PBS buffer with 0.1% glucose and 1% DMSO) were added and the fluorescence was measured for 20 minutes. All fluorescence measurements were preformed using a BioTek Cytation 5 Cell Imaging Multi-Mode Reader (35 °C, excitation at 350 nm and emission at 435 nm and 500 nm, time intervals of 23 seconds, orbital shaking (5 seconds at 548 rpm (2 mm) before each measurement). As a positive control, 50 mM benzyl alcohol was used, which is known to increase membrane fluidity.[16-18] As a negative control, the ribosome-targeting antibiotic clindamycin was used (2 µg/mL), as well as a blank run (no antibiotic added).

For the data analysis, the fluorescence intensities obtained for the background runs (no cells, only buffer+dye+antibiotic) were subtracted from the fluorescence intensities obtained for the runs with bacteria present. The Laurdan generalized polarization (GP) was then calculated as follows (with I_{435} the background-corrected fluorescence intensity at 435 nm, and I_{500} the background-corrected fluorescence intensity at 500 nm:

$$GP = \frac{I_{435} - I_{500}}{I_{435} + I_{500}}$$

The result for one of the biological repeats is shown in the main manuscript. The results of additional biological repeats are shown in **Figure S103** - **Figure S108**. Compound **1** and **3** both show an increase in membrane fluidity, comparable to positive control benzyl alcohol, with a more pronounced effect seen for compound **3** compared to compound **1**.

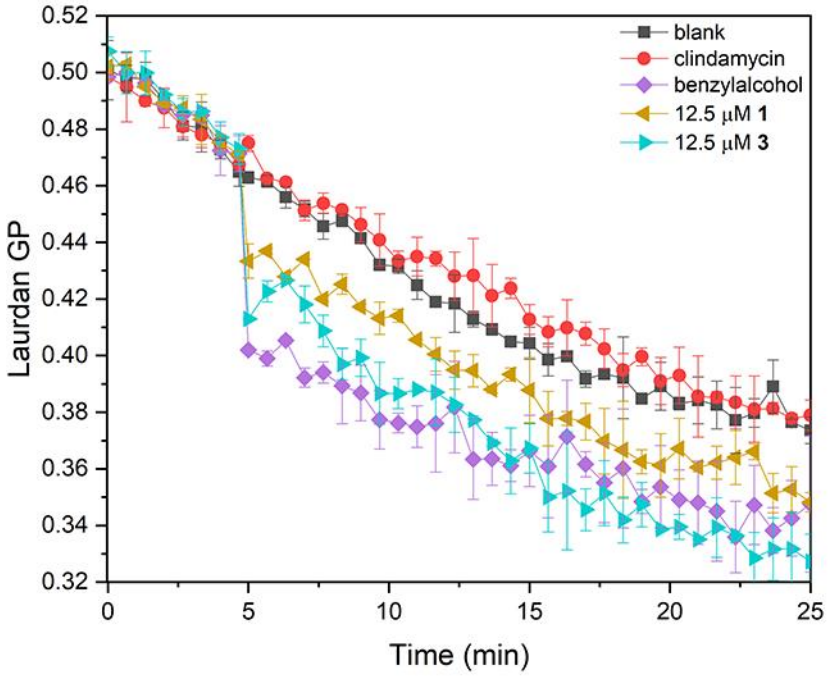

Figure S103. Laurdan generalized polarization (GP) in *B. subtilis* (OD_{600} = 0.2) stained with 10 µM Laurdan. Compounds were added at time *t* = 5 min: DMSO (1%, blank), clindamycin (2 µg/mL, negative control), benzyl alcohol (50 mM, positive control), 12.5 µM **1**, or 12.5 µM **3**. Results are the average of 2 technical repeats (error bars represent standard deviations).

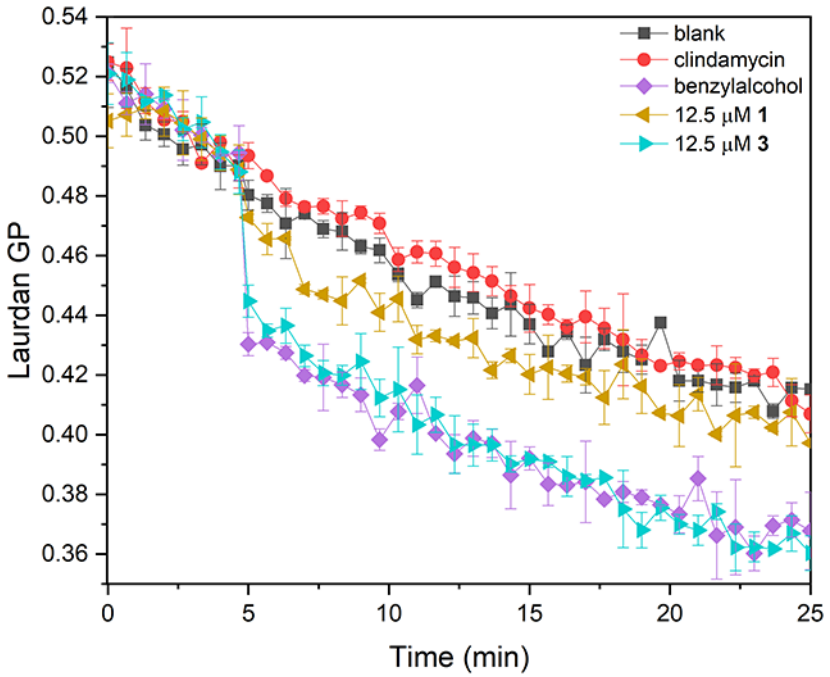

Figure S104. Laurdan generalized polarization (GP) in *B. subtilis* (OD_{600} = 0.2) stained with 10 µM Laurdan. Compounds were added at time *t* = 5 min: DMSO (1%, blank), clindamycin (2 µg/mL, negative control), benzyl alcohol (50 mM, positive control), 12.5 µM **1**, or 12.5 µM **3**. Results are the average of 2 technical repeats (error bars represent standard deviations).

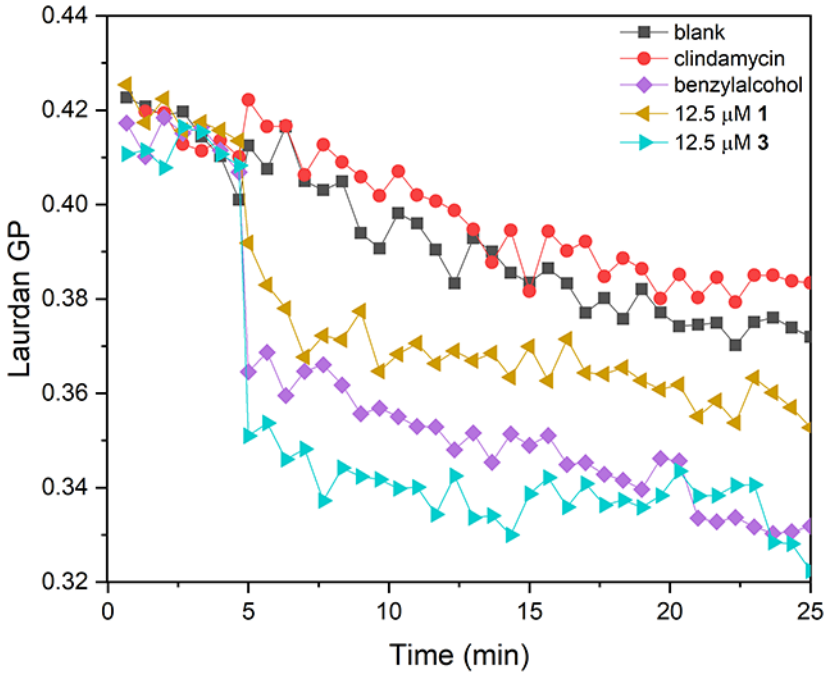

Figure S105. Laurdan generalized polarization (GP) in *B. subtilis* (OD_{600} = 0.45) stained with 10 µM Laurdan. Compounds were added at time *t* = 5 min: DMSO (1%, blank), clindamycin (2 µg/mL, negative control), benzyl alcohol (50 mM, positive control), 12.5 µM **1**, or 12.5 µM **3**. Data is the result of 1 technical repeat.

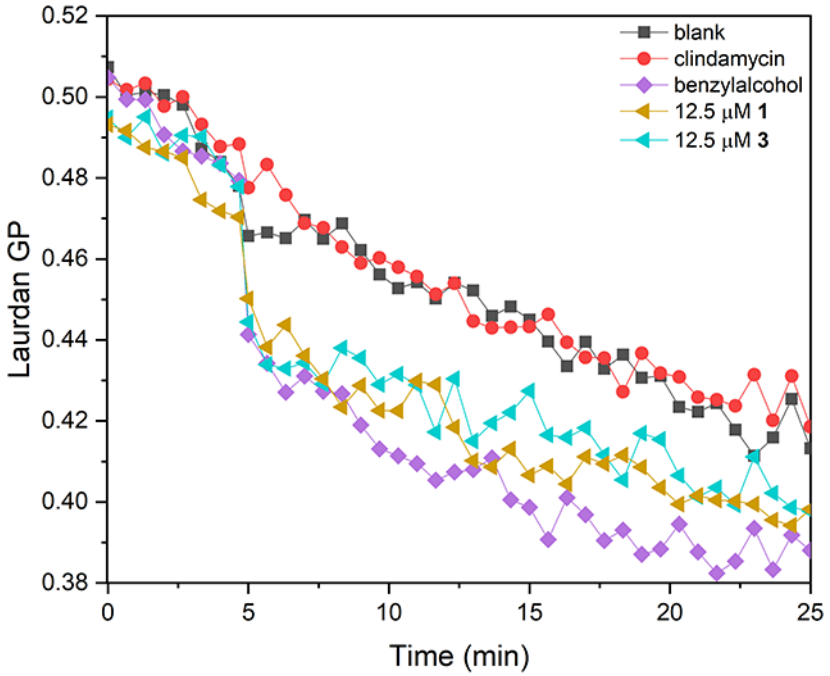

Figure S106. Laurdan generalized polarization (GP) in *B. subtilis* (OD_{600} = 0.45) stained with 10 µM Laurdan. Compounds were added at time *t* = 5 min: DMSO (1%, blank), clindamycin (2 µg/mL, negative control), benzyl alcohol (50 mM, positive control), 12.5 µM **1**, or 12.5 µM **3**. Data is the result of 1 technical repeat.

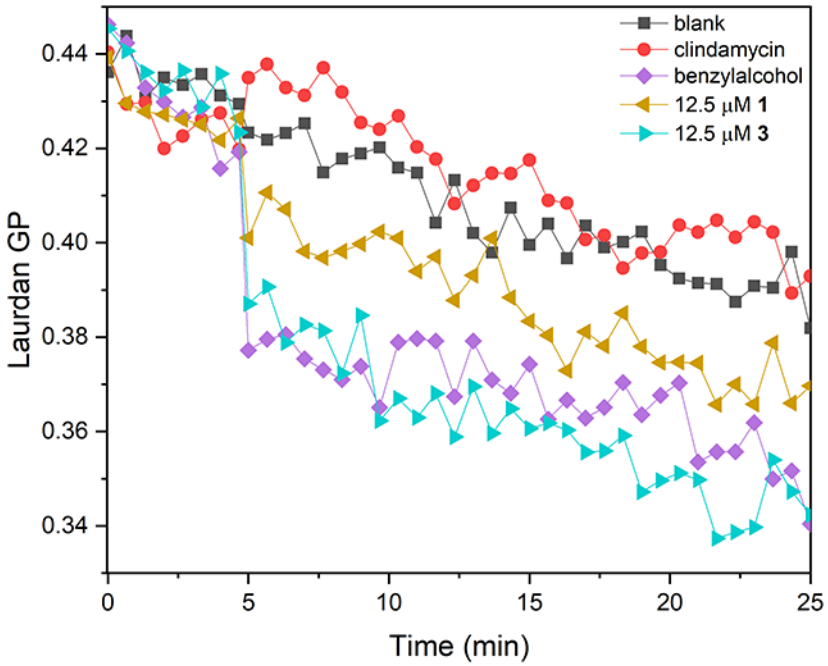

Figure S107. Laurdan generalized polarization (GP) in *B. subtilis* (OD_{600} = 0.45) stained with 10 µM Laurdan. Compounds were added at time *t* = 5 min: DMSO (1%, blank), clindamycin (2 µg/mL, negative control), benzyl alcohol (50 mM, positive control), 12.5 µM **1**, or 12.5 µM **3**. Data is the result of 1 technical repeat.

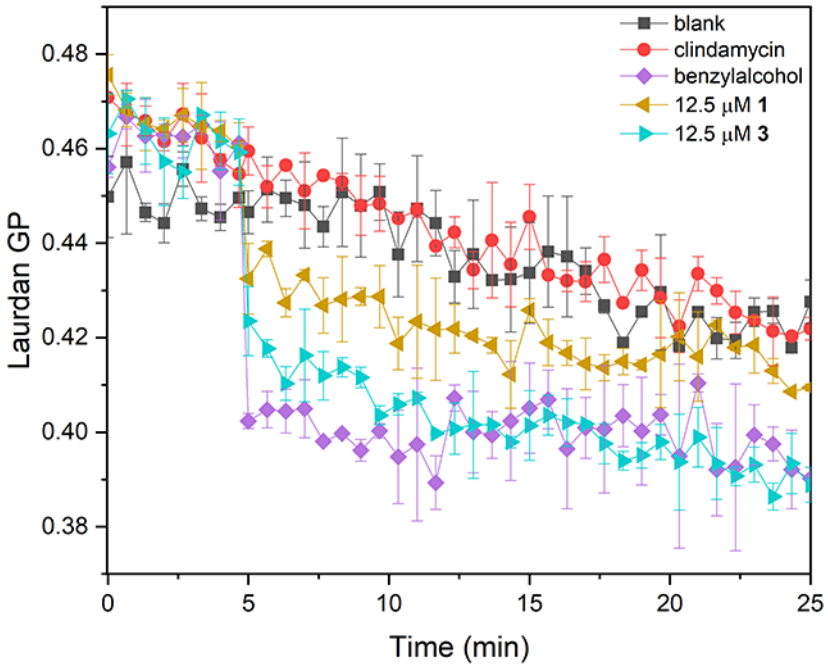

Figure S108. Laurdan generalized polarization (GP) in *B. subtilis* (OD_{600} = 0.45) stained with 10 µM Laurdan. Compounds were added at time *t* = 5 min: DMSO (1%, blank), clindamycin (2 µg/mL, negative control), benzyl alcohol (50 mM, positive control), 12.5 µM **1**, or 12.5 µM **3**. Data is the result of 1 technical repeat.

S6.5. DPH assay

The DPH (1,6-diphenyl-1,3,5-hexatriene) assay was performed according to a modified literature procedure.[19-22] For each experiment, a small amount of the *B. subtilis* glycerol stock was streaked onto a Müller-Hinton agar plate and the agar plate was incubated for 18-24 hours at 35 °C. The obtained colonies were aseptically transferred into sterile cation-adjusted Müller-Hinton broth and diluted to OD_{600} of 0.2 in 17x100 mm polystyrene culture tubes. To the culture tubes was then added an aliquot of a DMF stock solution of compounds **1**, **3** or clindamycin to achieve a final DMF amount of 1%, and the bacteria were incubated at 35 °C for 30 minutes with shaking (200 rpm). The cultures were then centrifuged at 3000 rpm for 5 mins and the pellets were washed 1x with PBS buffer and the final pellet was resuspended in PBS buffer to obtain an OD_{600} of 0.2-0.3. To the bacterial suspension was then added an aliquot of a DPH stock solution in DMF to achieve a final concentration of 10 µM DPH and 1% DMF, and the bacteria were incubated at 35 °C for 45 minutes with shaking (200 rpm). The cultures were then centrifuged at 3000 rpm for 5 mins and the pellets were washed 1x with PBS buffer supplemented with 1% DMF and the final pellet was resuspended in PBS buffer to obtain an OD_{600} of 0.2-0.3. The final solution was transferred to a disposable methacrylate macrocuvette (Fisherbrand #14-955-129), and the fluorescence anisotropy was measured using an Agilent Cary Eclipse fluorometer with manual polarizer (excitation = 355 nm, emission = 425 nm). The steady state fluorescence anisotropy was then calculated as:

$$anisotropy = \frac{I_{vv} - G \cdot I_{vh}}{I_{vv} + 2 \cdot G \cdot I_{vh}}$$

Where I_{vv} is the vertical component of fluorescence intensity measured using excitation with vertically polarized light, and I_{vh} is the horizontal component of the fluorescence intensity measured using excitation with vertically polarized light. G is a correction factor for the instrument, which was determined by the ratio of the fluorescence intensities of the horizontal and vertical components of a bacterial sample without any fluorophore when excited with light that is horizontally polarized ($G = I_{hv}/I_{hh}$), and was found to be 0.71208 for our fluorometer. The results are shown in the main manuscript.

S7. Hemolytic Activity

When designing a potential drug that targets the bacterial cellular membrane it is important to ensure it has a small effect on human erythrocytes. One of the simplest ways to determine a compound's toxicity towards human blood cells is by measuring the amount of hemoglobin release in response to the interaction. The following protocol was adapted from a protocol designed for antimicrobial peptides.[7]

Single donor human red blood cells were washed twice and diluted to 2.5 x 10^7 cells/mL in a 4% DMSO 1x PBS buffer. The assay was performed in a 96 well plate with a final volume of 200 µL. Boronic acid (BA) experimental concentrations of 250 µM, 200 µM, 125 µM, 100 µM, 62.5 µM, and 31.25 µM were created from serial dilutions of a 25 mM DMSO stock solution. 1% Triton X-100 was used as a positive control and 4% DMSO PBS buffer was used as a negative control. The plates were sealed with a protective film to prevent evaporation and incubated for 1 hour at 37˚C. After incubation, the 96 well plates were centrifuged at 3900 rpm for 5 min. 50 µL of each well's supernatant was then carefully transferred to a new 96 well plate, which was then centrifuged to remove any bubbles. Without any interfering bubbles, the absorbance of the supernatant was measured at 414 nm. The percent of hemolysis was calculated by the following formula:

$$\%\ Hemolysis = \frac{Abs\ (Sample) - Abs\ (Neg)}{Abs\ (Pos) - Abs\ (Neg)} \times 100$$

Where *Abs(Sample)* is each sample's absorption at 414 nm, *Abs(Neg)* is the negative control's average absorbance at 414 nm, and *Abs(Pos)* is the positive control's average absorption at 414 nm. The % hemolysis values were input into OriginPro 2018b (b9.5.5.409 (Academic)) and fitted with the DoseResp model with the maximum value set at 100% to determine HC_{50} from the inflection point.

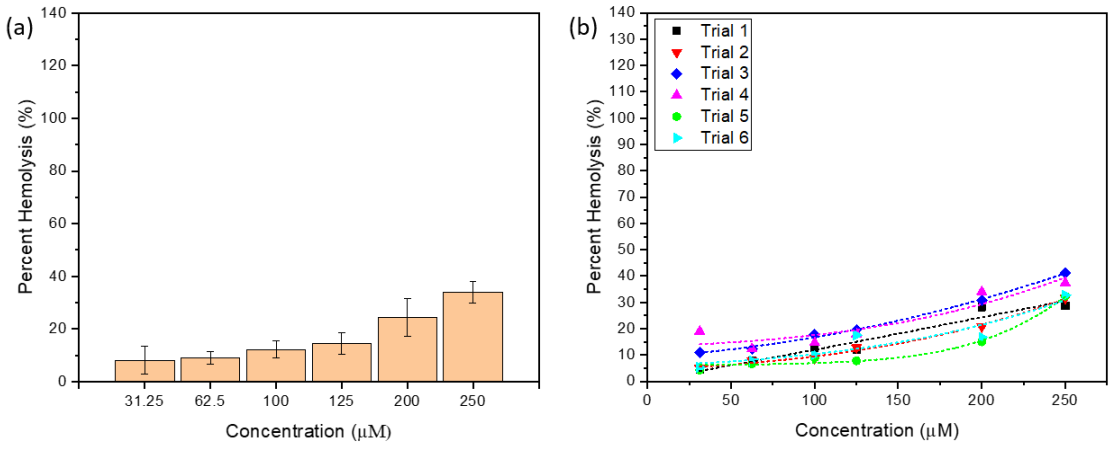

(c)

Model	DoseResp					
Equation	y = A1 + (100-A1)/(1 + 10^((LOGx0-x)*p))					
Trial	1	2	3	4	5	6
A1	-47.23 ± 149.81	1.49 ± 2.63	2.76 ± 3.28	11.12 ± 9.81	6.06 ± 1.10	3.50 ± 9.87
LOGx0	216.23 ± 599.18	328.98 ± 10.48	297.89 ± 5.14	313.94 ± 40.92	288.67 ± 8.58	334.81 ± 50.38
Adj. R-Squar	0.91055	0.98886	0.99476	0.78681	0.97457	0.81248

Figure S109. (a) Normalized hemolytic activity of **1** at varying concentrations. The results are the average of a minimum 2 biological x 2 technical repeats, and the error bars represent standard deviations. (b) HC_{50} calculations of **1** using the adjusted DoseResp model. The dashed lines represent the fit of the model. (c) HC_{50} output chart with inflection value (Logx0).

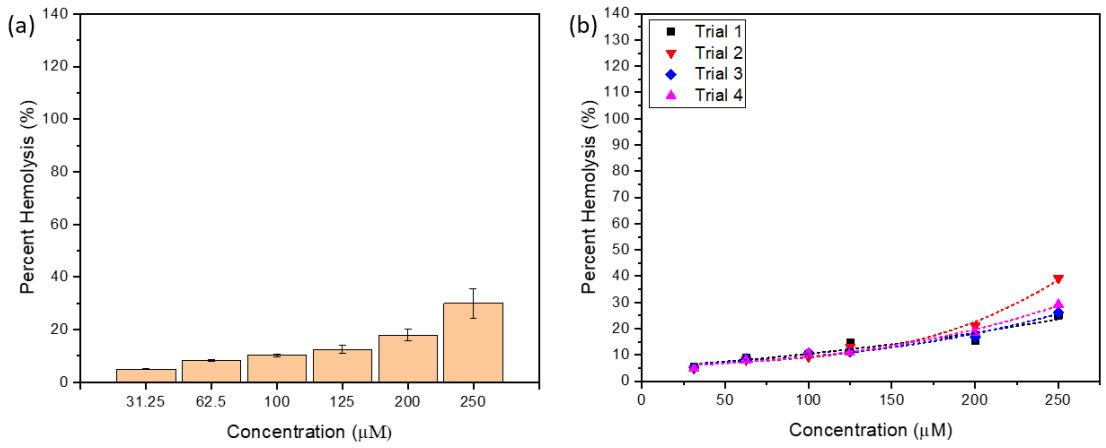

(c)

Model	DoseResp			
Equation	y = A1 + (100-A1)/(1 + 10^((LOGx0-x)*p))			
Trial	1	2	3	4
A1	-2.87 ± 21.17	5.66 ± 2.05	3.74 ± 3.74	3.17 ± 2.89
LOGx0	435.81 ± 82.72	285.15 ± 8.80	367.82 ± 33.79	342.07 ± 18.25
Adj. R-Square	0.86203	0.97507	0.95708	0.9776

Figure S110. (a) Normalized hemolytic activity of **2** at varying concentrations. The results are the average of a minimum 2 biological x 2 technical repeats, and the error bars represent standard deviations. (b) HC_{50} calculations of **1** using the adjusted DoseResp model. The dashed lines represent the fit of the model. (c) HC_{50} output chart with inflection value (Logx0).

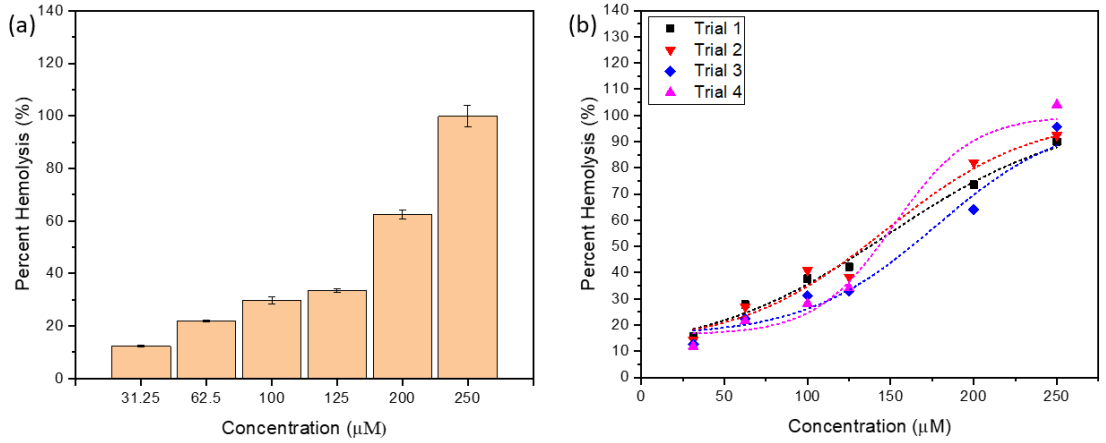

(c)

Model	DoseResp			
Equation	y = A1 + (100-A1)/(1 + 10^((LOGx0-x)*p))			
Trial	1	2	3	4
A1	8.82 ± 7.77	12.19 ± 10.29	15.88 ± 7.45	16.30 ± 6.01
LOGx0	147.86 ± 13.35	146.74 ± 16.83	177.42 ± 15.15	151.90 ± 21.15
Adj. R-Square	0.98506	0.95888	0.95158	0.96892

Figure S111. (a) Normalized hemolytic activity of **3** at varying concentrations. The results are the average of a minimum 2 biological x 2 technical repeats and the error bars represent standard deviations. (b) HC_{50} calculations of **1** using the adjusted DoseResp model. The dashed lines represent the fit of the model. (c) HC_{50} output chart with inflection value (Logx0).

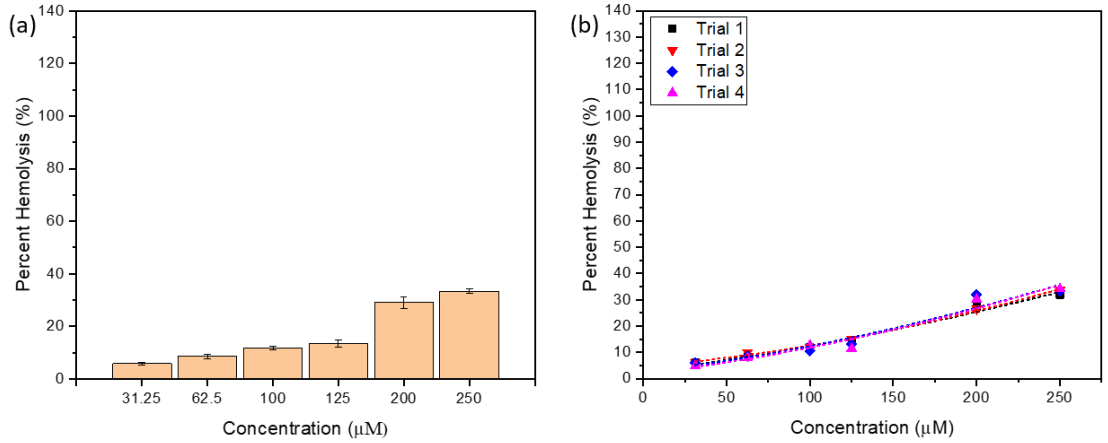

(c)

Model	DoseResp			
Equation	y = A1 + (100-A1)/(1 + 10^((LOGx0-x)*p))			
Trial	1	2	3	4
A1	-14.03 ± 16.99	-5.16 ± 5.30	-11.75 ± 29.77	-10.68 ± 21.95
LOGx0	313.39 ± 37.40	322.38 ± 7.60	296.09 ± 57.68	297.22 ± 38.91
Adj. R-Square	0.97959	0.99342	0.90798	0.93624

Figure S112. (a) Normalized hemolytic activity of **4** at varying concentrations. The results are the average of a minimum 2 biological x 2 technical repeats and the error bars represent standard deviations. (b) HC_{50} calculations of **1** using the adjusted DoseResp model. The dashed lines represent the fit of the model. (c) HC_{50} output chart with inflection value (Logx0).

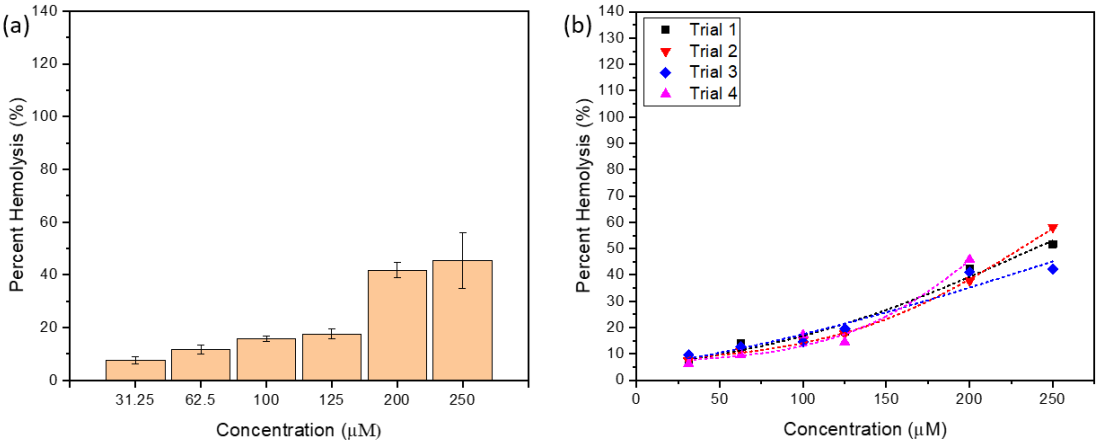

(c)

Model	DoseResp			
Equation	y = A1 + (100-A1)/(1 + 10^((LOGx0-x)*p))			
Trial	1	2	3	4
A1	-1.96 ± 9.90	5.75 ± 1.58	-11.38 ± 34.60	6.13 ± 4.93
LOGx0	235.27 ± 18.00	237.68 ± 2.87	245.67 ± 80.19	214.72 ± 8.99
Adj. R-Square	0.96945	0.9964	0.90782	0.94195

Figure S113. (a) Normalized hemolytic activity of **5** at varying concentrations. The results are the average of a minimum 2 biological x 2 technical repeats and the error bars represent standard deviations. (b) HC_{50} calculations of **1** using the adjusted DoseResp model. The dashed lines represent the fit of the model. (c) HC_{50} output chart with inflection value (Logx0).

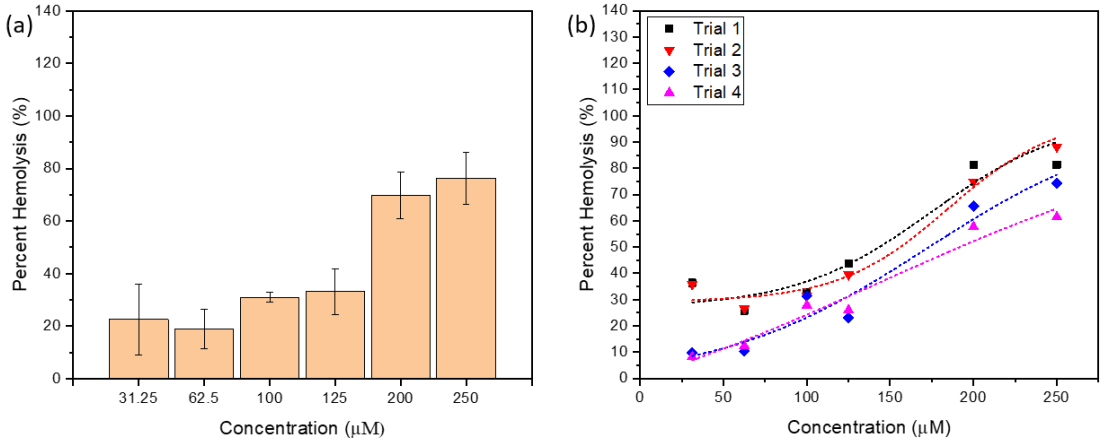

(c)

Model	DoseResp			
Equation	y = A1 + (100-A1)/(1 + 10^((LOGx0-x)*p))			
Trial	1	2	3	4
A1	26.95 ± 9.93	29.29 ± 4.35	-0.96 ± 17.62	-27.01 ± 46.60
LOGx0	174.88 ± 22.96	184.72 ± 11.02	172.02 ± 30.79	143.48 ± 91.02
Adj. R-Square	0.87909	0.96116	0.92113	0.94367

Figure S114. (a) Normalized hemolytic activity of **6** at varying concentrations. The results are the average of a minimum 2 biological x 2 technical repeats and the error bars represent standard deviations. (b) HC_{50} calculations of **1** using the adjusted DoseResp model. The dashed lines represent the fit of the model. (c) HC_{50} output chart with inflection value (Logx0).

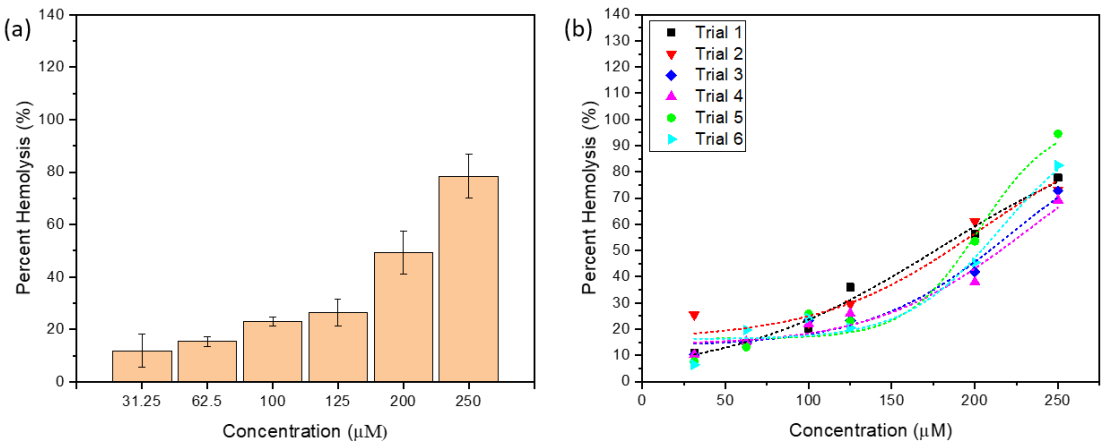

(c)

Model	DoseResp					
Equation	y = A1 + (100-A1)/(1 + 10^((LOGx0-x)*p))					
Plot	1	2	3	4	5	6
A1	1.60 ± 8.71	16.09 ± 7.61	13.46 ± 4.20	13.87 ± 4.99	16.36 ± 4.52	16.13 ± 4.33
LOGx0	178.15 ± 15.81	203.44 ± 16.18	222.20 ± 8.85	229.90 ± 10.57	202.72 ± 8.76	215.05 ± 9.42
Adj. R-Squar	0.97736	0.92663	0.957	0.93328	0.93824	0.92935

Figure S115. (a) Normalized hemolytic activity of **7** at varying concentrations. The results are the average of a minimum 2 biological x 2 technical repeats and the error bars represent standard deviations. (b) HC_{50} calculations of **1** using the adjusted DoseResp model. The dashed lines represent the fit of the model. (c) HC_{50} output chart with inflection value (Logx0).

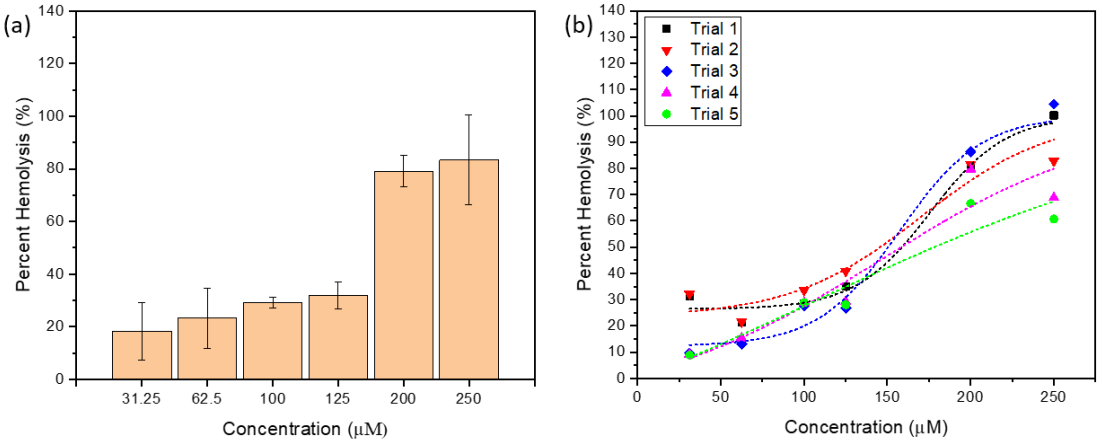

(c)

Model	DoseResp				
Equation	y = A1 + (100-A1)/(1 + 10^((LOGx0-x)*p))				
Trial	1	2	3	4	5
A1	26.35 ± 3.45	23.24 ± 9.18	12.21 ± 5.24	-10.18 ± 40.09	-40.92 ± 136.78
LOGx0	175.71 ± 9.18	170.43 ± 19.81	157.40 ± 10.06	145.44 ± 64.46	106.93 ± 247.65
Adj. R-Squ	0.97871	0.91013	0.97406	0.84519	0.82002

Figure S116. (a) Normalized hemolytic activity of **8** at varying concentrations. The results are the average of a minimum 2 biological x 2 technical repeats and the error bars represent standard deviations. (b) HC_{50} calculations of **1** using the adjusted DoseResp model. The dashed lines represent the fit of the model. (c) HC_{50} output chart with inflection value (Logx0).

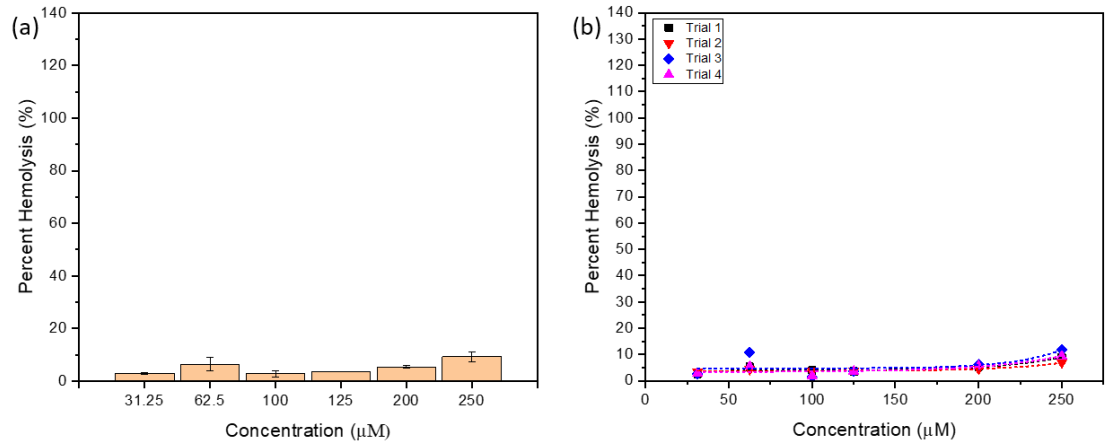

(c)

Model	DoseResp			
Equation	y = A1 + (100-A1)/(1 + 10^((LOGx0-x)*p))			
Trial	1	2	3	4
A1	3.75 ± 0.73	3.71 ± 0.25	4.69 ± 2.26	3.34 ± 1.06
LOGx0	365.93 ± 86.59	370.39 ± 55.10	319.24 ± 151.10	368.11 ± 99.23
Adj. R-Square	0.72719	0.89159	0.05282	0.66591

Figure S117. (a) Normalized hemolytic activity of **PBA** at varying concentrations. The results are the average of a minimum 2 biological x 2 technical repeats and the error bars represent standard deviations. (b) HC_{50} calculations of **1** using the adjusted DoseResp model. The dashed lines represent the fit of the model. (c) HC_{50} output chart with inflection value (Logx0).

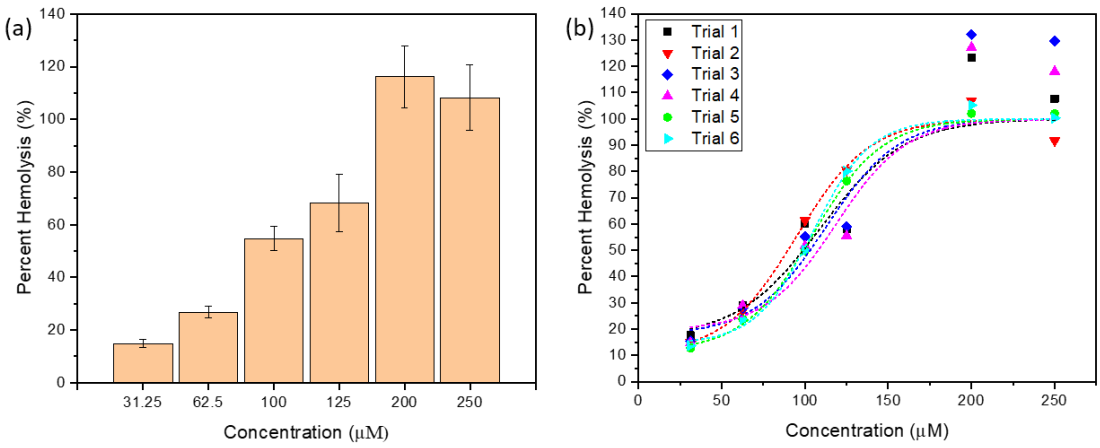

(c)

Model	DoseResp					
Equation	y = A1 + (100-A1)/(1 + 10^((LOGx0-x)*p))					
Trial	1	2	3	4	5	6
A1	16.64 ± 28.62	10.34 ± 11.47	17.80 ± 34.07	19.48 ± 24.30	11.58 ± 3.55	14.33 ± 4.09
LOGx0	109.14 ± 26.72	94.77 ± 9.60	112.67 ± 30.89	118.42 ± 22.97	104.57 ± 2.98	104.88 ± 3.42
Adj. R-Squar	0.81669	0.96755	0.70299	0.78309	0.99535	0.99063

Figure S118. (a) Normalized hemolytic activity of **indolicidin** at varying concentrations. The results are the average of a minimum 2 biological x 2 technical repeats and the error bars represent standard deviations. (b) HC_{50} calculations of **1** using the adjusted DoseResp model. The dashed lines represent the fit of the model. (c) HC_{50} output chart with inflection value (Logx0).

S8. References

1. S. Mothana, J.-M. Grassot and D. G. Hall, *Angew. Chem. Int. Ed.*, 2010, **49**, 2883-2887.
2. J. Reijenga, A. Van Hoof, A. Van Loon and B. Teunissen, *Analytical chemistry insights*, 2013, **8**, ACI. S12304.
3. J. Yan, G. Springsteen, S. Deeter and B. Wang, *Tetrahedron*, 2004, **60**, 11205-11209.
4. P. R. Westmark, S. J. Gardiner and B. D. Smith, *J. Am. Chem. Soc.*, 1996, **118**, 11093-11100.
5. D. Brynn Hibbert and P. Thordarson, *Chem. Commun.*, 2016, **52**, 12792-12805.
6. G. Springsteen and B. Wang, *Chem. Commun.*, 2001, DOI: 10.1039/B104895N, 1608-1609.
7. W. L. A. Brooks, C. C. Deng and B. S. Sumerlin, *ACS Omega*, 2018, **3**, 17863-17870.
8. Clinical and Laboratory Standards Institute, *Methods for dilution antimicrobial susceptibility tests for bacteria that grow aerobically; approved standard*, Clinical and Laboratory Standards Institute, Wayne, PA, 11th ed. CLSI standard M07 edn., 2018.
9. H. Zhao, J.-P. Mattila, J. M. Holopainen and P. K. J. Kinnunen, *Biophys. J.*, 2001, **81**, 2979-2991.
10. J. D. te Winkel, D. A. Gray, K. H. Seistrup, L. W. Hamoen and H. Strahl, *Front. Cell Dev. Biol.*, 2016, **4**.
11. D. A. Kelkar and A. Chattopadhyay, *Biochim. Biophys. Acta, Biomembr.*, 2007, **1768**, 2011-2025.
12. B. L. Roth, M. Poot, S. T. Yue and P. J. Millard, *Appl. Environ. Microbiol.*, 1997, **63**, 2421-2431.
13. Z. AlKhatib, M. Lagedroste, J. Zaschke, M. Wagner, A. Abts, I. Fey, D. Kleinschrodt and S. H. J. Smits, *MicrobiologyOpen*, 2014, **3**, 752-763.
14. Katharina M. Scherer, J.-H. Spille, H.-G. Sahl, F. Grein and U. Kubitscheck, *Biophys. J.*, 2015, **108**, 1114-1124.
15. K. Scheinpflug, O. Krylova and H. Strahl, in *Antibiotics: Methods and Protocols*, ed. P. Sass, Springer New York, New York, NY, 2017, DOI: 10.1007/978-1-4939-6634-9_10, pp. 159-174.
16. J. Reyes and R. Latorre, *Biophys. J.*, 1979, **28**, 259-279.
17. R. D. Sauerheber, J. A. Esgate and C. E. Kuhn, *Biochim. Biophys. Acta, Biomembr.*, 1982, **691**, 115-124.
18. T. Maula, B. Westerlund and J. P. Slotte, *Biochim. Biophys. Acta, Biomembr.*, 2009, **1788**, 2454-2461.
19. W. B. Yu and B. C. Ye, *J Basic Microbiol*, 2016, **56**, 502-509.
20. L. J. Bessa, M. Ferreira and P. Gameiro, *J. Photochem. Photobiol. B*, 2018, **181**, 150-156.
21. C. S. López, H. A. Garda and E. A. Rivas, *Arch. Biochem. Biophys.*, 2002, **408**, 220-228.
22. W. S. Sung, Y. Park, C.-H. Choi, K.-S. Hahm and D. G. Lee, *Biochem. Biophys. Res. Commun.*, 2007, **363**, 806-810.